Summer 9-1-2014

Characterization of the Role of R7-RGS Proteins in Mammalian Retina and Vision

Matthew D. Cain
Washington University in St. Louis

WASHINGTON UNIVERSITY IN ST. LOUIS
Division of Biology & Biomedical Sciences
Molecular Cell Biology

Dissertation Examination Committee:
Kendall J. Blumer, Chair
Thomas J. Baranski
David C. Beebe
Susan M. Culican
James E. Huettner
Daniel Kerschensteiner

Characterization of the Role of R7-RGS Proteins in Mammalian Retina and Vision

by

Matthew David Cain

A dissertation presented to the
Graduate School of Arts and Sciences
of Washington University in
partial fulfillment of the
requirements for the degree
of Doctor of Philosophy

August 2014

Saint Louis, Missouri

Table of Contents

List of Figures and Tables

Chapter 3

Chapter 4

Chapter 5

Acknowledgements

I would like to thank Dr. Kendall Blumer for providing an opportunity to conduct my doctoral thesis in his lab. Ken has been a wonderful mentor and performance coach over the years. Thank you for always making yourself available, for providing me independence, pushing me to answer my own questions, and reminding me to get out of my own head.

I would like to thank to my committee, Drs. Thomas J. Baranski, David C. Beebe, Susan M. Culican, James E. Huettner, and Daniel Kerschensteiner. I would like to especially thank Susan Culican and Daniel Kerschensteiner who have been wonderful collaborators throughout my thesis work. Without your willingness to open your labs to me, this work could not have been accomplished. I would also like to thank members of Department of Ophthalmology and Visual Sciences and VR core, especially Drs. Peter Lukaseiwicz, Vladimir Kefalov, and Anne Hennig for offering training and advice.

Thank you to all my other collaborators and colleagues in the Department of Cell Biology and Physiology and the Department of Ophthalmology and Visual Sciences.

I want to thank the present and past members of the Blumer lab. You have shown me how to be a successful scientist. You have inspired me to be a better senior student and mentor. Your advice and camaraderie is unmatched. I will very much miss our lunchtime discussions.

I could not have done this without my friends and family. Thank you for always being there. Thank you for believing that I could do this. Thank you for inspiring me to be better. Thank you for the endless love and support. I love you all.

Special thanks are required for Christy. She was my rock through the writing of this dissertation.

ABSTRACT OF THE DISSERTATION

Characterization of the Role of RGS7-family Proteins in Mammalian Retina and Vision

by

Matthew David Cain

Doctor of Philosophy in Biology and Biomedical Sciences

Molecular Cell Biology

Washington University in St. Louis, 2014

Professor Kendall J. Blumer, Chairperson

GPCR/G protein signaling is a critical component of neuronal signal transduction and function. G protein signaling is regulated by a family of regulator of G protein signaling (RGS) proteins that act as GTPase activating proteins (GAPs) for Gα subunits. In the retina, the R7-RGS family of RGS proteins which specifically act as GAPs toward Gi/o, are critical regulators of phototransduction and ON bipolar cell light responses in the outer retina. While R7-RGS proteins are expressed throughout the inner retina, their function there is unknown. The goal of this dissertation project is to characterize R7-RGS regulation on retina function and vision.

This dissertation is divided into four parts: i) analysis of inner retinal function in mature and developing R7BP$^{-/-}$ retinas, ii) characterization of composition and localization of R7-RGS/R7BP complexes in the dorsal lateral geniculate nucleus (dLGN), iii) characterization of blockade of RGS regulation of Gi2 and Go subunits on outer retina function, and iv) preliminary analysis of the effect of RGS6 ablation on vision. In part i), we found that R7BP is expressed in starburst amacrine cells (SAC) and retinal ganglion cells (RGC). R7BP regulates mesopic RGC light responses and glutamatergic wave burst duration in mature and developing retina,

respectively. In part ii), we found that R7PB is expressed in the dLGN. R7BP interacts with RGS6 and RGS7 in lateral geniculate nucleus lysates, but is not necessary for their membrane localization. In part iii), outer retinal phenotypes of RGS-insensitive Gi2 and Go mutant mice were characterized. RGS regulation of Gi2 is necessary for normal rod light responses. Heterozygous expression of RGS-insensitive Go subunits was not sufficient to perturb ON bipolar cell light responses or dendritic morphology. In part iv), we found that RGS6 is expressed in starburst amacrine cells. RGS6 localization to SAC plexi is independent of R7BP. We demonstrated that, although dispensable for normal phototransduction or ON bipolar light responses, RGS6 is necessary for normal spatial vision. Based on these findings, we suggest that RGS regulation of Gi/o signaling is necessary for normal retinal function and that R7-RGS proteins regulate inner retinal function. Additionally, we identified several new candidate circuits to further explore R7-RGS function in the visual system.

Chapter 1:

Introduction

Introduction

GPCRs and G protein Signaling

G-protein coupled receptors (GPCRs) are a superfamily of seven-transmembrane domain proteins which function to interact with signals from the extracellular environment and propagate these signals into the intracellular space to promote cellular responses. The diversity in expression, recognized ligands, and regulated cellular responses make them essential components for many physiological processes. Similarly, this diversity has made GPCRs the most abundant pharmaceutical targets, making up approximately 30% of all marketed drugs (Garland, 2013).

GPCRs are activated by an incredibly diverse set of ligands, including peptides, hormones, neurotransmitters, odorants, and photons. Upon activation, GPCRs undergo conformational change that allow them to act as guanine exchange factors (GEFs) for heterotrimeric G-proteins (Figure 1). Heterotrimeric G proteins consist of three subunits, Gα, Gβ, and Gγ. Gα is the nucleotide binding GTPase subunit. Gβ and Gγ form constitutive dimers (Gβγ) that associate with Gα depending on the guanine nucleotide (GDP or GTP) bound state of Gα. Prior to guanine nucleotide exchange, Gα binds GDP and Gβγ. As GEFs, activated GPCRs promote exchange of GDP for GTP and dissociation of the Gαβγ heterotrimer. Both GTP-bound Gα and Gβγ act on effectors to propagate intracellular signals.

There are a diversity of Gα subunits, grouped into four classes Gs, Gi/o, Gq, and G12/13. Each class of Gα has specific downstream effectors that modulate cell signaling. Gs activates adenylyl cyclase to generate the secondary messenger cAMP. Gi/o inhibits adenylyl cyclase. Gq activates phospholipase C and promote intracellular Ca^{2+} release. G12/13 promotes cytoskeletal

changes through Rho and RhoGEFs. There is similar diversity in Gβγ subunits and they also couple to downstream effectors, such as GIRK channels.

This study exclusively focuses on GPCR signaling cascades that couple to Gi/o subunits.

RGS Proteins

RGS (regulator of G protein signaling) protein are critical to the switch-like behavior of G protein signaling via their function as GTPase activating proteins (GAPs) toward Gα subunits. GAPs accelerate the inherently slow intrinsic GTPase activity of Gα subunits, promoting the hydrolysis of GTP to GDP by stabilizing the switch regions of Gα in a configuration that resembles the transition state (Ross and Wilkie, 2000; Srinivasa et al., 1998; Tesmer et al., 1997). GDP-bound Gα proteins have decreased affinity for effectors and re-associate with Gβγ. Therefore, in general RGS proteins act as inhibitors of G protein signaling and can act to attenuate the magnitude or control the kinetics of cellular responses (Ross and Wilkie, 2000).

Originally identified in yeast (Chan and Otte, 1982), RGS proteins now comprise a large superfamily of proteins characterized by the presence of a RGS domain (Figure 2). RGS proteins are subdivided into families based on both their structure and affinity for specific Gα subunits. Many families have accessory domains that facilitate interactions with non-Gα proteins or act as effector domains for secondary signaling cascades. Since their discovery, RGS proteins have been revealed as critical regulators of G protein signaling in human biology and diseases, including hypertension (Heximer et al., 2003), cardiac arrhythmia (Cifelli et al., 2008; Wydeven et al., 2014), opioid action (Garzón et al., 2003; Psifogeorgou et al., 2007; Terzi et al., 2011; Zachariou et al., 2003; Zhou et al., 2012a), depression (Stewart et al., 2014), learning and

memory (Lee et al., 2010; Ostrovskaya et al., 2014a), and Parkinson's disease (Gold et al., 2007; Kovoor et al., 2005). As such, they are being recognized as potential pharmaceutical targets for the treatment of human disease (Sjögren, 2011).

R7-RGS Heterotrimeric Complexes

This study will primarily focus on the biology of the regulator of G protein signaling 7 (R7-RGS) family. The R7-RGS family consists of four members (RGS6, 7, 9, and 11) which act as GAPs for Gi/o and are expressed throughout the central nervous system (Gold et al., 1997; Hooks et al., 2003; Song et al., 2007). R7-RGS family members have a conserved structure consisting of a C-terminal RGS domain, which is necessary and sufficient for GAP activity, and N-terminal DEP (disheveled, Egl-10, and pleckstrin), DHEX/R7H (DEP helical extension, or RGS7 homology) and GGL (G protein gamma-like) domains (Figure 3A). The GGL domain is structurally similar to the heterotrimeric Gγ subunit and facilitates the interaction with a divergent Gβ subunit Gβ5 (Cheever et al., 2008; Snow et al., 1998) (Figure 3B). This interaction is necessary for the folding of Gβ5 and mutual protection of Gβ5 and R7-RGS proteins from proteolytic degradation (Chen et al., 2003; Shim et al., 2012). Additionally, this interaction of R7-RGS proteins with Gβ5 provides additional interfaces by which R7-RGS complexes interact with traditional Gβγ effectors, including GIRK channels (Xie et al., 2010; Zhou et al., 2012a). The DEP domain facilitates interaction with two membrane associated proteins, RGS9 anchor protein (R9AP) and R7-family binding protein (R7BP) (Drenan et al., 2005; Hu and Wensel, 2002; Martemyanov et al., 2003, 2005). The DEP domain also facilitates binding to various GPCRs, including GPR158, GPR179 and M3 muscarinic receptor (Orlandi et al., 2012; Sandiford and Slepak, 2009).

R9AP and R7BP were originally identified as membrane targeting proteins for R7-RGS proteins (Drenan et al., 2005; Hu and Wensel, 2002). However, in recent years R9AP and R7BP have been shown to have more complex mechanisms of regulating R7-RGS/Gβ5 dimers. Both R9AP and R7BP are SNARE like proteins, distantly related to syntaxins (Drenan et al., 2005; Keresztes et al., 2003; Martemyanov et al., 2003, 2005) (Figure 3C). Both proteins localize to membranes by distinct mechanisms. R9AP is membrane-targeted by a C-terminal transmembrane domain (Hu and Wensel, 2002) while R7BP associates with membranes by two C-terminal palmitate moieties (Drenan et al., 2005). Both proteins protect RGS9 from degradation *in vivo* (Anderson et al., 2007a; Keresztes et al., 2004). R7BP is reciprocally protected from proteolytic degradation by its interaction with R7-RGS DEP domains (Anderson et al., 2007a; Grabowska et al., 2008) (Figure 3D). However, there is evidence that R7BP and R9AP have more divergent effects on R7-RGS function *in vivo*. R9AP is necessary for trafficking RGS9 to outer segments of rod photoreceptors, a function that cannot be rescued by R7BP (Cao et al., 2010; Martemyanov et al., 2003). It is unclear what role, if any, R7BP plays in trafficking of R7-RGS proteins *in vivo*. In transfected cells, R7BP targets the R7-RGS complex to the plasma membrane, augmenting their GAP activity and subsequently attenuating Gi/o signaling (Drenan et al., 2005). Additionally, there is strong evidence that R7BP also functions as an allosteric modulator of R7-RGS function, modulating R7-RGS GAP activity toward Gi/o and interaction with M3 receptors and GIRK channels (Masuho et al., 2013; Sandiford and Slepak, 2009; Zhou et al., 2012a). While the R7-RGS family is expressed throughout the central nervous system (Gold et al., 1997; Song et al., 2007) , this study focuses on exploring their function in the mammalian retina.

Retina Structure

The retina is the primary light sensing organ of the mammalian nervous system. It is comprised primarily of neuronal tissue that is structured into a series of layers. Photoreceptors are positioned in the outermost portion of the retina (Figure 4). Photoreceptors are highly specialized neurons that are responsible for phototransduction, or the conversion of photons into electrical signals in photoreceptors. Photoreceptors can be divided into two primary species, rods and cones which differ in their light sensitivity. Rods are highly sensitive and mediate low intensity or scotopic vision. Cones require higher light intensities and facilitate photopic vision. Cones can be further divide based on their wavelength absorption spectra and are responsible for mediating color vision. Structurally, phototransduction occurs in the outer segments of photoreceptors. Photoreceptors synapse onto bipolar cells in the outer plexiform layer (OPL). Bipolar cells can be divided into two primary groups, ON and OFF, based on whether they depolarize or hyperpolarize to light, respectively. Horizontal neurons also synapse in the outer plexiform layer, where they integrate and regulate photoreceptor input into bipolar cells. In this study, this section of the retina will be referred to as the outer retina. ON and OFF bipolar cells project to the inner and outer sublaminae of the inner plexiform layer (IPL), respectively. In the IPL, cone bipolar cells form glutamatergic synapses onto both retinal ganglion cells (RGCs) and amacrine cells. Rod bipolar cells synapse onto AII amacrine cells which allows them to couple to cone bipolar cells. In this study, the circuits formed between bipolar, amacrine, and retinal ganglion cells in the IPL are referred to as the inner retina. Amacrine cells are interneurons that primarily release inhibitory neurotransmitters GABA or glycine. However, some amacrine cell types release additional neurotransmitters, including dopamine and acetylcholine. Amacrine cell

neurotransmitter release modulates the input of bipolar cells into RGCs. RGCs are the final point of integration of retinal circuits and are responsible for transmitting visual information to vision centers of the brain.

G Protein Signaling in the Retina

G protein signaling is an essential component of phototransduction and transmission to retinal ganglions cells. Phototransduction occurs on optic discs of the photoreceptors when photons are captured by the GPCR rhodopsin. In periods of darkness, cGMP concentrations are high and bind to cGMP gated (CNG) channels. This opens CNG channels allowing for a steady inward current of Ca^{2+} and Na^{2+}, depolarization of the photoreceptor, and glutamate release. Photon absorption by the chromophore, retinal, in rhodopsin triggers isomerization of 11-cis-retinal to all-trans-retinal, activating rhodopsin. Activated of rhodopsin triggers GTP exchange in the transducin Gα subunit and subsequent activation of cGMP phosphodiesterase 6, accelerating the hydrolysis of cGMP to GMP. This reduction in cGMP results in closure of CNG channels, hyperpolarization of the photoreceptor, and a decrease in glutamate release from photoreceptor termini.

ON bipolar cells reverse the signal of photoreceptors through a metabotropic mechanism. In periods of darkness, the GPCR mGluR6 is bound by glutamate released from photoreceptors and maintains an active pool of Go1 Gα subunits (Dhingra et al., 2000a, 2002; Masu et al., 1995). Go1 inhibits constitutively-active TRPM1 channels, hyperpolarizing ON bipolar cells (Koike et al., 2010; Morgans et al., 2010). However, the mechanism of this inhibition is not well

understood. Upon exposure to light, the decrease in synaptic glutamate allows for inactivation of Go1, relief of TRPM1 inhibition, and ON bipolar cell depolarization.

In addition, there are a number of classic neurotransmitters (dopamine, glutamate, GABA, and acetylcholine) that activate GPCRs that act as modulators of inner retinal activity. Dopamine regulates the electrical coupling of amacrine cells (Gleason, 2012) and excitability of retinal ganglion cells (Chen and Yang, 2007; Hayashida et al., 2009; Ogata et al., 2012). With the exception of mGluR3 and mGluR6, all metabotropic glutamate receptors exhibit both pre- and post-synaptic expression in amacrine cells and post-synaptic expression in retinal ganglion cells (Dhingra and Vardi, 2012). In amacrine cells, mGluRs primarily regulate neurotransmitter release (Dhingra and Vardi, 2012). In retinal ganglion cells, mGluRs regulate voltage-gated calcium channels and excitability (Robbins et al., 2003; Yu et al., 2009) Muscarinic acetylcholine receptors are expressed throughout the inner retina (Strang et al., 2010), although our understanding of their regulation of inner retinal activity is limited (Baldridge, 1996; Neal and Cunningham, 1995). The extent RGS proteins regulate the endogenous signaling of these GPCRs is not known.

R7-RGS Complexes in Retina

R7-RGS family complexes are necessary for proper phototransduction and neurotransmission in the retina. RGS9-1 is the only R7-RGS family member expressed in the photoreceptors, where it has an obligate interaction with R9AP and accelerates the deactivation of transducin (Cowan et al., 1998; He et al., 1998; Keresztes et al., 2004; Makino et al., 1999). Because R9AP expression is necessary for RGS9 expression, $RGS9^{-/-}$ and $R9AP^{-/-}$ mice have

similar phenotypes (Keresztes et al., 2004). Patients with mutations in either RGS9 or R9AP have difficulty seeing moving, low-contrast objects and adapt slowly to abrupt changes in light intensity (Hartong et al., 2007; Nishiguchi et al., 2004).

RGS6, RGS7, and RGS9 are expressed differentially within the non-photoreactive layers of the retina (Liapis et al., 2012; Morgans et al., 2007; Song et al., 2007). RGS7 and RGS11 are localized to the dendritic tips of ON bipolar cells in the OPL through interaction with the orphan GPCR GPR179 (Orlandi et al., 2012). In the OPL, loss of both RGS7 and RGS11 results in a no-b-wave electroretinogram (ERG) phenotype indicating a failure of ON bipolar cells to depolarize in response to light (Cao et al., 2012; Rao et al., 2007; Shim et al., 2012). This loss of the b-wave can be attributed to both the misregulation of mGluR6-Go signaling and morphological defects in the OPL synapses between photoreceptors and bipolar cells. RGS7 and RGS11 function redundantly in synapses, as single knockouts only exhibit delayed ON bipolar cell responses (Cao et al., 2012; Chen et al., 2003; Mojumder et al., 2009; Shim et al., 2012).

RGS6 and RGS7 are also expressed in the inner retina (Liapis et al., 2012; Song et al., 2007; Witherow et al., 2000). However, it is unknown which Gi/o signaling cascades are regulated by these R7-RGS proteins. Similarly, whether R7-RGS proteins are necessary for visual function outside of the outer retina has not been explored.

Hypothesis

R7-RGS proteins are expressed in the inner retina, but we have been unable to determine their contribution to inner retinal G protein signaling and vision. This represents a significant

gap in our understanding of retinal R7-RGS function. It is apparent that R7-RGS proteins are critical regulators of G protein signaling in the CNS and outer retina. Both the expression of R7-RGS proteins and the presence of multiple Gi/o signaling cascades in the inner retina make it a reasonable hypothesis that R7-RGS proteins regulate Gi/o signaling in the inner retina. Additionally, the function of the R7-family binding protein (R7BP) *in vivo* is poorly understood. This dissertation is motivated by the hypothesis that R7-RGS proteins regulate Gi/o signaling in the inner retina, and that this regulation is necessary for normal inner retina function and vision.

References

Anderson, G.R., Lujan, R., Semenov, A., Pravetoni, M., Posokhova, E.N., Song, J.H., Uversky, V., Chen, C.-K., Wickman, K., and Martemyanov, K.A. (2007). Expression and Localization of RGS9-2/Gβ5/R7BP Complex In Vivo Is Set by Dynamic Control of Its Constitutive Degradation by Cellular Cysteine Proteases. J. Neurosci. *27*, 14117–14127.

Baldridge, W.H. (1996). Optical recordings of the effects of cholinergic ligands on neurons in the ganglion cell layer of mammalian retina. J. Neurosci. *16*, 5060–5072.

Cao, Y., Kolesnikov, A.V., Masuho, I., Kefalov, V.J., and Martemyanov, K.A. (2010). Membrane anchoring subunits specify selective regulation of RGS9·Gbeta5 GAP complex in photoreceptor neurons. J. Neurosci. *30*, 13784–13793.

Cao, Y., Pahlberg, J., Sarria, I., Kamasawa, N., Sampath, A.P., and Martemyanov, K.A. (2012). Regulators of G protein signaling RGS7 and RGS11 determine the onset of the light response in ON bipolar neurons. PNAS *109*, 7905–7910.

Chan, R.K., and Otte, C.A. (1982). Isolation and genetic analysis of Saccharomyces cerevisiae mutants supersensitive to G1 arrest by a factor and alpha factor pheromones. Mol. Cell. Biol. *2*, 11–20.

Cheever, M.L., Snyder, J.T., Gershburg, S., Siderovski, D.P., Harden, T.K., and Sondek, J. (2008). Crystal structure of the multifunctional Gbeta5-RGS9 complex. Nat. Struct. Mol. Biol. *15*, 155–162.

Chen, L., and Yang, X.-L. (2007). Hyperpolarization-activated cation current is involved in modulation of the excitability of rat retinal ganglion cells by dopamine. Neuroscience *150*, 299–308.

Chen, C.-K., Eversole-Cire, P., Zhang, H., Mancino, V., Chen, Y.-J., He, W., Wensel, T.G., and Simon, M.I. (2003). Instability of GGL domain-containing RGS proteins in mice lacking the G protein β-subunit Gβ5. PNAS *100*, 6604–6609.

Cifelli, C., Rose, R.A., Zhang, H., Voigtlaender-Bolz, J., Bolz, S.-S., Backx, P.H., and Heximer, S.P. (2008). RGS4 regulates parasympathetic signaling and heart rate control in the sinoatrial node. Circ. Res. *103*, 527–535.

Cowan, C.W., Fariss, R.N., Sokal, I., Palczewski, K., and Wensel, T.G. (1998). High expression levels in cones of RGS9, the predominant GTPase accelerating protein of rods. Proceedings of the National Academy of Sciences of the United States of America *95*, 5351.

Dhingra, A., and Vardi, N. (2012). mGlu receptors in the retina. Wiley Interdisciplinary Reviews: Membrane Transport and Signaling *1*, 641–653.

Dhingra, A., Lyubarsky, A., Jiang, M., Pugh, E.N., Jr, Birnbaumer, L., Sterling, P., and Vardi, N. (2000). The light response of ON bipolar neurons requires G[alpha]o. J. Neurosci. *20*, 9053–9058.

Dhingra, A., Jiang, M., Wang, T.-L., Lyubarsky, A., Savchenko, A., Bar-Yehuda, T., Sterling, P., Birnbaumer, L., and Vardi, N. (2002). Light Response of Retinal ON Bipolar Cells Requires a Specific Splice Variant of Gαo. J. Neurosci. *22*, 4878–4884.

Drenan, R.M., Doupnik, C.A., Boyle, M.P., Muglia, L.J., Huettner, J.E., Linder, M.E., and Blumer, K.J. (2005). Palmitoylation regulates plasma membrane–nuclear shuttling of R7BP, a novel membrane anchor for the RGS7 family. J Cell Biol *169*, 623–633.

Garland, S.L. (2013). Are GPCRs Still a Source of New Targets? J Biomol Screen *18*, 947–966.

Garzón, J., López-Fando, A., and Sánchez-Blázquez, P. (2003). The R7 subfamily of RGS proteins assists tachyphylaxis and acute tolerance at mu-opioid receptors. Neuropsychopharmacology *28*, 1983–1990.

Gleason, E. (2012). The influences of metabotropic receptor activation on cellular signaling and synaptic function in amacrine cells. Visual Neuroscience *29*, 31–39.

Gold, S.J., Ni, Y.G., Dohlman, H.G., and Nestler, E.J. (1997). Regulators of G-protein signaling (RGS) proteins: region-specific expression of nine subtypes in rat brain. J. Neurosci. *17*, 8024–8037.

Gold, S.J., Hoang, C.V., Potts, B.W., Porras, G., Pioli, E., Kim, K.W., Nadjar, A., Qin, C., LaHoste, G.J., Li, Q., et al. (2007). RGS9-2 negatively modulates L-3,4-dihydroxyphenylalanine-induced dyskinesia in experimental Parkinson's disease. J. Neurosci. *27*, 14338–14348.

Grabowska, D., Jayaraman, M., Kaltenbronn, K.M., Sandiford, S.L., Wang, Q., Jenkins, S., Slepak, V.Z., Smith, Y., and Blumer, K.J. (2008). Postnatal induction and localization of R7BP, a membrane-anchoring protein for regulator of G protein signaling 7 family-Gβ5 complexes in brain. Neuroscience *151*, 969–982.

Hartong, D.T., Pott, J.-W.R., and Kooijman, A.C. (2007). Six Patients with Bradyopsia (Slow Vision): Clinical Features and Course of the Disease. Ophthalmology *114*, 2323–2331.

Hayashida, Y., Rodríguez, C.V., Ogata, G., Partida, G.J., Oi, H., Stradleigh, T.W., Lee, S.C., Colado, A.F., and Ishida, A.T. (2009). Inhibition of adult rat retinal ganglion cells by D1-type dopamine receptor activation. J. Neurosci. *29*, 15001–15016.

He, W., Cowan, C.W., and Wensel, T.G. (1998). RGS9, a GTPase Accelerator for Phototransduction. Neuron *20*, 95–102.

Heximer, S.P., Knutsen, R.H., Sun, X., Kaltenbronn, K.M., Rhee, M.-H., Peng, N., Oliveira-dos-Santos, A., Penninger, J.M., Muslin, A.J., Steinberg, T.H., et al. (2003). Hypertension

and prolonged vasoconstrictor signaling in RGS2-deficient mice. Journal of Clinical Investigation *111*, 445–452.

Hooks, S.B., Waldo, G.L., Corbitt, J., Bodor, E.T., Krumins, A.M., and Harden, T.K. (2003). RGS6, RGS7, RGS9, and RGS11 stimulate GTPase activity of Gi family G-proteins with differential selectivity and maximal activity. J. Biol. Chem. *278*, 10087–10093.

Hu, G., and Wensel, T.G. (2002). R9AP, a membrane anchor for the photoreceptor GTPase accelerating protein, RGS9-1. Proc. Natl. Acad. Sci. U.S.A. *99*, 9755–9760.

Keresztes, G., Mutai, H., Hibino, H., Hudspeth, A.J., and Heller, S. (2003). Expression patterns of the RGS9-1 anchoring protein R9AP in the chicken and mouse suggest multiple roles in the nervous system. Mol. Cell. Neurosci. *24*, 687–695.

Keresztes, G., Martemyanov, K.A., Krispel, C.M., Mutai, H., Yoo, P.J., Maison, S.F., Burns, M.E., Arshavsky, V.Y., and Heller, S. (2004). Absence of the RGS9.Gbeta5 GTPase-activating complex in photoreceptors of the R9AP knockout mouse. J. Biol. Chem. *279*, 1581–1584.

Koike, C., Obara, T., Uriu, Y., Numata, T., Sanuki, R., Miyata, K., Koyasu, T., Ueno, S., Funabiki, K., Tani, A., et al. (2010). TRPM1 is a component of the retinal ON bipolar cell transduction channel in the mGluR6 cascade. Proc. Natl. Acad. Sci. U.S.A. *107*, 332–337.

Kovoor, A., Seyffarth, P., Ebert, J., Barghshoon, S., Chen, C.-K., Schwarz, S., Axelrod, J.D., Cheyette, B.N.R., Simon, M.I., Lester, H.A., et al. (2005). D2 Dopamine Receptors Colocalize Regulator of G-Protein Signaling 9-2 (RGS9-2) via the RGS9 DEP Domain, and RGS9 Knock-Out Mice Develop Dyskinesias Associated with Dopamine Pathways. J. Neurosci. *25*, 2157–2165.

Lee, S.E., Simons, S.B., Heldt, S.A., Zhao, M., Schroeder, J.P., Vellano, C.P., Cowan, D.P., Ramineni, S., Yates, C.K., Feng, Y., et al. (2010). RGS14 is a natural suppressor of both synaptic plasticity in CA2 neurons and hippocampal-based learning and memory. Proc. Natl. Acad. Sci. U.S.A. *107*, 16994–16998.

Liapis, E., Sandiford, S., Wang, Q., Gaidosh, G., Motti, D., Levay, K., and Slepak, V.Z. (2012). Subcellular localization of regulator of G protein signaling RGS7 complex in neurons and transfected cells. Journal of Neurochemistry *122*, 568–581.

Makino, E.R., Handy, J.W., Li, T., and Arshavsky, V.Y. (1999). The GTPase activating factor for transducin in rod photoreceptors is the complex between RGS9 and type 5 G protein beta subunit. Proc. Natl. Acad. Sci. U.S.A. *96*, 1947–1952.

Martemyanov, K.A., Lishko, P.V., Calero, N., Keresztes, G., Sokolov, M., Strissel, K.J., Leskov, I.B., Hopp, J.A., Kolesnikov, A.V., Chen, C.-K., et al. (2003). The DEP domain determines subcellular targeting of the GTPase activating protein RGS9 in vivo. J. Neurosci. *23*, 10175–10181.

Martemyanov, K.A., Yoo, P.J., Skiba, N.P., and Arshavsky, V.Y. (2005). R7BP, a Novel Neuronal Protein Interacting with RGS Proteins of the R7 Family. J. Biol. Chem. *280*, 5133–5136.

Masu, M., Iwakabe, H., Tagawa, Y., Miyoshi, T., Yamashita, M., Fukuda, Y., Sasaki, H., Hiroi, K., Nakamura, Y., Shigemoto, R., et al. (1995). Specific deficit of the ON response in visual transmission by targeted disruption of the mGIuR6 gene. Cell *80*, 757–765.

Masuho, I., Xie, K., and Martemyanov, K.A. (2013). Macromolecular Composition Dictates Receptor and G Protein Selectivity of Regulator of G Protein Signaling (RGS) 7 and 9-2 Protein Complexes in Living Cells. J. Biol. Chem. *288*, 25129–25142.

Mojumder, D.K., Qian, Y., and Wensel, T.G. (2009). Two R7 Regulator of G-Protein Signaling Proteins Shape Retinal Bipolar Cell Signaling. J. Neurosci. *29*, 7753–7765.

Morgans, C.W., Weiwei Liu, Wensel, T.G., Brown, R.L., Perez-Leon, J.A., Bearnot, B., and Duvoisin, R.M. (2007). Gβ5-RGS complexes co-localize with mGluR6 in retinal ON-bipolar cells. European Journal of Neuroscience *26*, 2899–2905.

Morgans, C.W., Brown, R.L., and Duvoisin, R.M. (2010). TRPM1: the endpoint of the mGluR6 signal transduction cascade in retinal ON-bipolar cells. Bioessays *32*, 609–614.

Neal, M.J., and Cunningham, J.R. (1995). Baclofen enhancement of acetylcholine release from amacrine cells in the rabbit retina by reduction of glycinergic inhibition. J. Physiol. (Lond.) *482 (Pt 2)*, 363–372.

Nishiguchi, K.M., Sandberg, M.A., Kooijman, A.C., Martemyanov, K.A., Pott, J.W.R., Hagstrom, S.A., Arshavsky, V.Y., Berson, E.L., and Dryja, T.P. (2004). Defects in RGS9 or its anchor protein R9AP in patients with slow photoreceptor deactivation. Nature *427*, 75–78.

Ogata, G., Stradleigh, T.W., Partida, G.J., and Ishida, A.T. (2012). Dopamine and full-field illumination activate D1 and D2-D5-type receptors in adult rat retinal ganglion cells. J. Comp. Neurol. *520*, 4032–4049.

Orlandi, C., Posokhova, E., Masuho, I., Ray, T.A., Hasan, N., Gregg, R.G., and Martemyanov, K.A. (2012). GPR158/179 regulate G protein signaling by controlling localization and activity of the RGS7 complexes. J. Cell Biol. *197*, 711–719.

Ostrovskaya, O., Xie, K., Masuho, I., Fajardo-Serrano, A., Lujan, R., Wickman, K., and Martemyanov, K.A. (2014). RGS7/Gβ5/R7BP complex regulates synaptic plasticity and memory by modulating hippocampal GABABR-GIRK signaling. Elife *3*, e02053.

Psifogeorgou, K., Papakosta, P., Russo, S.J., Neve, R.L., Kardassis, D., Gold, S.J., and Zachariou, V. (2007). RGS9-2 is a negative modulator of mu-opioid receptor function. J. Neurochem. *103*, 617–625.

Rao, A., Dallman, R., Henderson, S., and Chen, C.-K. (2007). Gβ5 Is Required for Normal Light Responses and Morphology of Retinal ON-Bipolar Cells. J. Neurosci. *27*, 14199–14204.

Robbins, J., Reynolds, A.M., Treseder, S., and Davies, R. (2003). Enhancement of low-voltage-activated calcium currents by group II metabotropic glutamate receptors in rat retinal ganglion cells. Mol. Cell. Neurosci. *23*, 341–350.

Ross, E.M., and Wilkie, T.M. (2000). GTPase-activating proteins for heterotrimeric G proteins: regulators of G protein signaling (RGS) and RGS-like proteins. Annu. Rev. Biochem. *69*, 795–827.

Sandiford, S.L., and Slepak, V.Z. (2009). The Gβ5−RGS7 Complex Selectively Inhibits Muscarinic M3 Receptor Signaling via the Interaction between the Third Intracellular Loop of the Receptor and the DEP Domain of RGS7†. Biochemistry *48*, 2282–2289.

Shim, H., Wang, C.-T., Chen, Y.-L., Chau, V.Q., Fu, K.G., Yang, J., McQuiston, A.R., Fisher, R.A., and Chen, C.-K. (2012). Defective Retinal Depolarizing Bipolar Cells in Regulators of G Protein Signaling (RGS) 7 and 11 Double Null Mice. J. Biol. Chem. *287*, 14873–14879.

Sjögren, B. (2011). Regulator of G protein signaling proteins as drug targets: current state and future possibilities. Adv. Pharmacol. *62*, 315–347.

Snow, B.E., Krumins, A.M., Brothers, G.M., Lee, S.-F., Wall, M.A., Chung, S., Mangion, J., Arya, S., Gilman, A.G., and Siderovski, D.P. (1998). A G protein γ subunit-like domain shared between RGS11 and other RGS proteins specifies binding to Gβ5 subunits. Proceedings of the National Academy of Sciences of the United States of America *95*, 13307.

Song, J.H., Song, H., Wensel, T.G., Sokolov, M., and Martemyanov, K.A. (2007). Localization and differential interaction of R7 RGS proteins with their membrane anchors R7BP and R9AP in neurons of vertebrate retina. Molecular and Cellular Neuroscience *35*, 311–319.

Srinivasa, S.P., Watson, N., Overton, M.C., and Blumer, K.J. (1998). Mechanism of RGS4, a GTPase-activating protein for G protein alpha subunits. J. Biol. Chem. *273*, 1529–1533.

Stewart, A., Maity, B., Wunsch, A.M., Meng, F., Wu, Q., Wemmie, J.A., and Fisher, R.A. (2014). Regulator of G-protein signaling 6 (RGS6) promotes anxiety and depression by attenuating serotonin-mediated activation of the 5-HT(1A) receptor-adenylyl cyclase axis. FASEB J. *28*, 1735–1744.

Strang, C.E., Renna, J.M., Amthor, F.R., and Keyser, K.T. (2010). Muscarinic Acetylcholine Receptor Localization and Activation Effects on Ganglion Response Properties. IOVS *51*, 2778–2789.

Terzi, D., Cao, Y., Agrimaki, I., Martemyanov, K.A., and Zachariou, V. (2011). R7BP Modulates Opiate Analgesia and Tolerance but not Withdrawal. Neuropsychopharmacology *37*, 1005–1012.

Tesmer, J.J.G., Berman, D.M., Gilman, A.G., and Sprang, S.R. (1997). Structure of RGS4 Bound to AlF4−-Activated Giα1: Stabilization of the Transition State for GTP Hydrolysis. Cell *89*, 251–261.

Witherow, D.S., Wang, Q., Levay, K., Cabrera, J.L., Chen, J., Willars, G.B., and Slepak, V.Z. (2000). Complexes of the G Protein Subunit Gβ5 with the Regulators of G Protein Signaling RGS7 and RGS9 CHARACTERIZATION IN NATIVE TISSUES AND IN TRANSFECTED CELLS. J. Biol. Chem. *275*, 24872–24880.

Wydeven, N., Posokhova, E., Xia, Z., Martemyanov, K.A., and Wickman, K. (2014). RGS6, but not RGS4, is the dominant regulator of G protein signaling (RGS) modulator of the parasympathetic regulation of mouse heart rate. J. Biol. Chem. *289*, 2440–2449.

Xie, K., Allen, K.L., Kourrich, S., Colón-Saez, J., Thomas, M.J., Wickman, K., and Martemyanov, K.A. (2010). Gbeta5 recruits R7 RGS proteins to GIRK channels to regulate the timing of neuronal inhibitory signaling. Nat. Neurosci. *13*, 661–663.

Yu, J., Daniels, B.A., and Baldridge, W.H. (2009). Slow Excitation of Cultured Rat Retinal Ganglion Cells by Activating Group I Metabotropic Glutamate Receptors. J Neurophysiol *102*, 3728–3739.

Zachariou, V., Georgescu, D., Sanchez, N., Rahman, Z., DiLeone, R., Berton, O., Neve, R.L., Sim-Selley, L.J., Selley, D.E., Gold, S.J., et al. (2003). Essential role for RGS9 in opiate action. PNAS *100*, 13656–13661.

Zhou, H., Chisari, M., Raehal, K.M., Kaltenbronn, K.M., Bohn, L.M., Mennerick, S.J., and Blumer, K.J. (2012). GIRK channel modulation by assembly with allosterically regulated RGS proteins. PNAS.

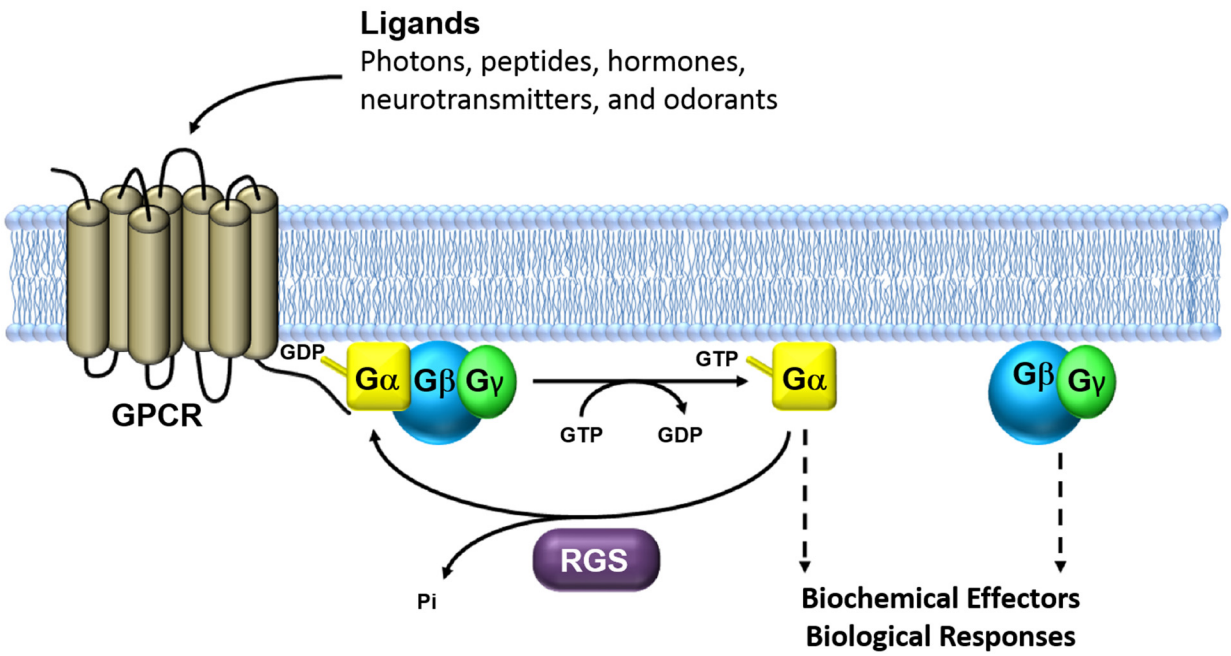

Figure 1. G Protein Cycle

GPCRs promote the exchange of GDP-bound Gα to GTP-bound Gα. GTP-bound Gα dissociates from Gβγ, enabling coupling to biochemical effectors. RGS proteins act as GTPase activating proteins (GAPs) promoting GTP hydrolysis.

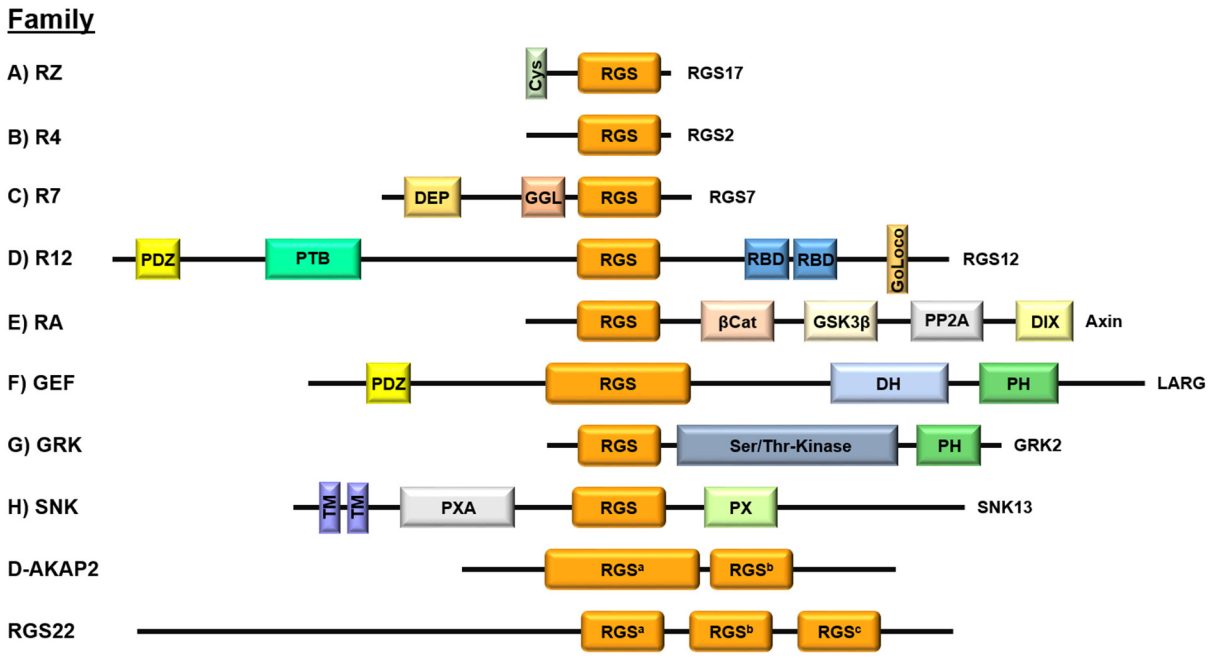

Figure 2. RGS Superfamily

All RGS proteins contain a RGS domain. RGS proteins are divided into families based on their Gα preference and accessory domain structure. Modified from (Siderovski and Willard, 2005).

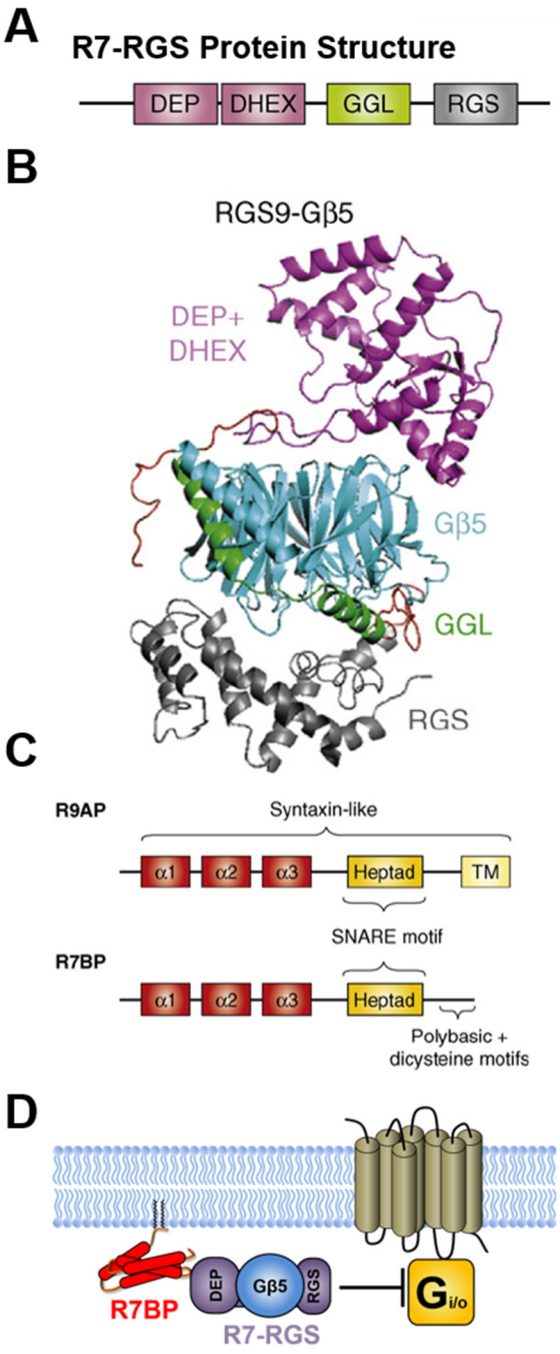

Figure 3. R7-RGS complexes act as GAPs for Gi/o.

A. Domain organization of R7-RGS proteins. R7-RGS family members have a conserved structure consisting C-terminal RGS domain, which is necessary and sufficient for GAP activity, and N-terminal DEP, DHEX/R7H, and GGL domains.

B. Crystal structure of RGS9-Gβ5 dimer. DEP+DHEX domain (purple), GGL domain (green), RGS domain (gray), and Gβ5 (cyan) Modified from (Cheever et al., 2008)

C. Syntaxin-like domain organization of R9AP and R7BP with conserved trihelical region (red), heptad/SNARE motif (orange), and C-terminal membrane targeting domain. R9AP C-terminal domain (yellow) is a transmembrane segment. R7BP C-terminus contains a palmitoylation signal.

D. R7BP interacts with R7-RGS DEP domain. R7-RGS complexes act as GAPs for Gi/o. Modified from (Jayaraman et al., 2009).

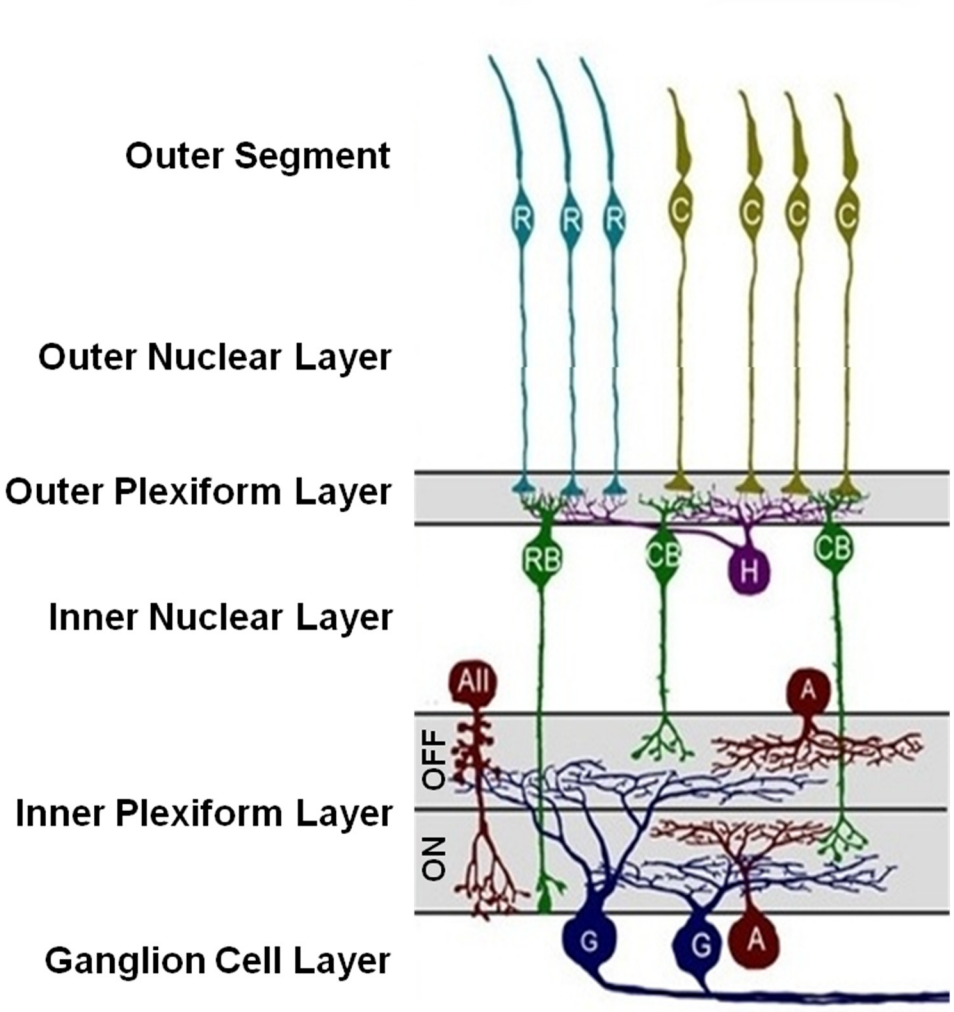

Figure 4. Diagram of mammalian retina

Laminated structure of the mammalian retina. The vertical pathway of the retina is glutamatergic. This pathway is composed of photoreceptors, rod (R) and cones (C), rod (RB) and cone (CB) bipolar cells and retinal ganglion cells (G). Horizontal (H) and amacrine (A) cells are interneurons that primarily release inhibitory neurotransmitters, GABA and glycine. Modified from (Webvision, 1995)

Chapter 2:

An allosteric regulator of R7-RGS proteins influences light-evoked activity and glutamatergic waves in the inner retina

Published in altered form as: PLoS ONE 8(12): e82276

Acknowledgements:

Ken Blumer conceived the project of studying the retina of R7BP$^{-/-}$ mice. Ken also was instrumental in helping establish the many collaborations that are represented in this work. Kevin Kaltenbronn designed the targeting constructs for generating R7BP$^{-/-}$ mice and was responsible for initial backcrossing and diligent colony management. ES cells were provided and injected into C57BL/6 mouse blastocysts by Washington University Murine Embryonic Stem Cell Core and Washington University's Pathology Microinjection Core Facility, respectively. Susan Culican and Bradly Vo were also critical to the initiation of the projection. Susan and Bradly performed preliminary anterograde labeling of R7BP$^{-/-}$ retinogeniculate projections that is not reported here but that motivated much of the work presented in this chapter. Stacey Peek performed anterograde labeling for experiments presented herein by performing intraocular injections and brain isolations. I processed brain slices and performed analysis. Susan and Rachel Lamb also assisted with training and coordination with Culican lab.

Daniel Kerschensteiner and the members of the Kerschensteiner lab were very helpful in providing advice, training, and discussion. Specifically, they provided instruction for retinal dissection, confocal microscopy, and MEA protocols. Daniel additionally contributed to the design and analysis of MEA experiments. I isolated retinas, performed MEA recordings, and sorted data.

Vladimir Kefalov and Sasha Kolesnikov contributed to the optomotor experiments. Specifically, Sasha trained me for the OptoMotry system and performed characterization of R7BP$^{-/-}$ optomotor responses. I performed characterization of Gβ5$^{-/-}$ mice with additional coordination with Kefalov lab.

ERG recordings were performed in collaboration with Anne Hennig and Peter Lukasiewicz. Anne performed R7BP ERG recordings and I performed analysis.

Robert Barlow, Yumiko Umino, and Eduardo Solessio (*SUNY* Upstate Medical University) helped me troubleshoot and calibrate the OptoMotry system.

Dennis Oakley (Bakewell Center) trained me for use of the FV500 confocal microscopes.

Gongfu Zhou (Siteman Cancer Center Biostatistics Core) assisted by developing and performing statistical analysis of MEA data.

I would like to thank members of the Blumer and Kerschensteiner labs for helpful advice and discussion.

This work was supported by grants from the National Institutes of Health (GM44592 and HL075632 (K.J.B), EY021855 (DK), EY019312 (VJK), EY016336 (SMC), and EY02687 (Department of Ophthalmology and Visual Sciences, Washington University) and from Research to Prevent Blindness, Inc. (DOVS). SMC and DK also received funding from the following foundations: Horncrest Foundation (S.M.C.), Hope for Vision Foundation, Edward Mallinckrodt Jr. Foundation, Alfred P. Sloan Foundation, and Whitehall Foundation (DK). During this work I was supported by predoctoral training grants from the NIH (GM 007067 and T32-EY013360).

Abstract

In the outer retina, G protein-coupled receptor (GPCR) signaling mediates phototransduction and synaptic transmission between photoreceptors and ON bipolar cells. In contrast, the functions of modulatory GPCR signaling networks in the inner retina are less well understood. We addressed this question by determining the consequences of augmenting modulatory Gi/o signaling driven by endogenous transmitters. This was done by analyzing the effects of genetically ablating the R7 RGS-binding protein (R7BP), a membrane-targeting protein and positive allosteric modulator of R7-RGS (regulator of the G protein signaling 7) family that deactivates Gi/oα subunits. We found that R7BP is expressed highly in starburst amacrine cells and retinal ganglion cells (RGCs). As indicated by electroretinography and multielectrode array recordings of adult retina, ablation of R7BP preserved outer retina function, but altered the firing rate and latency of ON RGCs driven by rods and cones but not rods alone. In developing retina, R7BP ablation increased the burst duration of glutamatergic waves whereas cholinergic waves were unaffected. This effect on glutamatergic waves did not result in impaired segregation of RGC projections to eye-specific domains of the dorsal lateral geniculate nucleus. R7BP knockout mice exhibited normal spatial contrast sensitivity and visual acuity as assessed by optomotor reflexes. Taken together these findings indicate that R7BP-dependent regulation of R7-RGS proteins shapes specific aspects of light-evoked and spontaneous activity of RGCs in mature and developing retina.

Introduction

Signal transduction by G protein-coupled receptors (GPCRs) in the outer retina converts visual stimulation ultimately to patterns of activity of retinal ganglion cells (RGCs). Visual opsins trigger light-evoked activation of transducin, and Go-coupled type 6 metabotropic glutamate receptors (mGluR6) regulate transmitter release by ON bipolar cells (Dhingra et al., 2000b; Masu et al., 1995). Gi/o-coupled receptors potentially modulate synaptic transmission in mature (Clark et al., 2009; Gleason, 2012; Huang et al., 2013; Jensen and Daw, 1986; Kothmann et al., 2009) and developing (Catsicas and Mobbs, 2001; Stellwagen et al., 1999; Syed et al., 2004) retina. However, the diversity of these modulatory GPCRs has impeded progress toward understanding their functions in the inner retina.

Functions of specific G protein signaling networks in the retina recently have been probed by studying the consequences of augmenting signaling evoked by light or endogenous neurotransmitters. This approach has utilized mice lacking one or more members of the R7-RGS (regulators of G protein signaling) family (RGS6, 7, 9, 11), which accelerate G protein deactivation by functioning as GTPase-activating proteins (GAPs) specific for Gi/oα subunits (Hooks et al., 2003). Each R7-RGS isoform forms an obligate heterodimer with Gβ5 (Snow et al., 1998; Witherow et al., 2000) to regulate Gi/o signaling (Garzón et al., 2005; Hooks et al., 2003; Xie et al., 2010, 2012; Zhou et al., 2012b) and has a distinct retinal expression pattern (Liapis et al., 2012; Morgans et al., 2007; Song et al., 2007). RGS9 is expressed in photoreceptor disk membranes where it deactivates transducin (Cowan et al., 1998; He et al., 1998). RGS7 and 11 are expressed in ON bipolar cells and deactivate Goα, thereby facilitating light-evoked depolarization (Cao et al., 2012; Chen et al., 2010; Mojumder et al., 2009; Rao et al., 2007; Shim et al., 2012; Zhang et al., 2010). RGS6 and 7 are expressed in the inner retina

(Liapis et al., 2012; Song et al., 2007; Witherow et al., 2000), suggesting that further studies of the R7-RGS family may reveal new functions for Gi/o signaling in retina.

Because the absence of RGS7 and RGS11 or the entire R7-RGS family disorganizes dendritic arborization of ON bipolar cells (Rao et al., 2007; Shim et al., 2012), these mutants are ill-suited to assess whether light-evoked responses in the inner retina are affected by augmenting Gi/o signaling. As an alternative, we hypothesized that R7-RGS function in the retina would be impaired rather than lost completely by disrupting R7 RGS-binding protein (R7BP), a palmitoylated SNARE-like protein that functions as a positive allosteric regulator of R7-RGS/Gβ5 heterodimers (Anderson et al., 2007b; Drenan et al., 2005, 2006; Jia et al., 2011; Martemyanov et al., 2005; Narayanan et al., 2007; Song et al., 2006; Zhou et al., 2012b). R7BP is highly expressed in the inner retina (Cao et al., 2008). It augments R7-RGS GAP activity (Drenan et al., 2006; Masuho et al., 2013), enables RGS7 regulation of Giα (Masuho et al., 2013), and facilitates recruitment of R7-RGS/Gβ5 complexes to GIRK channels (Zhou et al., 2012b). However, R7BP ablation does not perturb outer retina organization, rod-driven activity, membrane association of RGS7, or protein expression of RGS6, RGS7, or RGS11 in the retina (Cao et al., 2008). Therefore, ablation of R7BP may impair rather than eliminate activity of the R7-RGS protein family and modestly augment Gi/o signaling evoked by endogenous GPCR agonists in the inner retina.

Here we identify cell types in the inner retina that express R7BP and analyze the consequences of R7BP ablation. Our results provide evidence indicating that regulation of R7-

RGS proteins by R7BP shapes specific aspects of light-evoked and spontaneous wave activity in the inner retina.

Results

R7BP is expressed highly in starburst amacrine cells and retinal ganglion cells.

To investigate roles of Gi/o signaling regulated by R7-RGS/Gβ5 complexes under the control of R7BP, we first identified retinal cell types that express R7BP by probing vertical retinal slices of adult mice with affinity-purified polyclonal R7BP antibodies (Grabowska et al., 2008). Specific R7BP staining was expressed weakly in the outer plexiform layer (OPL) with stronger expression throughout the inner plexiform layer (IPL), especially in the S2 (OFF) and S4 (ON) sublaminae of the IPL, and in somata of the inner nuclear and ganglion cell layers (INL and GCL) (Figure 2A). No specific staining above background was observed in $R7BP^{-/-}$ retinas, demonstrating antibody specificity (Figure 2B). Several results indicated that nearly all starburst amacrine cells (SACs) express R7BP. First, co-staining of R7BP and choline acetyltransferase (ChAT, a marker of SACs) was evident in S2 and S4, indicating the presence of R7BP in SAC processes. Second, R7BP also was expressed strongly on the somatic plasma membrane of most ChAT-positive cells in the INL (92% ± 2%, n=3 retinas; Figure 2C, indicated by arrowheads) and a majority of displaced SACs (52% ± 1%) in the GCL. R7BP in the GCL also was detected on the somatic plasma membrane of some ChAT-negative cells (asterisks, Figure 2C). This suggests that R7BP is expressed in other cell types in the inner retina and is consistent with expression in other sublaminae of the IPL. Many of these ChAT-negative neurons were retinal ganglion cells (RGCs; 49% ± 3%; n=3 retinas) as indicated by co-staining with Brn3a (an RGC marker; arrowheads in Figure 2D) (Nadal-Nicolás et al., 2009). Thus, the overall pattern of R7BP expression in retina is similar to the aggregate expression of RGS6, 7, and 11 (Cao et al., 2008; Liapis et al., 2012; Song et al., 2007), supporting the notion that R7BP regulates the function of one or more of these R7-RGS proteins in the inner retina.

Next, we determined the expression pattern of R7BP during postnatal retinal development. This was examined because in brain the expression of R7BP/R7-RGS/Gβ5 complexes is induced postnatally during synaptic refinement (Anderson et al., 2007c; Grabowska et al., 2008) and because R7-RGS/Gβ5 heterodimers are required for normal development and dendritic organization in cerebellum, hippocampus, and retina (Rao et al., 2007; Shim et al., 2012; Zhang et al., 2011). At P8, we detected specific R7BP staining in the IPL but not in the INL or GCL (Figure 3). At P12, R7BP staining in the IPL and S2/S4 was more intense, and became detectable in the OPL, INL and GCL. An adult pattern of R7BP expression was evident at P30. Thus, R7BP is expressed before photoreceptors mature and is refined as retinal development is completed.

R7BP ablation does not disrupt outer retina function.

Previous investigations have shown that R7BP$^{-/-}$ mice exhibit normal retinal morphology and rod-driven light responses of ON bipolar cells (Cao et al., 2008). To determine whether R7BP ablation affects rod- or cone-driven responses over a full range of stimulus intensities, we performed electroretinography of dark-adapted (Figure 4A) and light-adapted mice (Figure 4F). In dark-adapted WT and R7BP$^{-/-}$ mice (n=5), we observed no difference in a-wave amplitude or latency corresponding to light-evoked hyperpolarization of rods (low light intensities) or rods and cones (higher intensities) (Figure 4B/C). The ERG b-wave, which primarily reports depolarization of ON-bipolar cells, exhibited a trend in R7BP$^{-/-}$ mice toward increased amplitude upon rod-specific stimulation but failed to reach the threshold for significance (Figure 4D). B-wave latency (time to b-wave peak after flash) was unaffected by the absence of R7BP (Figure

4E). Photopic (cone-specific) responses revealed by constant background illumination and high intensity flashes revealed no change in b-wave amplitude or latency (Figure 4G/H). Therefore, R7BP ablation had no significant effect on light-evoked responses in outer retina.

R7BP ablation affects the firing rate and latency of ON RGCs driven by rods and cones but not by rods alone.

Having shown that outer retina function is essentially preserved in R7BP$^{-/-}$ mice, we then analyzed inner retina function by performing multielectrode array (MEA) recordings of RGC activity. In dark-adapted retina (P20) we measured mean spike rates and latencies (time between flash and peak RGC firing rate) of transient ON RGCs under full field illumination at scotopic and mesopic intensities (5 and 200 Rh*/rod/sec, respectively). Under scotopic illumination, the absence of R7BP did not affect transient ON RGC mean spike rate (WT: 53±2 Hz, R7BP$^{-/-}$: 54±2 Hz; mean±SEM, WT: n=94, R7BP$^{-/-}$: n=150, Figure 5A) or latency (WT: 0.21±0.01 msec, R7BP$^{-/-}$: 0.21±0.01 msec, Figure 5B). In contrast, mesopic illumination of rods and cones indicated that transient ON RGCs in R7BP$^{-/-}$ retinas exhibited slower firing rates (WT: 59±3 Hz, R7BP$^{-/-}$: 50±2 Hz, $p<0.04$; Figure 5C) and longer latency (WT: 0.14±0.01 msec, R7BP$^{-/-}$: 0.19±0.02 msec, $p<0.03$, Figure 5D). R7BP ablation therefore affected light response of ON RGCs driven by mesopic but not scotopic illumination.

To characterize RGC light responses further we presented checkerboard Gaussian white noise illumination and calculated spike-triggered average (STA) stimuli through correlation of RGC spike trains to the patterns of light squares that evoked the spikes (see Methods for further description). Representative ON biphasic STAs are shown in Figure 5E (WT: n=58, R7BP$^{-/-}$:

n=63). The average size of WT and R7BP$^{-/-}$ RGCs receptive fields were calculated as a two-dimensional Gaussian fit of the spatial profile (Figure 5E, insets) at the STA temporal maximum (peak contrast, asterisks). This analysis indicated that time to peak (difference between STA temporal maximum and spike; WT: 120±3 msec, R7BP$^{-/-}$: 110±1 msec; mean±SEM; Figure 5F) and the average receptive field radius (WT: 110±3 μm; R7BP$^{-/-}$: 110±2 μm; Figure 5G) of WT and R7BP$^{-/-}$ ON RGCs were similar. Thus, whereas R7BP ablation did not affect the average size of ON RGC receptive fields, it did affect the light-evoked firing rate and latency of ON RGCs in response to full-field flashes.

R7BP ablation alters the burst duration of glutamatergic waves in developing retina.

Several considerations prompted us to investigate whether R7BP ablation affects spontaneous activity exhibited as propagating waves of correlated, high intensity firing of neighboring RGCs in developing retina (reviewed in (Torborg and Feller, 2005)). In P0-P10 murine retina, cholinergic waves driven by acetylcholine release from SACs activate nicotinic acetylcholine receptors (nAChRs) on RGCs (Bansal et al., 2000). From P11 to ~P16, cholinergic waves are replaced by glutamatergic waves in which ionotropic glutamate receptors on RGCs are stimulated by glutamate release from bipolar cells. Whether Gi/o-coupled receptor signaling regulated by R7-RGS proteins affects cholinergic or glutamatergic waves has not been investigated.

To address this question we used MEA recordings to analyze spontaneous waves in developing WT and R7BP$^{-/-}$ retinas. Because R7BP is not expressed detectably in the retina until ~P8, we analyzed spontaneous RGC activity in dark-adapted P8-9 and P12-13 retinas to examine

cholinergic and glutamatergic waves, respectively. Several properties of spontaneous waves were measured, including firing rate, burst duration, interwave interval, and correlation indices. At P8-9, both WT and R7BP$^{-/-}$ retinas exhibited correlated periodic bursting similar to previous descriptions of cholinergic waves (Demas et al., 2003). Characteristic of glutamatergic waves, bursting at P12-13 in both WT and R7BP$^{-/-}$ occurred more frequently and with shorter duration than at P8-9 (Figure 6A/C, Table 1). Thus, R7BP ablation apparently did not preclude transition between these two stages of waves. Furthermore, R7BP ablation did not affect cholinergic wave characteristics (Figure 6B, Table 1). Similarly, the correlation indices, spike rate, and interwave interval within glutamatergic waves were unaffected (Figure 6D, Table 1). However, burst duration of glutamatergic waves was longer in R7BP$^{-/-}$ retina (WT: 0.41±0.01 sec, R7BP$^{-/-}$: 0.55±0.02 sec, $p<0.03$, Figure 6E). Thus, R7BP-dependent regulation of R7-RGS proteins modulates distinct aspects of glutamatergic but not cholinergic waves in developing retina.

R7BP ablation does not impair segregation of retinogeniculate projections.

Retinal waves play important roles in organizing axonal projections of RGCs that innervate eye-specific domains of the dorsal lateral geniculate nucleus (dLGN) of the thalamus (reviewed in (Huberman et al., 2008; Torborg and Feller, 2005)). While it seemed unlikely that the modest change in glutamatergic wave burst duration observed in R7BP$^{-/-}$ retina would be sufficient to impair retinogeniculate segregation, we wanted to confirm segregation was intact.

To determine whether R7BP deficiency affects segregation of RGC projections into eye-specific domains in the dLGN, we injected Alexa 555 or Alexa 647 dye-conjugated cholera toxin B (CTB) as anterograde tracers into opposite eyes of WT and R7BP$^{-/-}$ mice. Representative

images of retinogeniculate labeling of the dLGN in WT and R7BP$^{-/-}$ are shown in Figure 7A/B. Images quantified by analyzing variance of R-values (log_{10} ratio of ipsilateral and contralateral fluorescence signals on a pixel by pixel basis) revealed no detectable difference in retinogeniculate segregation in R7BP$^{-/-}$ and WT littermates (Figure 7D). Similarly, areas occupied by contralateral, ipsilateral, or both projections were indistinguishable between WT and R7BP$^{-/-}$ animals (Figure 7D). Thus, R7BP ablation was insufficient to disrupt retinogeniculate segregation.

R7BP $^{-/-}$ mice exhibit normal spatial contrast sensitivity and visual acuity.

To assess whether R7BP ablation affects overall visual perception, we evaluated optomotor responses as a means of determining visual acuity and contrast sensitivity under scotopic (-4.5 log cd/m^2) and photopic (1.8 log cd/m^2) conditions (Figure 8) (Prusky et al., 2004). Results indicated that visual acuity in WT and R7BP$^{-/-}$ mice (n=5) was similar under both scotopic (WT: 0.34±0.03 cyc/deg, R7BP$^{-/-}$: 0.35±0.03 cyc/deg; mean±SEM) and photopic illumination (WT: 0.54±0.02 cyc/deg, R7BP$^{-/-}$: 0.50±0.04 cyc/deg). Similarly, no difference in contrast sensitivity was observed under scotopic (WT: 9.2±1.2, R7BP$^{-/-}$: 11±2.8) or photopic illumination (WT: 48±6, R7BP$^{-/-}$: 46±7). Thus, although R7BP deficiency affects light response of RGCs, it did not affect aspects of spatial vision required for normal optomotor reflexes.

Discussion

Our analysis of R7BP$^{-/-}$ mice indicates that Gi/o signaling evoked by endogenous transmitters and regulated by R7-RGS proteins modulates RGC activity in mature and developing inner retina. In mature retina, R7BP ablation had a modest but significant effect on mesopic transient ON RGC light responses, slowing the firing rate and increasing the latency, whereas ON RGC activity under scotopic illumination was unaffected. As R7BP is expressed most highly in inner retina and R7BP$^{-/-}$ mice exhibit relatively normal outer retina structure (Cao et al., 2008) and function, these phenotypes apparently are consequences of inner retina dysfunction. Whether R7BP is functioning postsynaptically in RGCs or presynaptically in amacrine cells is unclear, as both cell types express R7BP. However, the effects of R7BP on light responses are consistent with evidence that RGC hyperpolarization can be regulated by activation of Gi/o-coupled receptors in either cell type. Indeed, activation of Gi/o-coupled A1 adenosine receptors can reduce RGC spiking by activating G-protein-coupled inwardly rectifying K^+ (GIRK) and small conductance Ca^{2+}-activated K^+ (SK) channels (Clark et al., 2009). Alternatively, activation of Gi/o-coupled group III mGluRs increases GABA release from amacrine cells and inhibitory drive experienced by RGCs (Guimarães-Souza and Calaza, 2012).

In developing retina, ablation of R7BP increased the burst duration of RGCs driven by glutamatergic waves. This effect was specific for glutamatergic waves because loss of R7BP had no significant effect on cholinergic waves, consistent with low level expression of R7BP in the IPL and SACs at this stage of development (P8-9). The effect of R7BP ablation on glutamatergic wave burst duration in RGCs provides the first indication that regulation of Gi/o signaling by R7-RGS proteins modulates glutamatergic wave dynamics. Previous studies have

identified corresponding roles for R7-RGS complexes in the developing nervous system, including ON BPC synapse formation (Rao et al., 2007; Shim et al., 2012) and cerebral and hippocampal development (Zhang et al., 2011).

Ultimately, these effects of R7BP ablation on ON RGC light response and glutamatergic waves were modest and insufficient to affect downstream processes including spatial vision and retinogeniculate segregation. Because R7BP deficiency apparently results in modest impairment of R7-RGS-mediated regulation of Gi/o signaling in inner retina, it may be necessary to eliminate R7-RGS proteins in inner retinal cell types to elicit pronounced phenotypes. This approach may reveal how augmented Gi/o signaling affects inner retina development and function. Studies of R7-RGS isoforms in SACs may be of particular interest because Gi/o-coupled receptors modulate SAC neurotransmitter release to control direction-selective (DS) circuits (Jensen, 2006; Taylor and Smith, 2012).

Material and Methods

Animals

All animal procedures used protocols approved by the Washington University Animal Studies Committee (Protocol #20110184 and #20140036). $R7BP^{-/-}$ mice produced by targeted deletion of exon 2 have been described previously (Zhou et al., 2012b). Targeting strategy of the R7BP locus, characterization of nonconditional ($R7BP^{-}$) and conditional ($R7BP^{fl}$) knockout alleles are depicted in Figure 1. $R7BP^{+/-}$ mice were crossed six generations into the C57BL/6 background (Charles River Laboratories) and then interbred to produce WT and $R7BP^{-/-}$ littermates of either sex for analysis.

Tissue preparation and immunostaining

Mice were euthanized by CO_2 asphyxiation followed by cervical dislocation. Enucleated eyes were fixed with paraformaldehyde (4%) in PBS (pH 7.4). Retinas were isolated in PBS and embedded in 4% low-melting point agarose. For fixation of brain, euthanized mice were perfused intracardially with PBS followed by paraformaldehyde (4%) in PBS. Brains were removed and post-fixed overnight at 4 ºC. Vertical retina and coronal brain slices were cut (60 μm and 100 μm, respectively) with a vibratome. Slices were blocked with 10% normal horse serum (NHS) in PBS and incubated with primary antibodies overnight in 5% NHS and 0.05% Triton X-100 (Sigma-Aldrich). The following antibodies were used: affinity purified rabbit anti-R7BP (Grabowska et al., 2008), goat anti-ChAT (#AB143 Millipore; 1:100), goat anti-Brn3a (C20 Santa Cruz; 1:500), Alexa Fluor 568-conjugated anti-rabbit and Alexa Fluor 488-conjugated anti-goat (Invitrogen; 1:1000) antibodies. Slices were mounted using VectaShield (Vector Labs) and imaged with Olympus FluoView FV500 (Bakewell NeuroImaging

Laboratory, WUSM). Retinal immunofluorographs were median filtered (1 pixel surround) using NIH Fiji (Schindelin et al., 2012).

Electroretinography

Flash ERG measurements were performed with a UTAS-E3000 visual Electrodiagnostic System running EM for Windows (LKC Technologies). Mice (~3 months old) were dark-adapted overnight. Under dim red illumination, mice were anesthetized with a cocktail of 80 mg/kg ketamine and 15 mg/kg xylazine. The body temperature of the mice was maintained at 37 ^{o}C with a heating pad controlled by a rectal temperature probe. After positioning mice in the Ganzfeld dome, the recording electrodes (2.0 mm diameter platinum loops) were positioned on the corneal surface of each eye in a drop of 0.5% atropine sulfate (Bausch & Lomb) and 1.25% hydroxypropol methylcellulose (GONAK; Akorn Inc.). Reference and ground electrodes were placed at the vertex of the skull and back, respectively. For dark-adapted analysis, we recorded the responses to white light flashes of increasing intensity (-4.6 to 1.9 log cd s/m^2) in total darkness. Mice were then light-adapted to a constant white background illumination of 2.3 log cd s/m^2 for 10 min. Light-adapted responses to a series of light flashes (-0.01 to 2.67 log cd s/m^2) were obtained in the presence of constant background illumination. At each intensity, responses to multiple trials were averaged. The a- and b-wave amplitude and latency were measured and quantified for comparison.

Multielectrode array recordings of RGC activity

Mice were dark-adapted for at least 1 h prior to CO_2 asphyxiation. For light-evoked recordings, eyes were enucleated and retinas were isolated under IR illumination. For

spontaneous activity recordings, this step was performed under dim red illumination. During dissection, isolated retinas were maintained in cooled murine artificial cerebral spinal fluid (mACSF) (125 mM NaCl, 2.5 mM KCl, 1 mM $MgCl_2$, 1.25 mM NaH_2PO_4-H_2O, 20 mM glucose, 26 mM $NaHCO_3$, 2 mM $CaCl_2$) oxygenated with 95% O_2, 5% CO_2. Isolated retinas were placed ganglion cell layer down on a multi-electrode array (MEA), consisting of 252 electrodes at 100 μm spacing (MultiChannel Systems). To prevent movement of the retina, a transparent cell culture membrane (Corning) was placed over the retina and secured under a platinum ring. Retinas were allowed to equilibrate for 45-60 min before recording. While recording, retinas were superfused with oxygenated mACSF (30 ºC) at a rate of 1-1.5 mL/min.

Visual stimulation

Stimuli were generated using an organic light emitting display (OLED) mounted in place of the condenser of an inverted light microscope (10x objective). Stimulation protocols were programmed using Matlab (Mathworks). Full field illumination (4 sec) was attenuated to 5 or 200 Rh*/rod/sec by neutral density filters placed between the display and objective. For checkerboard Gaussian white noise stimulation, the field was divided into squares (66 μm sides) and the intensity of the squares was chosen at random from Gaussian distribution with a constant mean and standard deviation at 40 msec intervals.

Analysis of RGC light responses

Because MEA electrodes can record spikes from multiple RGCs, we used principal component analysis of waveforms (Offline Sorter, Plexon) to assign spike trains to individual RGCs. Individual RGCs were selected as those exhibiting spike trains in which less than 0.2%

of interspike intervals were less than 2 msec. This analysis was restricted to transient ON RGCs. Firing rate was calculated by quantifying the number of spikes during illumination (5 sec bin). Latency was calculated as the time to reach maximum firing rate. To study RGC space-time receptive fields, we generated and analyzed spike-trigger averages (STA), as described in detail previously (Chichilnisky, 2001). For STA analysis, retinas were stimulated with a Gaussian white noise checkerbox sequence. STA stimuli were the averages of the stimulus sequences (500 msec) preceding each spike for a given RGC. Because the quality of STAs depends on the number of spikes used to generated them, only RGCs with a robust total number of spikes were included for analysis (average number of spikes: WT: 4700±650, R7BP$^{-/-}$: 4700±630). The temporal structure of the receptive field response was calculated from the average of the stimulus squares that have a standard deviation (SD) three-fold greater than the SD of background squares. Receptive fields were estimated as the radius of a 1-SD ellipse from a two-dimension Gaussian fit of the spatial profile at the STA temporal maximum. The radius of the receptive field was calculated as: $r=\sqrt{r_{maj}r_{min}}$, where r_{maj} and r_{min} are the major and minor axes. Time to peak was calculated as the time between maximum STA contrast and the spike.

Analysis of RGC spontaneous wave activity

For recording of spontaneous waves, retinas were maintained in complete darkness for a recording period of 45 min. Individual RGCs were sorted as described above. Firing rate of RGCs was calculated as number of spikes at 5 sec bins. Burst duration was estimated by the width at half-maximum of a RGC's spike train autocorrelogram. Interwave interval was calculated as the average time between peaks in the population firing rate. To identify peaks, the firing rates of all RGCs from a retina were averaged and smoothed using an exponential filter:

$y(t) = \alpha$ x $y(t-1) + (1-\alpha)$ x $x(t)$, where α is the degree of smoothing (0.9), $x(t)$ is the mean firing rate, $y(t)$ is the smoothed version. The running average of the firing rate, calculated using a Loess filter (f = 0.67) multiplied by 1.5, was used as a threshold. Peaks were defined as the maximum point between two successive crossings of this threshold. Correlation indices were calculated as describe previously (Wong et al., 1993): $CI_{XY} = [N_{XY}(-\Delta t, +\Delta t)$ x $T] / [N_{X(O,T)}$ x $N_{Y(O,T)}$ x $2\Delta t]$ where N_{XY} is the number of spikes cell Y fired within ± Δt (0.1 sec) from spikes in cell X. T is the duration of the recording. $N_{X(O,T)}$ and $N_{Y(O,T)}$ are the total number spikes from cells X and Y, respectively.

Anterograde labeling and analysis of retinogeniculate projections

Alexa Fluor-647 or Alexa Fluor-555 dye-conjugated cholera toxin B subunit (CTB) (1-2 µL, 2 mg/mL, Invitrogen) was injected intravitreally into opposite eyes of anesthetized P19 mice with a Picospritzer III (Parker). After 2 days, mice were euthanized and perfused, and brain slices were prepared as described above. Coronal brain slices (80 µm) were mounted and imaged at 10x magnification. Retinogeniculate segregation was quantified as described previously (Torborg and Feller, 2004). Briefly, images were background subtracted using rolling ball subtraction (200 pixels) and the area surrounding the dLGN was masked. R-values for each pixel were calculated in Matlab Software (MathWorks) as $R = \mathrm{Log}_{10}(Fi/Fc)$, where Fi and Fc are the fluorescence of ipsilateral and contralateral channels, respectively. As a measure of segregation, the variance of R-values for the center four slices of each dLGN were averaged. To determine the area of contralateral and ipsilateral projections, background subtracted and masked images were thresholded (10%) and binarized. The total area of dLGN was set as the area of the dLGN mask and quantified using NIH Fiji, and the number of thresholded pixels for

contralateral and ipsilateral projections were quantified and expressed as percentage of the total dLGN area. For area of overlap, thresholded images were merged. Merged pixels were isolated using NIH Fiji (RG2B Colocalization) and quantified as described above.

Spatial vision measured by optomotor reflexes

For testing spatial vision, we measured optomotor responses in WT and R7BP$^{-/-}$ mice (~3 months old) using the OptoMotry virtual optomotor system (Cerebral Mechanics) (Prusky et al., 2004), which utilizes a reflex in which mice move their heads to track a moving vertical sine wave grating. Mice were placed on a pedestal surrounded by computer monitors that displayed the grating and monitored with a video camera under normal or IR illumination. Stimuli were presented for a period of 5 sec before returning to 50% gray illumination. The protocol implemented a two-alternative, forced choice method in which the observer was blind to the direction of rotation of the grating and was forced to identify the direction based on the mouse's observed head movement (Umino et al., 2006). A staircase paradigm was used for assessing contrast and spatial frequency thresholds, defined as a correct observer response of 70%. For determining contrast sensitivity, testing was performed under optimal tuning conditions in which spatial and temporal frequencies were set at 0.128 cyc/deg and 0.75 Hz, respectively (Umino et al., 2008). Contrast sensitivity was defined as the inverse of the contrast at threshold (Prusky et al., 2004). For testing visual acuity, contrast (100%) and speed (5.4 deg/s) were kept constant, while spatial frequency was gradually increased. Visual acuity was defined as the spatial frequency at threshold. During testing, the observer was blind to the genotype of the animal. For scotopic (-4.5 log cd/m^2) testing, mice were dark-adapted overnight and neutral density film filters were placed between mice and the computer monitors. For photopic (1.8 log cd/m^2)

testing, mice were light adapted, and the acuity and contrast sensitivity examinations were repeated without filters.

Statistics

Statistical analysis of electroretinograms was performed using repeated measures ANOVA, followed by Bonferroni's (Dunn) post-test. Significance was determined before Bonferroni. Analysis of MEA data implemented a linear/generalized linear mixed model framework. This framework allows analysis of data from individual neurons, while still accounting for the correlated nature of the activity of neurons recorded from the same retina and during correlated wave activity. Because each type of data obtained from MEA experiments exhibited different statistical distributions, we determined which type of statistical distribution for the random error in the linear/generalized linear mixed model best fit the data. RGC receptive field radius was analyzed using linear mixed model with normally distributed random error. Light-evoked and wave spike rate and wave burst duration were analyzed similarly after log transformation. Log transformation did not result in a normal distribution of data measuring latency, STA time-to-peak, or interwave interval. In these cases, a generalized linear mixed model was performed, the random error had a gamma distribution for latency measurements and a negative binomial distribution for STA-time-to-peak and interwave interval measurements. Model assumptions were examined by residual plots and other model diagnostics. Homogeneity within retinas from the same genotype was assessed by intra-class correlation coefficient analysis. Student's t-test was used to determine significance of the optomotor response and retinogeniculate segregation data. Statistical significance was defined as $p<0.05$.

References

Anderson, G.R., Semenov, A., Song, J.H., and Martemyanov, K.A. (2007a). The Membrane Anchor R7BP Controls the Proteolytic Stability of the Striatal Specific RGS Protein, RGS9-2. J. Biol. Chem. *282*, 4772–4781.

Anderson, G.R., Lujan, R., Semenov, A., Pravetoni, M., Posokhova, E.N., Song, J.H., Uversky, V., Chen, C.-K., Wickman, K., and Martemyanov, K.A. (2007b). Expression and Localization of RGS9-2/Gβ5/R7BP Complex In Vivo Is Set by Dynamic Control of Its Constitutive Degradation by Cellular Cysteine Proteases. J. Neurosci. *27*, 14117–14127.

Bansal, A., Singer, J.H., Hwang, B.J., Xu, W., Beaudet, A., and Feller, M.B. (2000). Mice lacking specific nicotinic acetylcholine receptor subunits exhibit dramatically altered spontaneous activity patterns and reveal a limited role for retinal waves in forming ON and OFF circuits in the inner retina. J. Neurosci. *20*, 7672–7681.

Cao, Y., Song, H., Okawa, H., Sampath, A.P., Sokolov, M., and Martemyanov, K.A. (2008). Targeting of RGS7/Gβ5 to the Dendritic Tips of ON-Bipolar Cells Is Independent of Its Association with Membrane Anchor R7BP. J. Neurosci. *28*, 10443–10449.

Cao, Y., Pahlberg, J., Sarria, I., Kamasawa, N., Sampath, A.P., and Martemyanov, K.A. (2012). Regulators of G protein signaling RGS7 and RGS11 determine the onset of the light response in ON bipolar neurons. PNAS *109*, 7905–7910.

Catsicas, M., and Mobbs, P. (2001). GABAB Receptors Regulate Chick Retinal Calcium Waves. J. Neurosci. *21*, 897–910.

Chen, F.S., Shim, H., Morhardt, D., Dallman, R., Krahn, E., McWhinney, L., Rao, A., Gold, S.J., and Chen, C.-K. (2010). Functional Redundancy of R7 RGS Proteins in ON-Bipolar Cell Dendrites. IOVS *51*, 686–693.

Chichilnisky, E.J. (2001). A Simple White Noise Analysis of Neuronal Light Responses. Network *12*, 199–213.

Clark, B.D., Kurth-Nelson, Z.L., and Newman, E.A. (2009). Adenosine-Evoked Hyperpolarization of Retinal Ganglion Cells Is Mediated by G-Protein-Coupled Inwardly Rectifying K+ and Small Conductance Ca2+-Activated K+ Channel Activation. J. Neurosci. *29*, 11237–11245.

Cowan, C.W., Fariss, R.N., Sokal, I., Palczewski, K., and Wensel, T.G. (1998). High expression levels in cones of RGS9, the predominant GTPase accelerating protein of rods. Proceedings of the National Academy of Sciences of the United States of America *95*, 5351.

Demas, J., Eglen, S.J., and Wong, R.O.L. (2003). Developmental Loss of Synchronous Spontaneous Activity in the Mouse Retina Is Independent of Visual Experience. J. Neurosci. *23*, 2851–2860.

Dhingra, A., Lyubarsky, A., Jiang, M., Pugh, E.N., Birnbaumer, L., Sterling, P., and Vardi, N. (2000). The Light Response of ON Bipolar Neurons Requires Gαo. J. Neurosci. *20*, 9053–9058.

Drenan, R.M., Doupnik, C.A., Boyle, M.P., Muglia, L.J., Huettner, J.E., Linder, M.E., and Blumer, K.J. (2005). Palmitoylation regulates plasma membrane–nuclear shuttling of R7BP, a novel membrane anchor for the RGS7 family. J Cell Biol *169*, 623–633.

Drenan, R.M., Doupnik, C.A., Jayaraman, M., Buchwalter, A.L., Kaltenbronn, K.M., Huettner, J.E., Linder, M.E., and Blumer, K.J. (2006). R7BP Augments the Function of RGS7·Gβ5 Complexes by a Plasma Membrane-targeting Mechanism. J. Biol. Chem. *281*, 28222–28231.

Garzón, J., Rodríguez-Muñoz, M., López-Fando, A., and Sánchez-Blázquez, P. (2005). Activation of mu-opioid receptors transfers control of Galpha subunits to the regulator of G-protein signaling RGS9-2: role in receptor desensitization. J. Biol. Chem. *280*, 8951–8960.

Gleason, E. (2012). The influences of metabotropic receptor activation on cellular signaling and synaptic function in amacrine cells. Visual Neuroscience *29*, 31–39.

Grabowska, D., Jayaraman, M., Kaltenbronn, K.M., Sandiford, S.L., Wang, Q., Jenkins, S., Slepak, V.Z., Smith, Y., and Blumer, K.J. (2008). Postnatal induction and localization of R7BP, a membrane-anchoring protein for regulator of G protein signaling 7 family-Gβ5 complexes in brain. Neuroscience *151*, 969–982.

Guimarães-Souza, E. m., and Calaza, K. c. (2012). Selective activation of group III metabotropic glutamate receptor subtypes produces different patterns of γ-aminobutyric acid immunoreactivity and glutamate release in the retina. Journal of Neuroscience Research *90*, 2349–2361.

He, W., Cowan, C.W., and Wensel, T.G. (1998). RGS9, a GTPase Accelerator for Phototransduction. Neuron *20*, 95–102.

Hooks, S.B., Waldo, G.L., Corbitt, J., Bodor, E.T., Krumins, A.M., and Harden, T.K. (2003). RGS6, RGS7, RGS9, and RGS11 stimulate GTPase activity of Gi family G-proteins with differential selectivity and maximal activity. J. Biol. Chem. *278*, 10087–10093.

Huang, H., Wang, Z., Weng, S.-J., Sun, X.-H., and Yang, X.-L. (2013). Neuromodulatory role of melatonin in retinal information processing. Prog Retin Eye Res *32*, 64–87.

Huberman, A.D., Feller, M.B., and Chapman, B. (2008). Mechanisms Underlying Development of Visual Maps and Receptive Fields. Annual Review of Neuroscience *31*, 479–509.

Jensen, R.J. (2006). Activation of group II metabotropic glutamate receptors reduces directional selectivity in retinal ganglion cells. Brain Research *1122*, 86–92.

Jensen, R.J., and Daw, N.W. (1986). Effects of dopamine and its agonists and antagonists on the receptive field properties of ganglion cells in the rabbit retina. Neuroscience *17*, 837–855.

Jia, L., Linder, M.E., and Blumer, K.J. (2011). Gi/o Signaling and the Palmitoyltransferase DHHC2 Regulate Palmitate Cycling and Shuttling of RGS7 Family-binding Protein. J. Biol. Chem. *286*, 13695–13703.

Kothmann, W.W., Massey, S.C., and O'Brien, J. (2009). Dopamine-Stimulated Dephosphorylation of Connexin 36 Mediates AII Amacrine Cell Uncoupling. J. Neurosci. *29*, 14903–14911.

Liapis, E., Sandiford, S., Wang, Q., Gaidosh, G., Motti, D., Levay, K., and Slepak, V.Z. (2012). Subcellular localization of regulator of G protein signaling RGS7 complex in neurons and transfected cells. Journal of Neurochemistry *122*, 568–581.

Martemyanov, K.A., Yoo, P.J., Skiba, N.P., and Arshavsky, V.Y. (2005). R7BP, a Novel Neuronal Protein Interacting with RGS Proteins of the R7 Family. J. Biol. Chem. *280*, 5133–5136.

Masu, M., Iwakabe, H., Tagawa, Y., Miyoshi, T., Yamashita, M., Fukuda, Y., Sasaki, H., Hiroi, K., Nakamura, Y., Shigemoto, R., et al. (1995). Specific deficit of the ON response in visual transmission by targeted disruption of the mGIuR6 gene. Cell *80*, 757–765.

Masuho, I., Xie, K., and Martemyanov, K.A. (2013). Macromolecular Composition Dictates Receptor and G Protein Selectivity of Regulator of G Protein Signaling (RGS) 7 and 9-2 Protein Complexes in Living Cells. J. Biol. Chem. *288*, 25129–25142.

Mojumder, D.K., Qian, Y., and Wensel, T.G. (2009). Two R7 Regulator of G-Protein Signaling Proteins Shape Retinal Bipolar Cell Signaling. J. Neurosci. *29*, 7753–7765.

Morgans, C.W., Weiwei Liu, Wensel, T.G., Brown, R.L., Perez-Leon, J.A., Bearnot, B., and Duvoisin, R.M. (2007). Gβ5-RGS complexes co-localize with mGluR6 in retinal ON-bipolar cells. European Journal of Neuroscience *26*, 2899–2905.

Nadal-Nicolás, F.M., Jiménez-López, M., Sobrado-Calvo, P., Nieto-López, L., Cánovas-Martínez, I., Salinas-Navarro, M., Vidal-Sanz, M., and Agudo, M. (2009). Brn3a as a Marker of Retinal Ganglion Cells: Qualitative and Quantitative Time Course Studies in Naïve and Optic Nerve–Injured Retinas. IOVS *50*, 3860–3868.

Narayanan, V., Sandiford, S.L., Wang, Q., Keren-Raifman, T., Levay, K., and Slepak, V.Z. (2007). Intramolecular Interaction between the DEP Domain of RGS7 and the Gβ5 Subunit†. Biochemistry *46*, 6859–6870.

Prusky, G.T., Alam, N.M., Beekman, S., and Douglas, R.M. (2004). Rapid Quantification of Adult and Developing Mouse Spatial Vision Using a Virtual Optomotor System. IOVS *45*, 4611–4616.

Rao, A., Dallman, R., Henderson, S., and Chen, C.-K. (2007). Gβ5 Is Required for Normal Light Responses and Morphology of Retinal ON-Bipolar Cells. J. Neurosci. *27*, 14199–14204.

Schindelin, J., Arganda-Carreras, I., Frise, E., Kaynig, V., Longair, M., Pietzsch, T., Preibisch, S., Rueden, C., Saalfeld, S., Schmid, B., et al. (2012). Fiji: an open-source platform for biological-image analysis. Nat. Methods *9*, 676–682.

Shim, H., Wang, C.-T., Chen, Y.-L., Chau, V.Q., Fu, K.G., Yang, J., McQuiston, A.R., Fisher, R.A., and Chen, C.-K. (2012). Defective Retinal Depolarizing Bipolar Cells in Regulators of G Protein Signaling (RGS) 7 and 11 Double Null Mice. J. Biol. Chem. *287*, 14873–14879.

Snow, B.E., Krumins, A.M., Brothers, G.M., Lee, S.-F., Wall, M.A., Chung, S., Mangion, J., Arya, S., Gilman, A.G., and Siderovski, D.P. (1998). A G protein γ subunit-like domain shared between RGS11 and other RGS proteins specifies binding to Gβ5 subunits. Proceedings of the National Academy of Sciences of the United States of America *95*, 13307.

Song, J.H., Waataja, J.J., and Martemyanov, K.A. (2006). Subcellular Targeting of RGS9-2 Is Controlled by Multiple Molecular Determinants on Its Membrane Anchor, R7BP. J. Biol. Chem. *281*, 15361–15369.

Song, J.H., Song, H., Wensel, T.G., Sokolov, M., and Martemyanov, K.A. (2007). Localization and differential interaction of R7 RGS proteins with their membrane anchors R7BP and R9AP in neurons of vertebrate retina. Molecular and Cellular Neuroscience *35*, 311–319.

Stellwagen, D., Shatz, C.J., and Feller, M.B. (1999). Dynamics of Retinal Waves Are Controlled by Cyclic AMP. Neuron *24*, 673–685.

Syed, M.M., Lee, S., Zheng, J., and Zhou, Z.J. (2004). Stage-dependent dynamics and modulation of spontaneous waves in the developing rabbit retina. J Physiol *560*, 533–549.

Taylor, W. r., and Smith, R. g. (2012). The role of starburst amacrine cells in visual signal processing. Visual Neuroscience *29*, 73–81.

Torborg, C.L., and Feller, M.B. (2004). Unbiased analysis of bulk axonal segregation patterns. Journal of Neuroscience Methods *135*, 17–26.

Torborg, C.L., and Feller, M.B. (2005). Spontaneous patterned retinal activity and the refinement of retinal projections. Progress in Neurobiology *76*, 213–235.

Umino, Y., Frio, B., Abbasi, M., and Barlow, R. (2006). A two-alternative, forced choice method for assessing mouse vision. Adv. Exp. Med. Biol. *572*, 169–172.

Umino, Y., Solessio, E., and Barlow, R.B. (2008). Speed, Spatial, and Temporal Tuning of Rod and Cone Vision in Mouse. J. Neurosci. *28*, 189–198.

Witherow, D.S., Wang, Q., Levay, K., Cabrera, J.L., Chen, J., Willars, G.B., and Slepak, V.Z. (2000). Complexes of the G Protein Subunit Gβ5 with the Regulators of G Protein Signaling RGS7 and RGS9 CHARACTERIZATION IN NATIVE TISSUES AND IN TRANSFECTED CELLS. J. Biol. Chem. *275*, 24872–24880.

Wong, R.O.L., Meister, M., and Shatz, C.J. (1993). Transient period of correlated bursting activity during development of the mammalian retina. Neuron *11*, 923–938.

Xie, K., Allen, K.L., Kourrich, S., Colón-Saez, J., Thomas, M.J., Wickman, K., and Martemyanov, K.A. (2010). Gbeta5 recruits R7 RGS proteins to GIRK channels to regulate the timing of neuronal inhibitory signaling. Nat. Neurosci. *13*, 661–663.

Xie, K., Masuho, I., Brand, C., Dessauer, C.W., and Martemyanov, K.A. (2012). The complex of G protein regulator RGS9-2 and Gβ(5) controls sensitization and signaling kinetics of type 5 adenylyl cyclase in the striatum. Sci Signal *5*, ra63.

Zhang, J., Jeffrey, B.G., Morgans, C.W., Burke, N.S., Haley, T.L., Duvoisin, R.M., and Brown, R.L. (2010). RGS7 and -11 Complexes Accelerate the ON-Bipolar Cell Light Response. IOVS *51*, 1121–1129.

Zhang, J.-H., Pandey, M., Seigneur, E.M., Panicker, L.M., Koo, L., Schwartz, O.M., Chen, W., Chen, C.-K., and Simonds, W.F. (2011). Knockout of G protein β5 impairs brain development and causes multiple neurologic abnormalities in mice. Journal of Neurochemistry *119*, 544–554.

Zhou, H., Chisari, M., Raehal, K.M., Kaltenbronn, K.M., Bohn, L.M., Mennerick, S.J., and Blumer, K.J. (2012). GIRK channel modulation by assembly with allosterically regulated RGS proteins. Proc. Natl. Acad. Sci. U.S.A. *109*, 19977–19982.

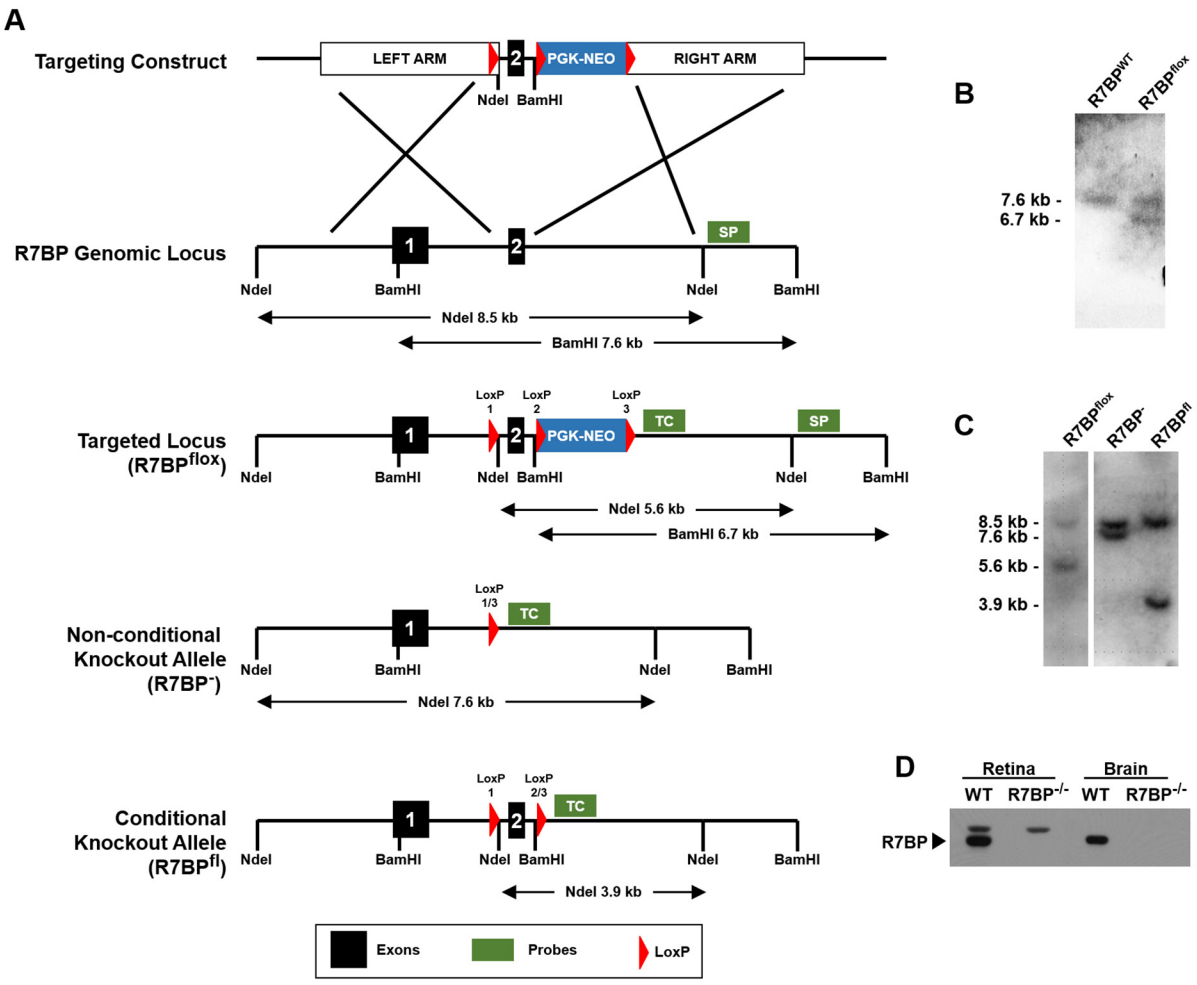

Figure 1. Generation and characterization of R7BP^{-} and R7BP^{fl} alleles.

A. Targeting strategy for generation of nonconditional (R7BP^{-}) and conditional (R7BP^{fl}) alleles. Cre mediated excision between LoxP1 and LoxP3 generates nonconditional allele (R7BP^{-}) Cre mediated excision between LoxP2 and LoxP3 generates conditional knockout allele (R7BP^{fl}). **B.** Southern analysis of BamHI digested genomic DNA from targeted embryonic stem cells using southern blot probes (SP) demonstrate homologous recombination. **C.** Southern analysis of NdeI digested targeted embryonic stem cells after Cre-mediated excision of exon 2 and the PGK Neo cassette (R7BP^{-}) or only the PGK-Neo cassette (R7BP^{fl}) using the TC probe. **D.** Western blot of whole retina or whole brain lysates from WT or R7BP$^{-/-}$ mice

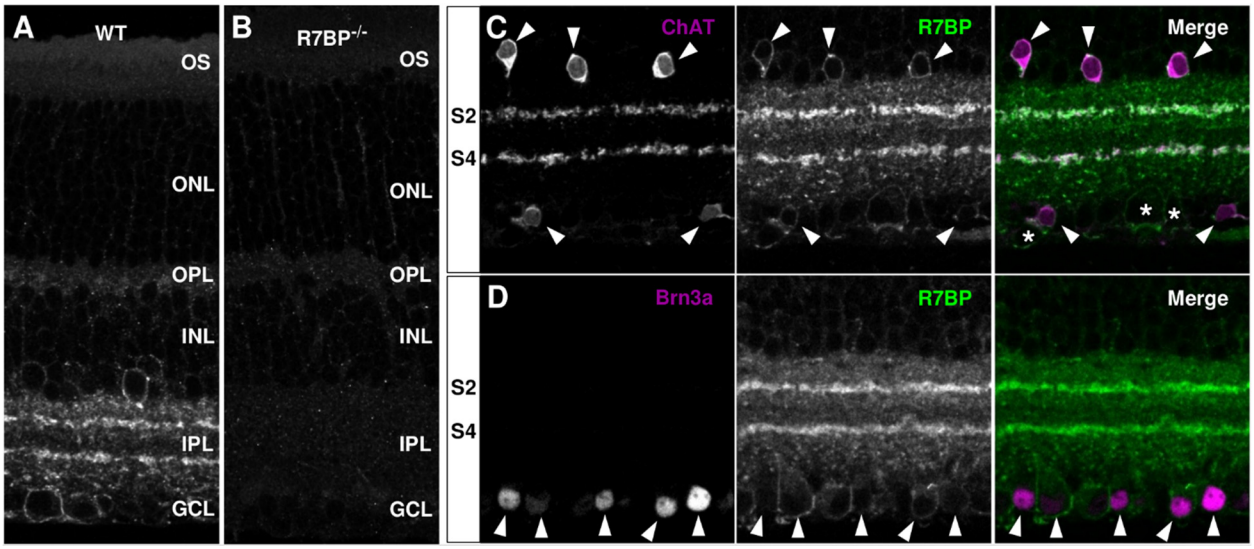

Figure 2. R7BP is expressed in starburst amacrine cells and Brn3a-positive RGCs.

A-B. R7BP is expressed in the OPL, INL, IPL, and GCL in wild-type retina (A) as compared to R7BP$^{-/-}$ retina (B). **C.** Expression of R7BP in starburst amacrine cells (SACs). Co-staining of the SAC marker (ChAT; magenta) and R7BP (green) in the S2/S4 sublaminae of the IPL and somata of the INL and GCL. Arrowheads mark ChAT-positive somata. Asterisks indicate R7BP-positive, ChAT-negative somata. **D.** Somatic expression of R7BP (green) in Brn3a-positive retinal ganglion cells (magenta). Arrowheads mark Brn3a-positive nuclei. Abbreviations are as follows: outer segment (OS), outer nuclear layer (ONL), outer plexiform layer (OPL), inner nuclear layer (INL), inner plexiform layer (IPL), ganglion cell layer (GCL).

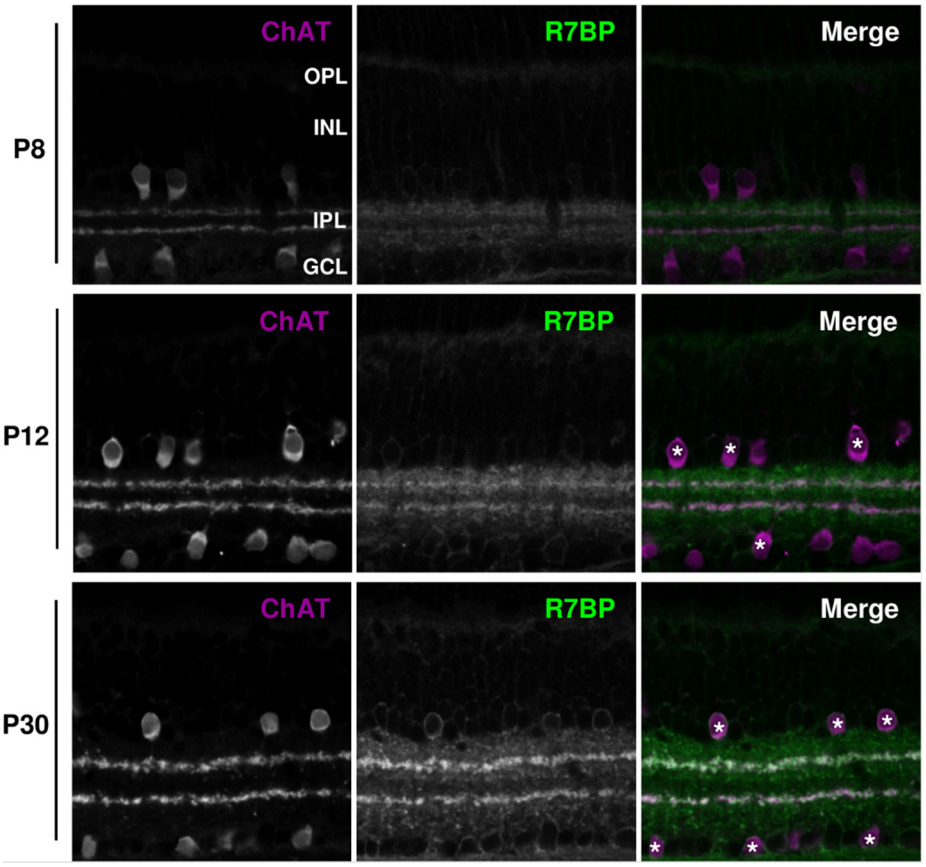

Figure 3. R7BP is induced during postnatal development.

At P8, R7BP (green) is expressed in the OPL, INL, IPL, and GCL. SACs (ChAT-positive cells; magenta) are indicated. R7BP expression in retina is increased at P12 and P30 relative to P8. Asterisks indicate R7BP-positive, ChAT-positive SACs.

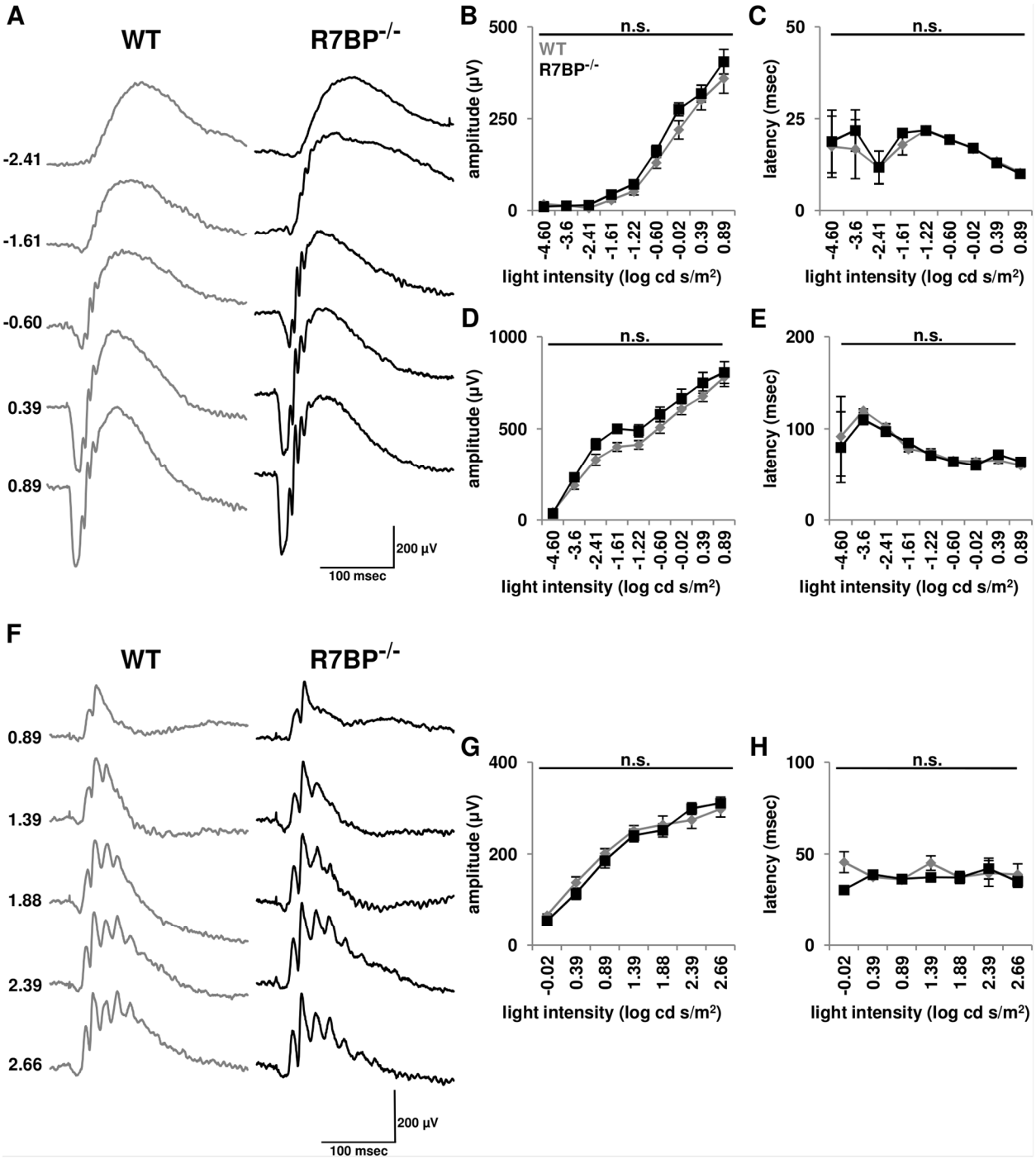

Figure 4. R7BP$^{-/-}$ mice have essentially normal light-evoked photoreceptor and ON bipolar cell activity.

A. Representative ERG responses from dark-adapted WT and R7BP$^{-/-}$ mice (~3 months) were obtained over the indicated range of flash intensities (log cd s/m^2). **B-C.** Quantification of ERG

a-wave peak amplitude (B) and latency (C) in adult dark-adapted WT (gray) and R7BP$^{-/-}$ (black) mice. **D-E.** Ablation of R7BP does not alter dark-adapted b-wave peak amplitude (D) or latency (E). **F.** Representative ERG responses of light-adapted WT and R7BP$^{-/-}$ mice over the photopic range of flash intensities (log cd s/m^2). **G-H.** Similar ERG b-wave peak amplitude (G) and latency (H) in light-adapted WT and R7BP$^{-/-}$ mice were observed. Error bars represent ±SEM.

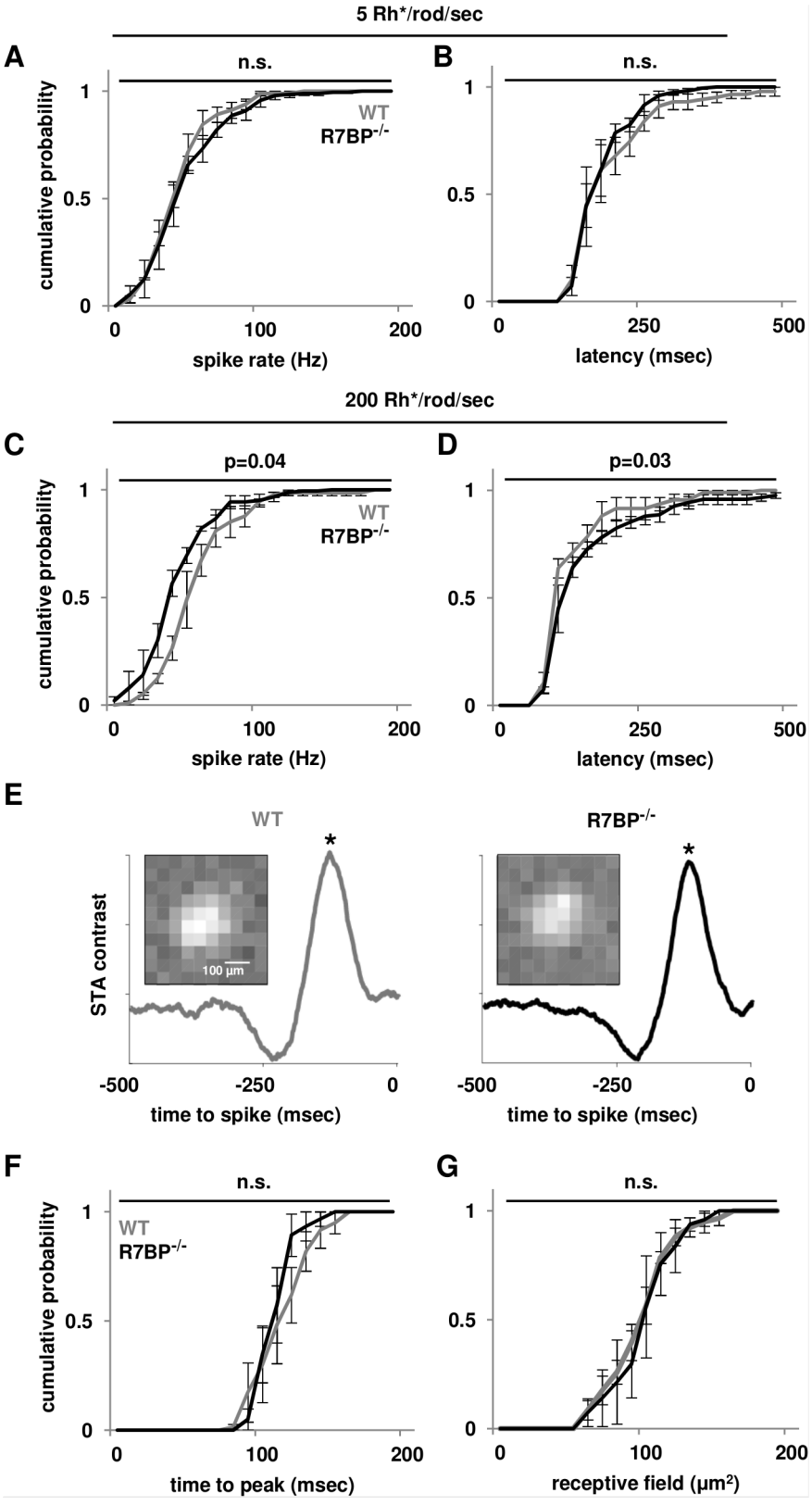
5 Rh*/rod/sec
A
n.s.
WT
R7BP-/-
cumulative probability
spike rate (Hz)
B
n.s.
latency (msec)
200 Rh*/rod/sec
C
p=0.04
D
p=0.03
E
WT
R7BP-/-
STA contrast
100 µm
time to spike (msec)
F
time to peak (msec)
G
receptive field (µm²)

Figure 5. Ablation of R7BP alters mesopic but not scotopic ON RGC light responses.

A-B. Distribution of mean spike rate (B) and latency (C) of P20-21 WT (gray lines) and R7BP$^{-/-}$ (black lines) ON RGCs is similar under scotopic illumination. **C-D.** Ablation of R7BP decreases the mean spike rate (D) and increases the latency (E) of P20-21 ON RGCs under mesopic illumination. **E.** Representative spike trigger average (STA) stimuli of WT (gray) and R7BP$^{-/-}$ (black) ON RGCs. Inset: Corresponding receptive field as revealed by images of STAs at peak contrast, asterisks. **F.** Time-to-peak between stimulus (STA peak contrast, asterisks) and response (spike) of WT and R7BP$^{-/-}$ ON RGCs. **G.** Receptive field sizes of ON RGCs in P20-21 WT and R7BP$^{-/-}$ retina were similar. Error bars represent ±SEM.

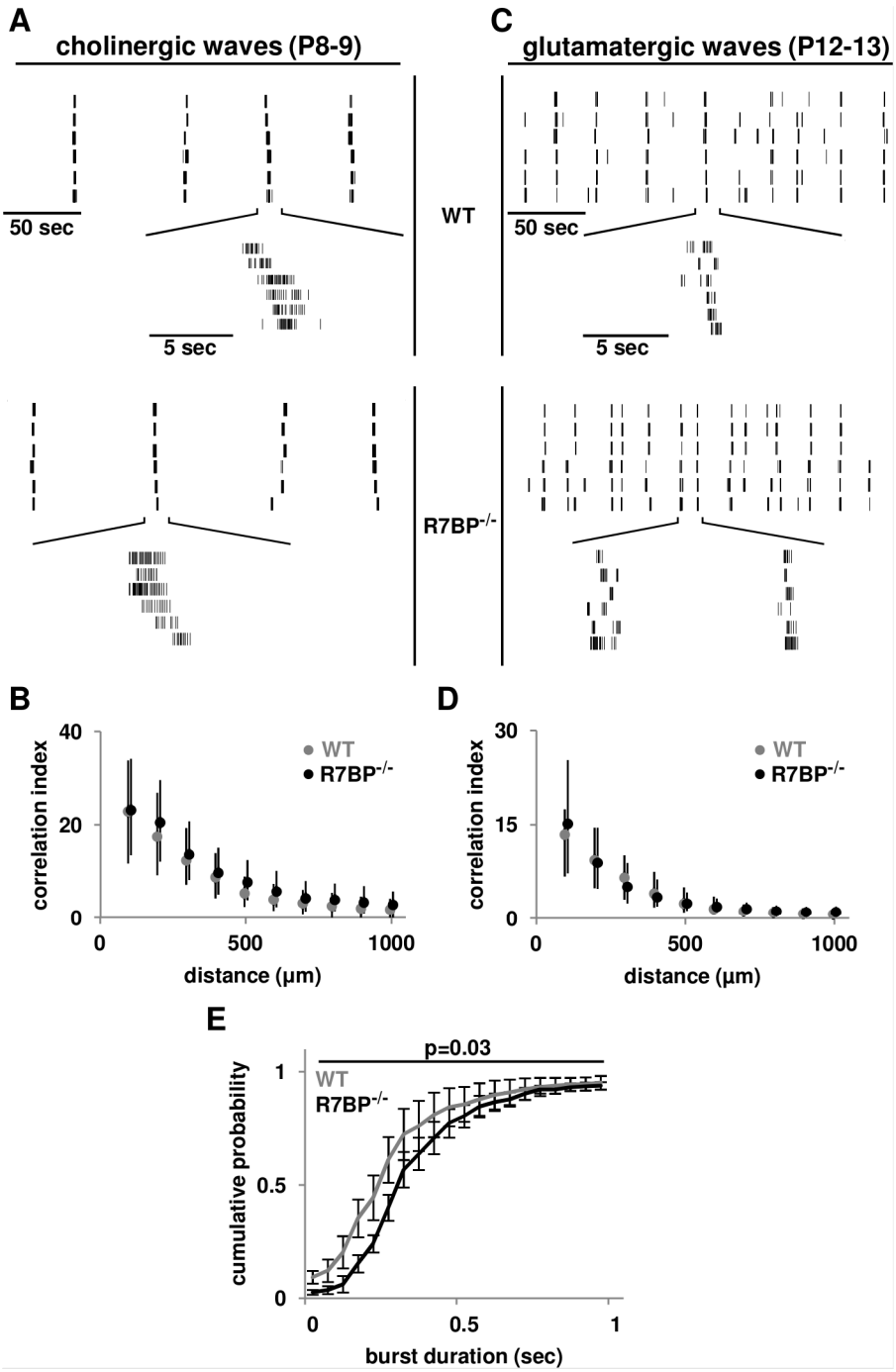

Figure 6. Ablation of R7BP increases glutamatergic wave burst duration.

A. Representative raster plots of cholinergic waves from P8-9 WT and R7BP$^{-/-}$ RGCs obtained by MEA recordings. **B.** Correlated firing of cholinergic waves is preserved in R7BP$^{-/-}$ retina. Correlation indexes from P8-9 WT (gray) and R7BP$^{-/-}$ (black) RGCs plotted as function of

distance between the recording electrodes. Circles indicate the median. Lower and upper error bars indicate the 25th and 75th percentile, respectively. **C.** Representative raster plots of glutamatergic waves in P12-13 WT and R7BP$^{-/-}$ RGCs. **D.** Correlated firing during glutamatergic waves is similar in WT (gray) and R7BP$^{-/-}$ (black) retinas. **E.** Ablation of R7BP increases the burst duration of glutamatergic waves in P12-13 retina. Error bars represent ±SEM.

	P8-9		P12-13	
	WT	**R7BP$^{-/-}$**	**WT**	**R7BP$^{-/-}$**
# of Neurons [Retinas]	190 [3]	180 [3]	594 [4]	365 [4]
Firing Rate (Hz)				
Mean±SEM	0.21±0.01	0.22±0.01	0.44±0.02	0.37±0.02
25%	0.12	0.13	0.17	0.18
50%	0.19	0.20	0.32	0.30
75%	0.28	0.29	0.58	0.47
p Value	p = 0.75		p = 0.83	
Burst Duration (sec)				
Mean±SEM	0.94±0.04	0.95±0.04	0.41±0.01	0.55±0.02
25%	0.47	0.59	0.24	0.30
50%	0.80	0.89	0.30	0.42
75%	1.2	1.3	0.42	0.60
p Value	p = 0.79		**p = 0.03***	
Interwave Interval (sec)				
Mean±SEM	60±3.5	68±3.1	22±8.1	23±8.1
25%	30	55	11	10
50%	54	75	20	21
75%	83	92	28	32
p Value	p = 0.67		p = 0.98	

Table 1: Spatiotemporal properties of cholinergic and glutamatergic waves of WT and R7BP$^{-/-}$ RGCs.

Quantification of firing rate, burst duration, and interwave interval of cholinergic (P8-9) and glutamatergic (P12-13) retinal waves determined by MEA recordings.

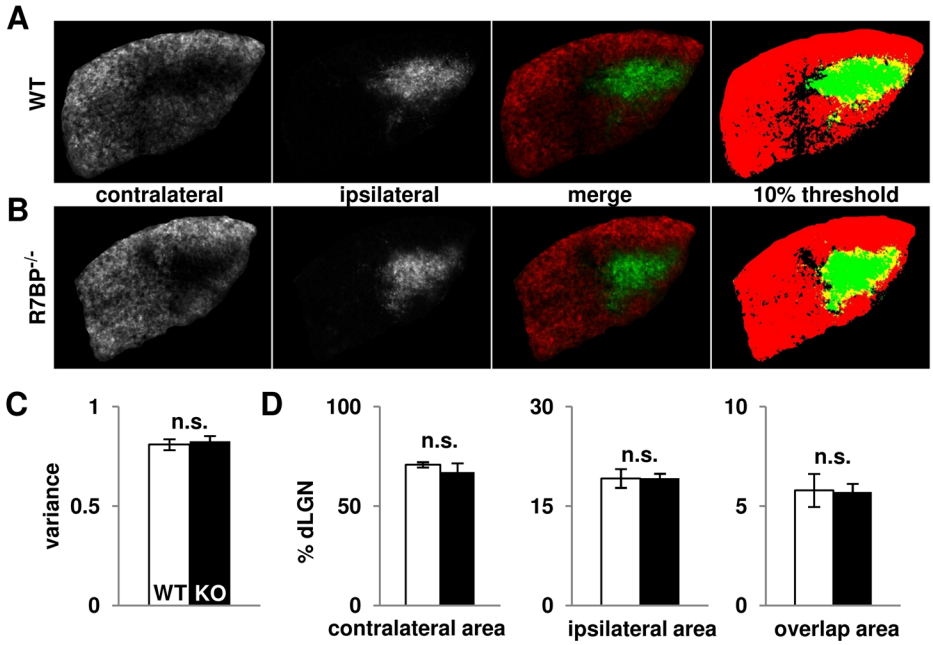

Figure 7. R7BP is dispensable for segregation of retinogeniculate projections.

A-B. Representative fluorescent labeling of contralateral (red) and ipsilateral (green) retinogeniculate projections of P21 WT (A) or R7BP$^{-/-}$ (B) dLGN using intraocularly injected, Alexa-conjugated cholera toxin B subunit (CTB) as anterograde tracers. Binarized images were thresholded at 10% to determine the area occupied by either contralateral (red), ipsilateral (green), or both (yellow) projections. **C.** Segregation of eye-specific domains is similar in WT (white bar) or R7BP$^{-/-}$ (black bar) dLGN as measured by mean variance of R-value distributions from CTB-labeled retinogeniculate projections. **D.** Ablation of R7BP does not alter the area of dLGN innervated by contralateral, ipsilateral, or both projections. Error bars represent ±SEM.

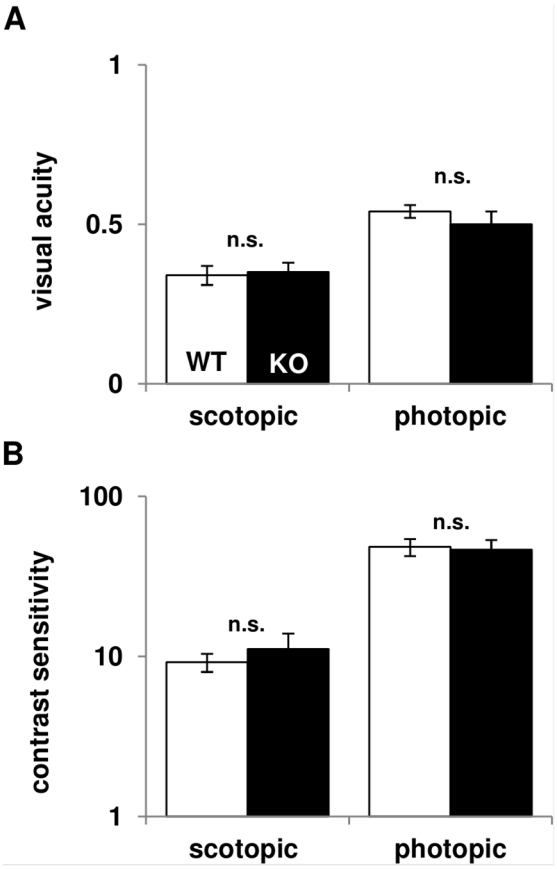

Figure 8. Normal visual acuity and spatial contrast sensitivity in R7BP$^{-/-}$ mice.

A. Similar visual acuity of WT (white bar) and R7BP$^{-/-}$ (black bar) mice under scotopic and photopic conditions as measured by optomotor response. **B.** Ablation of R7BP does not disrupt scotopic and photopic contrast sensitivity. Error bars represent ±SEM.

Chapter 3:

R7BP interacts with R7-RGS/Gβ5 complexes in the dLGN but does not regulate R7-RGS/Gβ5 membrane association

Acknowledgements:

This work is an extension of the work presented in Chapter 2. Patrick Osei-Owusu taught me intracardial perfusion. Murali Jayaraman and Hao Zhou helped train me in brain dissections. Jillian Smith assisted with the development and execution of brain and lateral geniculate nucleus dissection. Susan Culican provided the Six3-Cre mouse line. Rory Fisher (U. of Iowa) and Ted Wensel (Baylor College of Medicine) provided RGS6 and RGS7 antibodies, respectively. I would like to thank members of the Blumer lab for helpful advice and discussion. This work was supported by grants from the National Institutes of Health (GM44592 and HL075632 (K.J.B). During this work I was supported by predoctoral training grants from the NIH (GM 007067 and T32-EY013360).

Abstract

The visual system extends beyond the retina into multiple structures in the brain. Here we show that R7BP is highly expressed throughout the neuropil of the dorsal lateral geniculate nucleus (dLGN), a region of the brain that is an important component of the visual system, acting as the relay center for the retino-geniculo-cortical pathway that connects the retina to the primary visual cortex. The dLGN was also critical to a preliminary phenotype we were characterizing in $R7BP^{-/-}$ mice. Similar to retina, R7BP expression in the dLGN is induced during postnatal development. In adult lateral geniculate nucleus (LGN), R7BP interacts with RGS6 and RGS7 but is not necessary for membrane association of R7-RGS complexes in LGN lysates. Although these data have been collected within the context of a disproven preliminary phenotype, these findings indicate that R7-RGS complexes may function elsewhere in the visual system. Furthermore, the data demonstrate that R7BP likely regulates R7-RGS function independently of membrane targeting in the dLGN.

Introduction

Preliminary data of anterograde labeling of R7BP$^{-/-}$ retinas suggested a desegregation phenotype of retinogeniculate projections beginning at P12 (data not shown). This preliminary phenotype did not correlate with any deficits in retinal waves found in mice with similar desegregation phenotypes (Demas et al., 2006) or with observed deficits in R7BP$^{-/-}$ retinal waves (Cain et al., 2013). We began to explore the hypothesis that R7BP functions postsynaptically of retinal ganglion cells in the dLGN to regulate retinogeniculate segregation. Therefore, it was critical to understand the mechanism by which R7BP regulates R7-RGS proteins and Gi/o signaling to maintain segregation of retinogeniculate segregation.

Because we demonstrated that retinogeniculate segregation is normal in R7BP$^{-/-}$ (Cain et al., 2013), we shifted our focus to characterize the relationship between R7BP and R7-RGS at the third synapse of the visual system in the dLGN. The data from this study complements previous studies that have investigated the role of R7BP in membrane targeting of R7-RGS proteins in both retina and brain.

R7BP was originally predicted to function as a membrane-targeting binding partner for R7-RGS family members (Drenan et al., 2005). R7BP is necessary for plasma membrane localization of R7-RGS proteins *in vitro*, where it augments R7-RGS function (Drenan et al., 2006). Trafficking of R7BP/R7-RGS complexes is dependent on the presence of two C-terminal palmitate moieties (Drenan et al., 2005). When palmitoylated, R7BP likely cycles between plasma membrane and perinuclear endomembranes. Alternatively, unpalmitoylated R7BP

accumulates in the nucleus via a polybasic nuclear localization sequence (Drenan et al., 2005, 2006; Jia et al., 2011).

The extent to which R7BP is necessary for localization of R7-RGS proteins *in vivo* remains an open question. R7BP localizes to dendrites and spines in striatum and has been reported to recruit RGS7 to postsynaptic densities (Anderson et al., 2009; Grabowska et al., 2008). However, loss of R7BP in the retina or hippocampus only minimally deters RGS7 membrane association (Cao et al., 2008; Ostrovskaya et al., 2014b), suggesting that R7BP may not be necessary for R7-RGS membrane localization *in vivo*.

Together, this study characterizes the *in vivo* role of R7BP on R7-RGS protein localization and function in the dLGN. Specifically, we demonstrated that R7BP is highly expressed in the dLGN and that R7BP interacts with both RGS6 and RGS7. However, ablation of R7BP does not dramatically affect membrane association of R7-RGS/Gβ5 complexes.

Results

R7BP is expressed in the dLGN

In addition to the retina, we examined the expression of R7BP in other areas of the visual system. As the primary relay center between the retina and visual cortex, the dLGN is an essential component of the visual system. Additionally, preliminary data of retinogeniculate projections in dLGN indicated that loss of R7BP resulted in a desegregation of retinogeniculate projections (data not shown) that did not coincide with strong deficits in retinal waves (Chapter 2, Figure 6), suggesting that R7BP may function postsynaptically in dLGN. We probed for R7BP expression in coronal brain slices using affinity-purified R7BP antibodies. R7BP is strongly expressed in the dLGN (Figure 1A), only weakly expressed in ventral lateral geniculate nucleus (vLGN), and absent from the intergeniculate leaflet (IGL) (data not shown).

As R7BP is expressed in a subset of RGCs (Ch. 2, Figure 2), it was important to determine if R7BP staining originated from the RGCs innervating the dLGN or from neurons of the dLGN. We utilized a conditional R7BP knockout allele ($R7BP^{fl}$), in which exon 2 is flanked by loxP sites (Ch. 2, Figure 1), crossed to a retinal Cre line, Six3-Cre (Furuta et al., 2000). The Six3-Cre line expresses Cre enzyme throughout the retina and frontal cortex as early as E9. Specifically, $R7BP^{fl/fl}$ mice were bred to $R7BP^{+/-}$, Six3-Cre^{+} mice to generate $R7BP^{fl/-}$, Six3-Cre^{+} mice and their Cre-only littermate control ($R7BP^{fl/+}$, Six3-Cre^{+}). R7BP was still expressed throughout $R7BP^{fl/+}$, Six3-Cre^{+} control retina and dLGN (Figure 1B). R7BP expression was absent from a majority of the $R7BP^{fl/-}$, Six3-Cre^{+} retina, similar to $R7BP^{-/-}$ retinas. Weak residual R7BP expression was observed in the peripheral retina (data not shown). However, R7BP expression in the dLGN was maintained in $R7BP^{fl/-}$, Six3-Cre^{+} mice, indicating that R7BP

was expressed in neurons in the dLGN. High magnification confocal imaging revealed staining throughout the neuropil of the dLGN (Figure 1C). Although the density of staining prevented distinguishing somatic R7BP staining from the density of the neuropil, R7BP expression can be observed surrounding somata of dLGN neurons. This suggests that R7BP is expressed in dLGN neurons.

We also examined the onset of R7BP expression in the dLGN. This was originally done to correlate R7BP expression to onset of the preliminary desegregation phenotype which began at P12. R7BP expression was low but detectable above background at P4. Expression increased over the next two weeks to adult levels (Figure 2). Therefore, R7BP expression undergoes similar induction in multiple compartments of the visual system (Cain et al., 2013).

R7BP interacts with RGS6 and RGS7 in dLGN

As R7BP primarily regulates cell signaling through its interaction with R7-RGS complexes, it was important to understand which R7-RGS proteins R7BP coupled with in dLGN. We dissected the lateral geniculate nucleus region of the thalamus. As R7BP expression was predominately in the dLGN and not the IGL or vLGN, the primary contribution of R7BP will be from the dLGN. To confirm that our dissections were isolating R7BP-enriched dLGN, we determined R7BP expression level in immunoprecipitated R7BP from multiple R7BP-expressing brain regions (cortex, hippocampus, and striatum) and the LGN (Figure 3A). R7BP was highly expressed in LGN lysates compared to other brain regions. Additionally, we were successful in co-immunoprecipitating Gβ5, demonstrating our ability to collect full R7-RGS/Gβ5 heterotrimers. Interestingly, only a small fraction of Gβ5 (<10%) co-immunoprecipitated with

R7BP, suggesting that R7BP interacts with a subpopulation of R7-RGS/Gβ5 dimers, or that interaction is dynamic and labile. In addition to Gβ5, we also co-immunoprecipitated RGS6 (Figure 3B) and RGS7 (Figure 3C). Immunoprecipitation was dependent on R7BP as neither RGS6 nor RGS7 co-immunoprecipitated from $R7BP^{-/-}$ lysates. RGS9 and RGS11 expression was not detected in LGN lysates using available antibodies.

R7BP is not necessary for R7-RGS/Gβ5 membrane association or localization to synapses

As R7BP is considered a R7-RGS membrane targeting protein, especially *in vitro* (Drenan et al., 2005), we wanted to determine if R7BP was necessary for membrane localization of R7-RGS complexes *in vivo*. We performed crude membrane fractionation of dLGN preparations to determine if R7BP ablation perturbed R7-RGS/Gβ5 membrane association, using Gβ5 as a surrogate for all R7-RGS/Gβ5 dimers in the LGN. Gβ5 was highly associated with the membrane, with minimal cytosolic localization (Figure 4A). Similar to what was observed in retina (Cao et al., 2008), R7BP was dispensable for Gβ5 localization to crude membrane fractions. However, the extent to which R7BP traffics R7-RGS proteins to specific membrane or subcellular structures is unclear.

Discussion

We demonstrated that R7BP is highly expressed throughout the neuropil of the dLGN and can be detected surrounding the somata dLGN neurons, suggesting that R7-RGS complexes may regulate Gi/o signaling in the dLGN. There are two dLGN resident neurons that are part of the retino-geniculo-cortical system which relay visual information from retina projections to the primary visual cortex, thalamocortical relay neurons and inhibitory thalamic interneurons. Both neurons receive input from retinal ganglion cells (RGCs), corticothalamic neurons, and thalamic reticular nucleus neurons (TRN). Additionally, Gi/o signaling regulates the action of these neurons. Both GABA(B) and mGluR receptor signaling have been demonstrated to regulate thalamocortical relay neurons (Bickford et al., 2010a; Govindaiah and Cox, 2006; Perreault et al., 2003). Therefore, it is interesting to consider whether R7-RGS/R7BP complexes expressed in dLGN neurons regulate transmission of visual information outside of the retina.

The onset of R7BP expression is similar to that observed in whole brain lysates and coincides with periods of synaptic refinement (Grabowska et al., 2008). Similar synaptic refinement occurs in the dLGN during this period, including synaptic pruning and organization of retinogeniculate projections into eye specific domains (Bickford et al., 2010a; Huberman et al., 2008). Although R7BP was dispensable for normal organization of retinogeniculate projections (Cain et al., 2013), it is interesting to consider whether RGS7 and RGS6, which interact with R7BP in the dLGN, would have a significant effect on segregation.

We determined that R7/Gβ5 membrane association is independent of R7BP in LGN preparations. Similar trends have been observed in retina and hippocampus, in which ablation of

R7BP results in only minor reduction in membrane association of R7-RGS proteins (Cao et al., 2008; Ostrovskaya et al., 2014b). How RGS6 and RGS7 target to membranes in the dLGN is an open question. Do R7-RGS complex with GPCRs and other integral membrane proteins as in the retina (Orlandi et al., 2012)? It remains possible that R7BP membrane association may target R7-RGS complexes to relevant signaling regions of the plasma membrane that are not distinguishable by fractionation. Alternatively, these data may favor the hypothesis that R7BP primarily acts as a positive allosteric regulator for a specific pool of R7-RGS complexes (Masuho et al., 2013; Zhou et al., 2012b).

While originally designed to explore mechanisms underlying an invalidated desegregation phenotype, this study reveals a novel tissue in which R7-RGS complexes may regulate Gi/o signaling in the visual system. Additionally, we contribute to the ongoing description of R7BP regulation of R7-RGS complex *in vivo*.

Material and Methods

Animals

All animal procedures used protocols approved by the Washington University Animal Studies Committee (Protocol #20110184 and #20140036). $R7BP^{-/-}$ mice produced by targeted deletion of exon 2 have been described previously (Zhou et al., 2012b). $R7BP^{+/-}$ mice were crossed six generations into the C57BL/6 background (Charles River Laboratories) and then interbred to produce WT and $R7BP^{-/-}$ littermates of either sex for analysis. For generation of $R7BP^{fl}$ allele see Chapter 2, Figure 1. Retina-specific R7BP knockouts were generated as such: Six3-Cre^{+} mice were first crossed with $R7BP^{-/-}$ mice. $R7BP^{+/-}$, Six3-Cre^{+} mice then were crossed with $R7BP^{fl/fl}$ to generate $R7BP^{fl/-}$, Six3-Cre^{+} mice and their littermate control ($R7BP^{fl/+}$, Six3-Cre^{+}) of either sex for analysis.

Tissue preparation and immunostaining

Mice were euthanized by CO_2 asphyxiation followed by cervical dislocation. Enucleated eyes were fixed with paraformaldehyde (4%) in PBS (pH 7.4). Retinas were isolated in PBS and embedded in 4% low-melting point agarose. For fixation of brain, euthanized mice were perfused intracardially with PBS followed by paraformaldehyde (4%) in PBS. Brains were removed and post-fixed overnight at 4 ºC. Vertical retina and coronal brain slices were cut (60 μm and 100 μm, respectively) with a vibratome. Slices were blocked with 10% normal horse serum (NHS) in PBS and incubated with primary antibodies overnight in 5% NHS and 0.05% Triton X-100 (Sigma-Aldrich). The following antibodies were used: affinity purified rabbit anti-R7BP (Grabowska et al., 2008) and Alexa Fluor 488-conjugated anti-rabbit (Invitrogen; 1:1000) antibodies. Slices were mounted using VectaShield (Vector Labs) and imaged with Olympus

FluoView FV500 (Bakewell NeuroImaging Laboratory, WUSM). Retinal immunofluorographs were median filtered (1 pixel surround) using NIH Fiji (Schindelin et al., 2012). For quantification of postnatal induction of R7BP expression, mean fluorescence values were measured for R7BP-positive dLGN and normalized to R7BP-negative intergeniculate leaflet, as background.

LGN isolation

Mice were euthanized by CO_2 asphyxiation followed by cervical dislocation. Brains were removed and dissected in PBS. Specifically, the cortex and hippocampus were first isolated to expose the thalamus. The crude LGN was separated from the thalamus by isolating the tissue lateral and dorsal to the innervation of the optic tract in the thalamus. Following LGN isolation, striatum was dissected.

Immunoprecipitation

Brain regions were homogenized in 1% Triton X-100 in PBS (pH 8.0) using Teflon microcentrifuge tube pestle. Homogenates were further lysed by rotating at 4 °C for 30 min. Lysates were cleared by centrifugation at 16,000xg (20 min) and 100,000xg (1 hr). Soluble fractions were quantified using BioRad Bradford reagent. 100 μg of protein incubated with chicken anti-R7BP (#4827) and washed PrecipHen beads overnight at 4 °C. Protein was eluted in SDS Sample Buffer by boiling. For western blots, samples were electrophoresed through 10% SDS-polyacrylamide gels and transferred to PVDF membranes (Millipore). Membranes were blocked with 5% milk in TBST (1 hr) and incubated overnight at 4 °C with primary antibody in TBST or 5% milk in TBST. The following antibodies were used: affinity purified rabbit anti-

R7BP (1:1000), rabbit anti-Gβ5 (ATDG) (1:1000), provided by William Simonds, rabbit anti-RGS6 (1:1000), provided by Rory Fisher, and rabbit anti-RGS7 (1:1000), provided by Ted Wensel. Blots were washed three times in TBST (10 min) prior to incubation with HRP-conjugated anti-rabbit antibody in TBST. Secondary antibody was washed three times with TBST (10 min) and blots were imaged using ECL reagent (General Electric).

Membrane Fractionation

Dissected brain tissue was isolated as described above. Tissue was homogenized in hypotonic buffer (5 mM Tris pH 7.4, 1mM EDTA pH 8.0, 1mM EGTA pH 8.0, 10 mM KCl, 2 mM $MgCl_2$, 1 mM DTT, 0.25 M Sucrose) using a microcentrifuge tube pestle and incubated rotating at 4 °C. Cell debris was cleared by centrifugation at 1000xg for 20 min. Lysates were quantified as described above. Crude membrane fractions were isolated from cytosolic fractions by ultracentrifugation at 100,000xg (30 min), washed with small volume of hypotonic buffer, and re-pelleted at 100,000xg (20 min) before being solubilized in MCLB buffer (50 mM Tris pH 8.0), 5 mM EDTA, 0.5% IGEPAL, 100 mM NaCl, 1 mM sodium orthovanadate). Equivalent volumes of cleared lysates (total), cytosolic, and membrane fractions were resolved using SDS-PAGE and imaged using western blot as described above.

References

Anderson, G.R., Lujan, R., and Martemyanov, K.A. (2009). Changes in Striatal Signaling Induce Remodeling of RGS Complexes Containing Gβ5 and R7BP Subunits. Mol. Cell. Biol. *29*, 3033–3044.

Bickford, M.E., Slusarczyk, A., Dilger, E.K., Krahe, T.E., Kucuk, C., and Guido, W. (2010). Synaptic development of the mouse dorsal lateral geniculate nucleus. J. Comp. Neurol. *518*, 622–635.

Cain, M.D., Vo, B.Q., Kolesnikov, A.V., Kefalov, V.J., Culican, S.M., Kerschensteiner, D., and Blumer, K.J. (2013). An allosteric regulator of R7-RGS proteins influences light-evoked activity and glutamatergic waves in the inner retina. PLoS ONE *8*, e82276.

Cao, Y., Song, H., Okawa, H., Sampath, A.P., Sokolov, M., and Martemyanov, K.A. (2008). Targeting of RGS7/Gβ5 to the Dendritic Tips of ON-Bipolar Cells Is Independent of Its Association with Membrane Anchor R7BP. J. Neurosci. *28*, 10443–10449.

Demas, J., Sagdullaev, B.T., Green, E., Jaubert-Miazza, L., McCall, M.A., Gregg, R.G., Wong, R.O.L., and Guido, W. (2006). Failure to Maintain Eye-Specific Segregation in nob, a Mutant with Abnormally Patterned Retinal Activity. Neuron *50*, 247–259.

Drenan, R.M., Doupnik, C.A., Boyle, M.P., Muglia, L.J., Huettner, J.E., Linder, M.E., and Blumer, K.J. (2005). Palmitoylation regulates plasma membrane–nuclear shuttling of R7BP, a novel membrane anchor for the RGS7 family. J Cell Biol *169*, 623–633.

Drenan, R.M., Doupnik, C.A., Jayaraman, M., Buchwalter, A.L., Kaltenbronn, K.M., Huettner, J.E., Linder, M.E., and Blumer, K.J. (2006). R7BP Augments the Function of RGS7·Gβ5 Complexes by a Plasma Membrane-targeting Mechanism. J. Biol. Chem. *281*, 28222–28231.

Furuta, Y., Lagutin, O., Hogan, B.L.M., and Oliver, G.C. (2000). Retina- and ventral forebrain-specific Cre recombinase activity in transgenic mice. Genesis *26*, 130–132.

Govindaiah, G., and Cox, C.L. (2006). Metabotropic Glutamate Receptors Differentially Regulate GABAergic Inhibition in Thalamus. J. Neurosci. *26*, 13443–13453.

Grabowska, D., Jayaraman, M., Kaltenbronn, K.M., Sandiford, S.L., Wang, Q., Jenkins, S., Slepak, V.Z., Smith, Y., and Blumer, K.J. (2008). Postnatal induction and localization of R7BP, a membrane-anchoring protein for regulator of G protein signaling 7 family-Gβ5 complexes in brain. Neuroscience *151*, 969–982.

Huberman, A.D., Feller, M.B., and Chapman, B. (2008). Mechanisms Underlying Development of Visual Maps and Receptive Fields. Annual Review of Neuroscience *31*, 479–509.

Jia, L., Linder, M.E., and Blumer, K.J. (2011). Gi/o Signaling and the Palmitoyltransferase DHHC2 Regulate Palmitate Cycling and Shuttling of RGS7 Family-binding Protein. J. Biol. Chem. *286*, 13695–13703.

Masuho, I., Xie, K., and Martemyanov, K.A. (2013). Macromolecular Composition Dictates Receptor and G Protein Selectivity of Regulator of G Protein Signaling (RGS) 7 and 9-2 Protein Complexes in Living Cells. J. Biol. Chem. *288*, 25129–25142.

Orlandi, C., Posokhova, E., Masuho, I., Ray, T.A., Hasan, N., Gregg, R.G., and Martemyanov, K.A. (2012). GPR158/179 regulate G protein signaling by controlling localization and activity of the RGS7 complexes. J. Cell Biol. *197*, 711–719.

Ostrovskaya, O., Xie, K., Masuho, I., Fajardo-Serrano, A., Lujan, R., Wickman, K., and Martemyanov, K.A. (2014). RGS7/Gβ5/R7BP complex regulates synaptic plasticity and memory by modulating hippocampal GABABR-GIRK signaling. Elife *3*, e02053.

Perreault, M.-C., Qin, Y., Heggelund, P., and Zhu, J.J. (2003). Postnatal development of GABAergic signalling in the rat lateral geniculate nucleus: presynaptic dendritic mechanisms. J Physiol *546*, 137–148.

Schindelin, J., Arganda-Carreras, I., Frise, E., Kaynig, V., Longair, M., Pietzsch, T., Preibisch, S., Rueden, C., Saalfeld, S., Schmid, B., et al. (2012). Fiji: an open-source platform for biological-image analysis. Nat. Methods *9*, 676–682.

Zhou, H., Chisari, M., Raehal, K.M., Kaltenbronn, K.M., Bohn, L.M., Mennerick, S.J., and Blumer, K.J. (2012). GIRK channel modulation by assembly with allosterically regulated RGS proteins. Proc. Natl. Acad. Sci. U.S.A. *109*, 19977–19982.

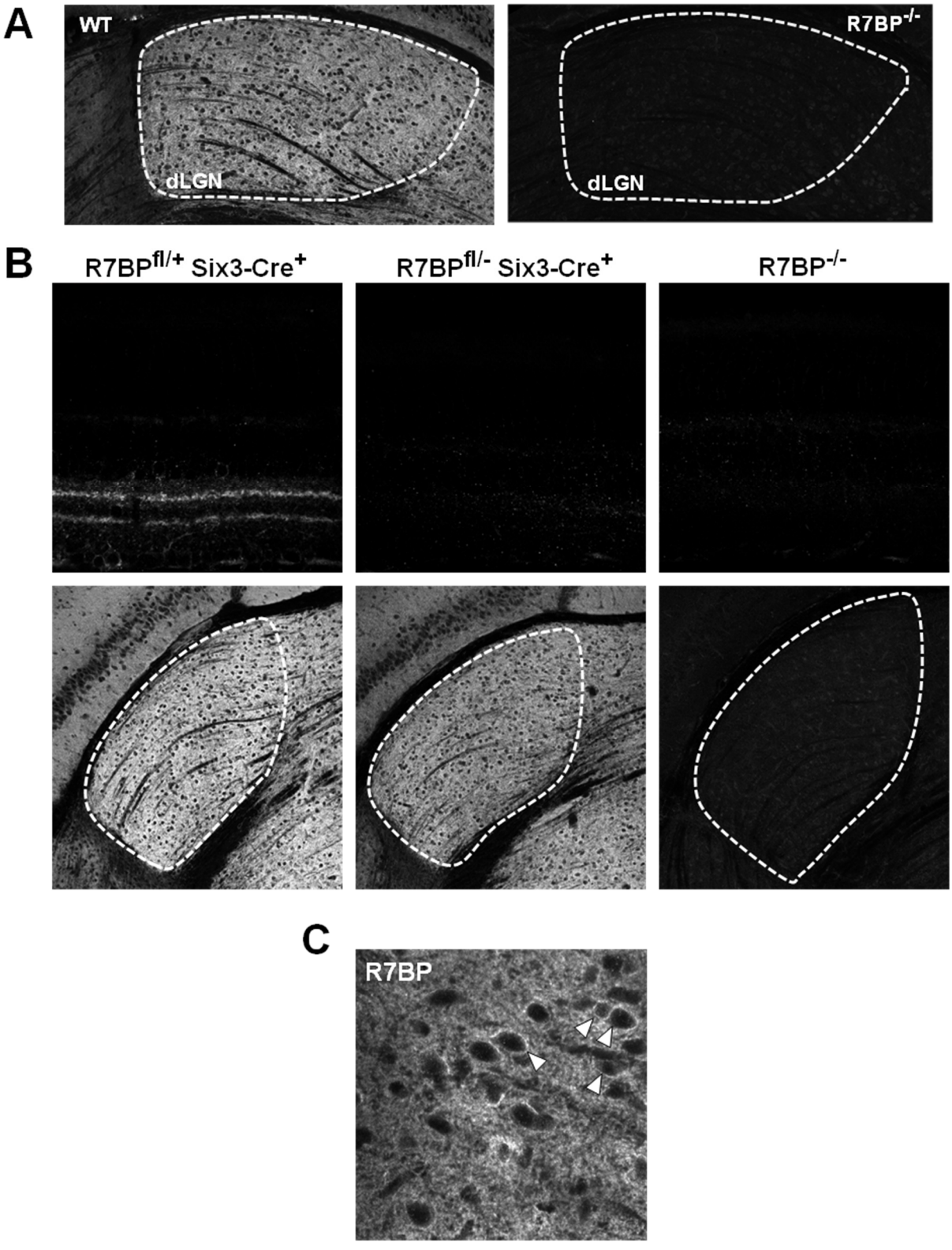
A
WT
dLGN
R7BP-/-
dLGN
B
R7BPfl/+ Six3-Cre+
R7BPfl/- Six3-Cre+
R7BP-/-
C
R7BP

Figure 1. R7BP is expressed in the dorsal lateral geniculate nuclei (dLGN).

A. R7BP is expressed in adult WT dLGN (traced by dashed white line) but absent from $R7BP^{-/-}$ dLGN. **B.** R7BP expression in dLGN persists in retina-specific R7BP knockouts. Immunostaining of R7BP in retina and dLGN of controls ($R7BP^{fl/+}$ Six3-Cre+). R7BP expression in dLGN of retina-specific R7BP knockouts ($R7BP^{fl/-}$ Six3-Cre+) is preserved. Loss of R7BP immunostaining in retina and dLGN of $R7BP^{-/-}$ controls**. C.** R7BP is expressed throughout the neuropil of dLGN. Arrowheads indicate somata surrounded by R7BP staining.

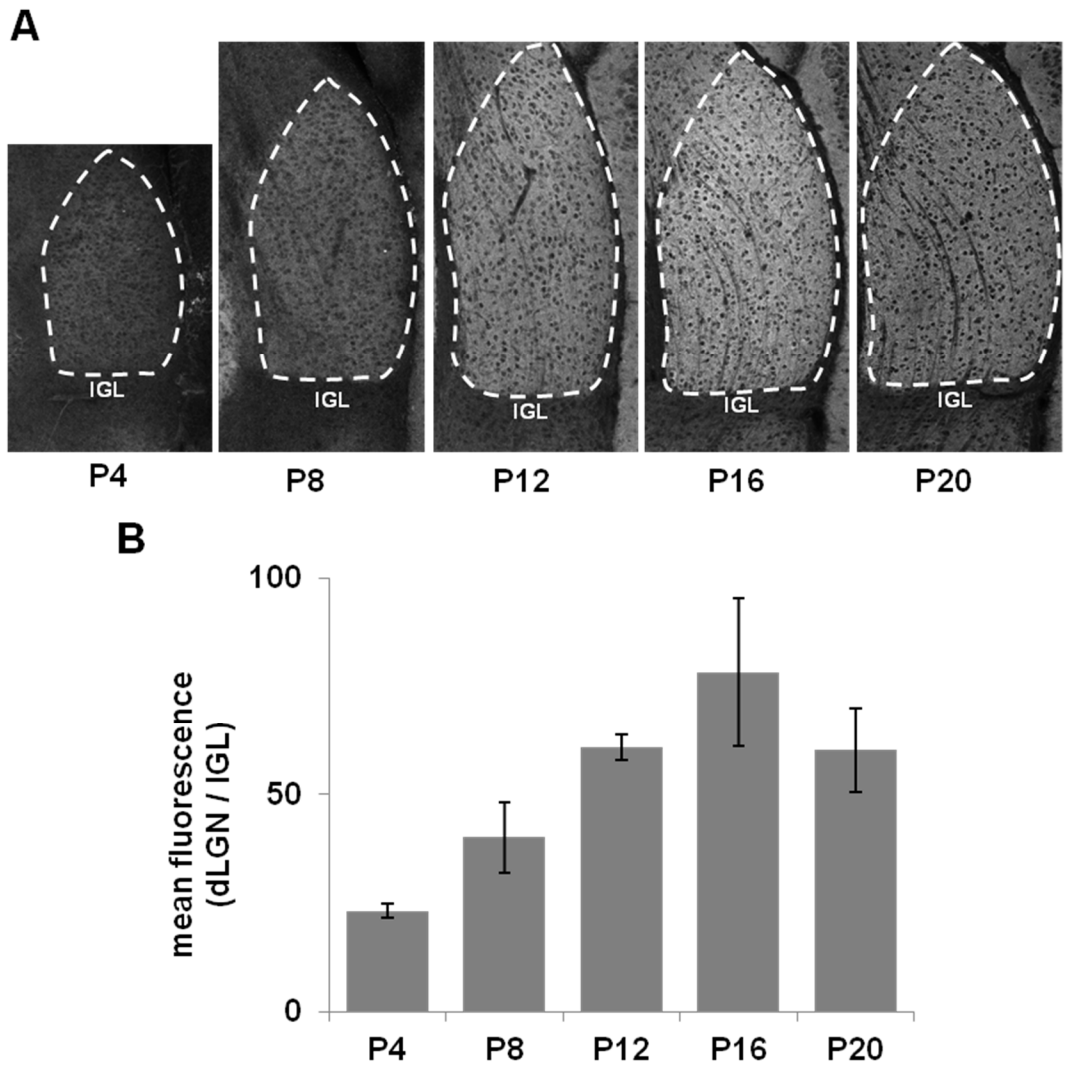

Figure 2. R7BP dLGN expression is induced during postnatal development.

A. Representative immunofluorographs of R7BP in wild-type dLGN (traced by dashed white line) at various ages. At P4, R7BP is barely detectable in dLGN, but increases to adult levels over two week of postnatal development. **B.** Quantification of mean fluorescence of dLGN R7BP immunostaining normalized to background fluorescence in the intergeniculate leaflet (IGL).

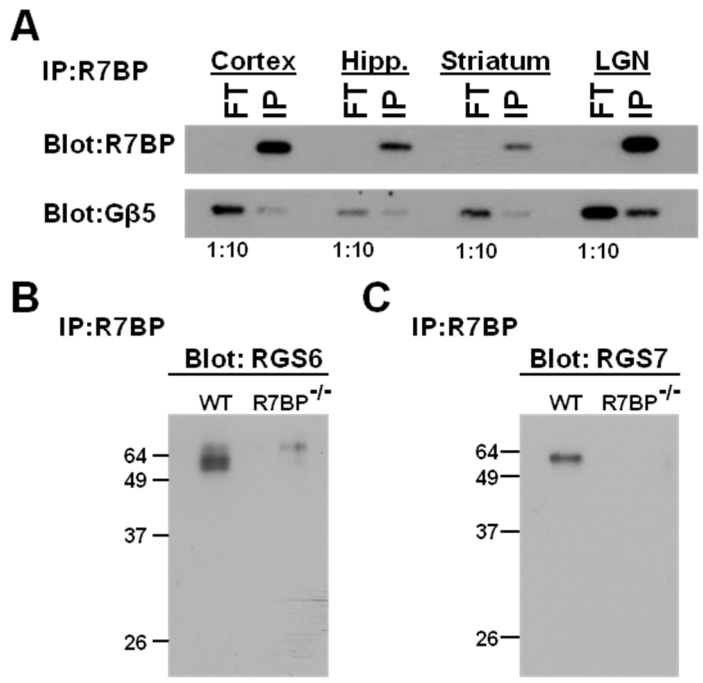

Figure 3. R7BP is highly expressed in crude geniculate lysates and interacts with both RGS6 and RGS7.

A. Co-immunoprecipitation of R7BP and Gβ5 from cortical, hippocampal, striatal and crude geniculate lysates using anit-R7BP antibody. R7BP and Gβ5 were resolved by SDS-PAGE and western blotting. **B.** Co-immunoprecipitation of RGS6 with anti-R7BP antibody from LGN lysates. $R7BP^{-/-}$ lysates demonstrate specificity of immunoprecipitation. **C.** Co-immunoprecipitation of RGS7 with anti-R7BP antibody from LGN lysates. $R7BP^{-/-}$ LGN lysates act as a negative control.

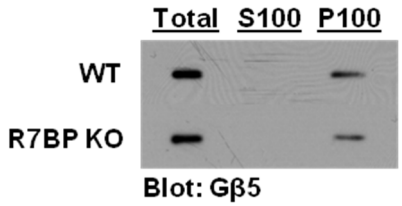

Figure 4. Ablation of R7BP does not disrupt RGS7/Gβ5 plasma membrane association. Subcellular fractionation of dLGN lysates into soluble cytosolic (S100) and insoluble crude membrane (P100) fractions. Membrane association of Gβ5 is indistinguishable between WT and $R7BP^{-/-}$ dLGN lysates.

Chapter 4:

Effect of expression of RGS-insensitive Gi2 and Go mutants on outer retinal function

Acknowledgements

This project was initially spearheaded by Jillian Smith, who performed the majority of the initial ERG recordings for RGS-insensitive Go and Gi2 mutants. I contributed intellectually to the design of the experiments, performed additional ERG recordings that are represented in the data presented herein, and performed all analysis. Special thanks go to Anne Hennig for training Jill and me on the ERG machines. Robert Johnson helped by providing discussion and instruction on using MATLAB. Robert also contributed code to the MATLAB scripts used for ERG analysis. RGS-insensitive Gi2 and Go mice were provided by Rick Neubig (Michigan State U.). Diana Schorry Brightman provided retinal cDNA used to clone murine TRPM1 that was utilized in experiments that are not presented here. Vladimir Kefalov and Peter Lukasiewicz provided helpful discussion. I would like to thank members of the Blumer lab for helpful advice and discussion. This work was supported by grants from the National Institutes of Health (GM44592 and HL075632 (K.J.B) and EY02687 (Department of Ophthalmology and Visual Sciences, Washington University) and from Research to Prevent Blindness, Inc. (DOVS). During this work I was supported by predoctoral training grants from the NIH (GM 007067 and T32-EY013360).

Abstract

Functional redundancy in GAP activity toward Gi/o may preclude identification of retinal signaling sensitive to RGS regulation when using single knockout strategies. In this study we characterize the outer retinal function of two RGS-insensitive knock-in mutant strains for Go and Gi2 in order to 1) directly inhibit RGS regulation of specific Gi/o Gα subunits and 2) investigate RGS regulation of Gi/o that may be independent of R7-RGS proteins. We report that heterozygous RGS-insensitive Go mutants have normal dark-adapted ERG b wave phenotypes and normal rod dendritic morphology. We also demonstrate a novel finding that RGS regulation of Gi2 is necessary for maximal rod light responses.

Introduction

Genetic ablation of the R7-RGS (regulator of G protein signaling) Gi/o GTPase activating proteins (GAPs) RGS7, RGS9, and RGS11 has led to the identified of multiple outer retinal GPCR signaling cascades that are dependent on GAP activity (Cao et al., 2012; Chen et al., 2010; Cowan et al., 1998; He et al., 1998; Mojumder et al., 2009; Rao et al., 2007; Shim et al., 2012; Zhang et al., 2010). However, two challenges have arisen in attempting to identify novel retina GPCR cascades that are regulated by R7-RGS proteins via single R7-RGS knockouts. The first challenge is functional redundancy; RGS7 and RGS11 have both been shown to regulate metabotropic glutamate receptor 6 (mGluR6)/Go cascades (Cao et al., 2012; Shim et al., 2012). R7-RGS proteins also have overlapping expression (Song et al., 2007) and may be redundant with other GAPs expressed in the retina (Faurobert et al., 1999; Ivanov et al., 2006; Ji et al., 2011). The second challenge is that strategies designed to circumvent this redundancy, such as ablating all R7-RGS proteins in $G\beta5^{-/-}$ mice, result in disruption of outer retinal light responses (Rao et al., 2007). This disruption prevents analysis of RGS function elsewhere in the retina. Here we used an alternative approach by characterizing knock-in mutants of Gi/o subunits that have been rendered insensitive to RGS regulation. In either Go or Gi2, the G184S mutation in Gα subunit prevents both interaction and GAP activity of RGS proteins without disrupting Gα interaction with receptors, Gβγ, or effectors (Fu et al., 2004; Lan et al., 1998).

The first mutant characterized was $Gi2^{G184S}$. Homozygous RGS-insensitive Gi2 ($Gi2^{GS/GS}$) mice have been useful for the identification of novel RGS regulation of several signaling cascades in hippocampal and cortical 5-HT1A signaling and isoflurane anesthesia

(Icaza et al., 2009; Talbot et al., 2010). Despite the abundance of Gi/o coupled receptors in the retina (Catsicas and Mobbs, 2001; Clark et al., 2009; Gleason, 2012; Huang et al.; Jensen, 2006; Jensen and Daw, 1986; Kothmann et al., 2009; Masu et al., 1995), Gi has yet to be demonstrated as the target of RGS regulation in retina. Importantly, Gi2 is not modeled to be a component of phototransduction or ON bipolar cell light responses (Dhingra et al., 2000b). Therefore, we hypothesized that disrupting RGS regulation and augmenting Gi2 signaling may reveal retinal functions that are sensitive to both RGS regulation and Gi2 signaling.

The second mutant was a heterozygous RGS-insensitive Go ($Go^{+/GS}$) mouse. Homozygous $Go^{GS/GS}$ mice are not viable (Goldenstein et al., 2009). However, $Go^{+/GS}$ mice have been used to identify novel RGS regulation of alpha2A adrenergic receptor signaling in CA3 hippocampal epileptiform activity and opioid supraspinal antinociception (Goldenstein et al., 2009; Lamberts et al., 2013). Unlike $Gi2^{GS/GS}$, $Go^{+/GS}$ has predicted deficits in rod bipolar cell light responses. Indeed, loss of RGS regulation of Go resulted in a no-b-wave ERG phenotype (Rao et al., 2007). Consequently, we hypothesize that presence of a RGS-insensitive Go^{G184S} would have a dominant effect on ERG b-waves; this effect is similar to either the increased b-wave latency in $RGS7^{-/-}$ or $RGS11^{-/-}$ mice or the no-b-wave phenotype observed upon loss of both RGS7 and RGS11 (Cao et al., 2012; Chen et al., 2010; Mojumder et al., 2009; Rao et al., 2007; Shim et al., 2012; Zhang et al., 2010). However, coincident to these no-b-wave phenotypes were morphological abnormalities in rod bipolar cell dendritic arborization (Rao et al., 2007; Shim et al., 2012). These morphological abnormalities were not observed in $Go^{-/-}$ or $mGlur6^{-/-}$ mice (Dhingra et al., 2000b; Tagawa et al., 1999), suggesting that they were not caused by the no-b-wave phenotype. Instead they are caused by either augmented Go signaling or loss of RGS regulation of another Gi/o subunit or signaling cascade. Therefore, we characterized

both ERG and rod bipolar cell morphology of $Go^{+/GS}$ mice to potentially delineate the relationship between these two phenotypes.

Our results provide novel evidence that Gi2 is necessary for rod function. We also demonstrate that Go^{G184S} does not function dominantly in ON bipolar cell light responses. Implications of this observation on existing models of mGluR6/Go/TRPM1 signaling are discussed.

Results

Blockade of RGS regulation of Gi2 diminishes rod light responses.

While R7-RGS proteins have been demonstrated to regulate transducin and Go signaling in retina (Cao et al., 2012; Chen et al., 2010; Cowan et al., 1998; He et al., 1998; Mojumder et al., 2009; Rao et al., 2007; Shim et al., 2012; Zhang et al., 2010), RGS regulation of Gi in retina has not been demonstrated. Moreover, very little is known about which retinal functions are regulated by specific Gi isoforms. Therefore, we performed electroretinography of dark-adapted (Figure 1A) and light-adapted (Figure 1F) WT and homozygous RGS-insensitive Gi2 ($Gi2^{GS/GS}$) knock-in mutant mice. Such a mutation would be expected to augment Gi2 signaling and reveal circuits sensitive to both Gi2 signaling and RGS regulation of Gi2. In dark-adapted WT and $Gi2^{GS/GS}$ mice ($n \geq 8$), we observed significant decrease in a-wave amplitude, especially at higher intensities, but no change in a-wave latency (Figure 1B/C). Similarly, the dark-adapted ERG b-wave amplitude in $Gi2^{GS/GS}$ mice was also diminished compared to WT (Figure 1D). This decrease was proportional to the decrease in a-wave amplitude (data not shown) which suggested that this result was a defect primarily in photoreceptors. B-wave latency (time to b-wave peak after flash) was unaffected by the expression of $Gi2^{G184S}$ (Figure 1E). $Gi2^{GS/GS}$ light-adapted photopic b-wave amplitude and latency were indistinguishable from WT mice. This result suggests the previous dark-adapted phenotype is due to diminished rod light responses at higher light intensities but not impaired cone function (Figure 1G/H). Therefore, RGS regulation of Gi2 is necessary for maximal rod light responses.

Heterozygous RGS-insensitive Go mutants have normal outer retinal function.

Inactivation of Go by RGS7 and RGS11 is modeled to be a necessary step in TRPM1 gating and ON bipolar cell depolarization (Cao et al., 2012; Shim et al., 2012); therefore, we predicted that the presence of a RGS-insensitive Go^{G184S} mutant would have a dominant negative effect on ERG b-waves. The effect may be similar to either the increase in b-wave latency observed in $RGS7^{-/-}$ or $RGS11^{-/-}$ mice or to the no-b-wave phenotype observed upon loss of both RGS7 and RGS11(Cao et al., 2012; Chen et al., 2010; Mojumder et al., 2009; Rao et al., 2007; Shim et al., 2012). To determine whether heterozygous RGS-insensitive Go mutants ($Go^{+/GS}$) affect rod- and cone-driven responses over a full range of stimulus intensities, we performed electroretinography of dark-adapted (Figure 2A) and light-adapted (Figure 2F) mice. In dark-adapted WT and $Go^{+/GS}$ mice ($n \geq 7$), we observed no difference in a-wave amplitude or latency corresponding to light-evoked hyperpolarization of rods (low light intensities) or rods and cones (higher intensities) (Figure 2B/C). Interestingly the dark-adapted ERG b-wave amplitude in $Go^{+/GS}$ mice was indistinguishable from WT at all intensities (Figure 2D). Similarly, B-wave latency (time to b-wave peak after flash) was unaffected by the expression of Go^{G184S} (Figure 2E). Photopic (cone-specific) responses revealed by constant background illumination and high intensity flashes displayed no change in b-wave latency but a significantly decreased $Go^{+/GS}$ b-wave amplitude at 2.4 log cd s/m^2 (Figure 2G/H). This ERG data is neither consistent with the prediction that Go^{G184S} would act dominantly nor is it consistent with accepted models of RGS regulation of the mGluR6/Go/TRPM1 cascade regulating ON bipolar cell light responses.

$Go^{+/GS}$ mice display normal Go retinal expression and rod bipolar cell morphology.

It is unclear why Go^{G184S} did not perturb ON bipolar cell light responses. One possibility is that Go^{G184S} does not correctly traffic to rod bipolar cell dendritic tips. Unfortunately, no antibodies are available to distinguish between Go^{WT} and Go^{G184S} subunits; therefore, determining if Go^{G184S} subunits correctly traffic to ON bipolar cell dendritic tips is not possible in this heterozygous background. We did immunostaining of WT and $Go^{+/GS}$ in vertical slices, but we observed no abnormal Go localization that could be attributable to Go^{G184S} in $Go^{+/GS}$ slices (Figure 3A).

Due to the predicted dominant effect of Go^{G184S}, we were also interested in assessing rod bipolar cell dendritic morphology in $Go^{+/GS}$ retina. Loss of RGS7 and RGS11 complexes in the outer plexiform layer (OPL) results in disorganized OPL and shorter ON bipolar cell dendrites (Rao et al., 2007; Shim et al., 2012). Using R7-RGS models, it is unclear if these morphological abnormalities were caused by augmented mGluR6/Go signaling or loss of RGS regulation of another Gi/o subunit and/or signaling cascade. However, the Go^{G184S} mutant allowed us to assess rod bipolar cell morphology in the absence of RGS regulation of Go specifically. Using immunostaining of Go as a marker for rod bipolar cell dendrites, we observed no discernible difference in dendritic morphology in WT and $Go^{+/GS}$ vertical slices (Figure 3B). These results indicate that the expression of Go^{G184S} under endogenous promoter is insufficient to perturb rod dendritic morphology.

Discussion

Our characterization of the ERGs of $Gi2^{GS/GS}$ mutants reveals that RGS regulation of Gi2 is necessary for proper rod function. $Gi2^{GS/GS}$ mutants also exhibit decreased b-wave amplitude that we interpret as being secondary to photoreceptor dysfunction. Interestingly, $Gi2^{-/-}$ mice have similarly reduced b-wave amplitude (Young et al., 2011). Whether or not the b-wave phenotype of $Gi2^{-/-}$ mice also coincides with a diminished a-wave was not reported in the previous study. Regardless, these data suggest that RGS regulation of Gi2 is necessary for proper rod photoreceptor function and that augmented Gi2 signaling can disrupt rod function. The mechanism by which Gi2 regulates rod function is an open question. Interestingly, ablation of RGS9 or Gβ5 does not alter the amplitude of rod light responses, suggesting that a non-R7-RGS GAP regulates Gi2 in this system.

In periods of darkness, sustained glutamate release from photoreceptors occupies mGluR6 to maintain a pool of active Go in dendritic tips of ON bipolar cells (Dhingra et al., 2000b; Masu et al., 1995). Active Go is modeled to directly or indirectly inhibit the constitutively-active transient receptor potential melastatin 1 (TRPM1) channel and cause hyperpolarization of ON bipolar cells (Koike et al., 2010; Morgans et al., 2010). R7-RGS proteins (RGS7 and RGS11) are modeled as Go GAPs (Cao et al., 2012; Shim et al., 2012) which allow for timely inactivation of Go in response to light stimuli, TRPM1 opening, and ON bipolar cell depolarization. Despite predictions that Go^{G184S} would have a dominant function to suppress ON bipolar cell light responses, $Go^{+/GS}$ mice exhibit normal dark-adapted ERGs. We observed no significant delay in b-wave latency or amplitude. How does a Go^{G184S} subunit that does not act dominantly fit into our current model of mGluR6/Go/TRPM1 cascade? We discuss

potential models that could explain the observed $Go^{+/GS}$ phenotypes below. Further testing of these models may elucidate the importance of R7-RGS proteins in ON bipolar cell synapses. Additionally, such studies may also reveal insights into Go regulation of TRPM1.

1) Go^{GS} does not couple to mGluR6 in ON bipolar cells. Go^{G184S} mutation is not predicted to disrupt Go interaction with GPCRs (Fu et al., 2004). Therefore, this result may be due to loss of Go^{GS} expression or failure to traffic to dendritic tips. While we cannot directly assay Go^{GS} expression or localization for Go^{GS}, we observed normal distribution of Go in $Go^{+/GS}$ rod bipolar cells.

2) Go^{GS} no longer inhibits TRPM1. This result may be due to the G184S mutation preventing the direct or indirect inhibition of TRPM1. The mechanism of Go-TRPM1 regulation is unknown. However, G184S mutation does not disrupt classic effector binding (Fu et al., 2004), but it is possible that this mutation may reflect a novel interface for TRPM1 regulation. Alternatively, Go may no longer interact with TRPM1 due to dissociation from the macromolecular signaling complexes with which TRPM1 interacts (Cao et al., 2011; Ray et al., 2014). Go may require interaction with R7-RGS proteins or continuous cycling between active and inactive states by R7-RGS GAPs to sustain interaction with TRPM1.

3) Go^{GS} cannot be dominant to Go^{WT} in ON bipolar cells. One mechanism that fits this model is inactive Go sequesters the hypothetical factor that inhibits TRPM1. The presence of Go^{WT} subunits in $Go^{+/GS}$ ON bipolar cells may be sufficient to sequester such a factor and allow for proper gating of TRPM1 despite a population of Go^{GS} subunits. Such a model has been proposed in which free Gβγ inhibits TRPM1, and inactivation of Go sequesters Gβγ in G protein

heterotrimers (Shen et al., 2012). Therefore, $Go^{+/GS}$ may have a sufficient pool of Go^{WT} to adequately sequester Gβγ during light responses.

.

Material and Methods

Animals

All animal procedures used protocols approved by the Washington University Animal Studies Committee (Protocol #20110184 and #20140036). Generation of Go^{G184S} mutants and $Gi2^{GS}$ mutants have been described previously (Fu et al., 2004; Huang et al., 2006). $Go^{+/GS}$ mice were interbred with $Go^{+/+}$ mice to produced WT and $Go^{+/GS}$ mice of either sex for analysis. $Gi2^{+/GS}$ mice were interbred to produce WT and $Gi2^{GS/GS}$ mice of either sex for analysis.

Electroretinography

Flash ERG measurements were performed with a UTAS-E3000 visual Electrodiagnostic System running EM for Windows (LKC Technologies). Mice (~3 months old) were dark-adapted overnight. Under dim red illumination, mice were anesthetized with a cocktail of 80 mg/kg ketamine and 15 mg/kg xylazine. The body temperature of the mice was maintained at 37 ^{o}C with a heating pad controlled by a rectal temperature probe. After positioning mice in the Ganzfeld dome, the recording electrodes (2.0 mm diameter platinum loops) were positioned on the corneal surface of each eye in a drop of 0.5% atropine sulfate (Bausch & Lomb) and 1.25% hydroxypropol methylcellulose (GONAK; Akorn Inc.). Reference and ground electrodes were placed at the vertex of the skull and back, respectively. For dark-adapted analysis, we recorded the responses to white light flashes of increasing intensity (-4.6 to 1.9 log cd s/m^2) in total darkness. Mice were then light-adapted to a constant white background illumination of 2.3 log cd s/m^2 for 10 min. Light-adapted responses to a series of light flashes (-0.01 to 2.67 log cd s/m^2) were obtained in the presence of constant background illumination. Responses to multiple

trials were averaged for each intensity. The a-wave amplitude and latency were measured and quantified for comparison. B-wave amplitude and latency were measured by using a custom MatLab script. Briefly, ERG curves were filtered using a lowpass zero-phase Butterworth digital filter (15 Hz) to remove high frequency oscillations. B-wave peak was defined as the maximum post-flash amplitude from lowpass filtered curves.

Tissue preparation and immunostaining

Mice were euthanized by CO_2 asphyxiation followed by cervical dislocation. Enucleated eyes were fixed with paraformaldehyde (4%) in PBS (pH 7.4). Retinas were isolated in PBS and embedded in 4% low-melting point agarose. Vertical retina slices were cut (60 μm) with a vibratome. Slices were blocked with 10% normal horse serum (NHS) in PBS and incubated with primary antibodies overnight in 5% NHS and 0.05% Triton X-100 (Sigma-Aldrich). The following antibodies were used: affinity purified mouse anti-Go (MAB-3073, Millipore; 1:500) and Alexa Fluor 488-conjugated anti-mouse (Invitrogen; 1:1000) antibodies. Slices were also stained with NeuroTrace Red Nissl stain (Invitrogen). Slices were mounted using VectaShield (Vector Labs) and imaged with Olympus FluoView FV500 (Bakewell NeuroImaging Laboratory, WUSM). Retinal immunofluorographs were median filtered (1 pixel surround) using NIH Fiji (Schindelin et al., 2012).

Statistics

Statistical analysis of electroretinograms was performed using repeated measures ANOVA, followed by Holm-Sidak post-test. Significance was determined before post-test. Statistical significance was defined as $p<0.05$.

References

Cao, Y., Posokhova, E., and Martemyanov, K.A. (2011). TRPM1 forms complexes with nyctalopin in vivo and accumulates in postsynaptic compartment of ON-bipolar neurons in mGluR6-dependent manner. J. Neurosci. *31*, 11521–11526.

Cao, Y., Pahlberg, J., Sarria, I., Kamasawa, N., Sampath, A.P., and Martemyanov, K.A. (2012). Regulators of G protein signaling RGS7 and RGS11 determine the onset of the light response in ON bipolar neurons. PNAS *109*, 7905–7910.

Catsicas, M., and Mobbs, P. (2001). GABAB Receptors Regulate Chick Retinal Calcium Waves. J. Neurosci. *21*, 897–910.

Chen, F.S., Shim, H., Morhardt, D., Dallman, R., Krahn, E., McWhinney, L., Rao, A., Gold, S.J., and Chen, C.-K. (2010). Functional Redundancy of R7 RGS Proteins in ON-Bipolar Cell Dendrites. IOVS *51*, 686–693.

Clark, B.D., Kurth-Nelson, Z.L., and Newman, E.A. (2009). Adenosine-Evoked Hyperpolarization of Retinal Ganglion Cells Is Mediated by G-Protein-Coupled Inwardly Rectifying K+ and Small Conductance Ca2+-Activated K+ Channel Activation. J. Neurosci. *29*, 11237–11245.

Cowan, C.W., Fariss, R.N., Sokal, I., Palczewski, K., and Wensel, T.G. (1998). High expression levels in cones of RGS9, the predominant GTPase accelerating protein of rods. Proceedings of the National Academy of Sciences of the United States of America *95*, 5351.

Dhingra, A., Lyubarsky, A., Jiang, M., Pugh, E.N., Birnbaumer, L., Sterling, P., and Vardi, N. (2000). The Light Response of ON Bipolar Neurons Requires Gαo. J. Neurosci. *20*, 9053–9058.

Faurobert, E., Scotti, A., Hurley, J.B., and Chabre, M. (1999). RET-RGS, a retina-specific regulator of G-protein signaling, is located in synaptic regions of the rat retina. Neurosci. Lett. *269*, 41–44.

Fu, Y., Zhong, H., Nanamori, M., Mortensen, R.M., Huang, X., Lan, K., and Neubig, R.R. (2004). RGS-insensitive G-protein mutations to study the role of endogenous RGS proteins. Meth. Enzymol. *389*, 229–243.

Gleason, E. (2012). The influences of metabotropic receptor activation on cellular signaling and synaptic function in amacrine cells. Visual Neuroscience *29*, 31–39.

Goldenstein, B.L., Nelson, B.W., Xu, K., Luger, E.J., Pribula, J.A., Wald, J.M., O'Shea, L.A., Weinshenker, D., Charbeneau, R.A., Huang, X., et al. (2009). Regulator of G protein signaling protein suppression of Galphao protein-mediated alpha2A adrenergic receptor

inhibition of mouse hippocampal CA3 epileptiform activity. Mol. Pharmacol. *75*, 1222–1230.

He, W., Cowan, C.W., and Wensel, T.G. (1998). RGS9, a GTPase Accelerator for Phototransduction. Neuron *20*, 95–102.

Huang, H., Wang, Z., Weng, S.-J., Sun, X.-H., and Yang, X.-L. Neuromodulatory role of melatonin in retinal information processing. Progress in Retinal and Eye Research.

Huang, X., Fu, Y., Charbeneau, R.A., Saunders, T.L., Taylor, D.K., Hankenson, K.D., Russell, M.W., D'Alecy, L.G., and Neubig, R.R. (2006). Pleiotropic phenotype of a genomic knock-in of an RGS-insensitive G184S Gnai2 allele. Mol. Cell. Biol. *26*, 6870–6879.

Icaza, E.E., Huang, X., Fu, Y., Neubig, R.R., Baghdoyan, H.A., and Lydic, R. (2009). Isoflurane-induced changes in righting response and breathing are modulated by RGS proteins. Anesth. Analg. *109*, 1500–1505.

Ivanov, D., Dvoriantchikova, G., Nathanson, L., McKinnon, S.J., and Shestopalov, V.I. (2006). Microarray analysis of gene expression in adult retinal ganglion cells. FEBS Lett. *580*, 331–335.

Jensen, R.J. (2006). Activation of group II metabotropic glutamate receptors reduces directional selectivity in retinal ganglion cells. Brain Research *1122*, 86–92.

Jensen, R.J., and Daw, N.W. (1986). Effects of dopamine and its agonists and antagonists on the receptive field properties of ganglion cells in the rabbit retina. Neuroscience *17*, 837–855.

Ji, M., Zhao, W.-J., Dong, L.-D., Miao, Y., Yang, X.-L., Sun, X.-H., and Wang, Z. (2011). RGS2 and RGS4 modulate melatonin-induced potentiation of glycine currents in rat retinal ganglion cells. Brain Res. *1411*, 1–8.

Koike, C., Obara, T., Uriu, Y., Numata, T., Sanuki, R., Miyata, K., Koyasu, T., Ueno, S., Funabiki, K., Tani, A., et al. (2010). TRPM1 is a component of the retinal ON bipolar cell transduction channel in the mGluR6 cascade. Proc. Natl. Acad. Sci. U.S.A. *107*, 332–337.

Kothmann, W.W., Massey, S.C., and O'Brien, J. (2009). Dopamine-Stimulated Dephosphorylation of Connexin 36 Mediates AII Amacrine Cell Uncoupling. J. Neurosci. *29*, 14903–14911.

Lamberts, J.T., Smith, C.E., Li, M.-H., Ingram, S.L., Neubig, R.R., and Traynor, J.R. (2013). Differential control of opioid antinociception to thermal stimuli in a knock-in mouse expressing regulator of G-protein signaling-insensitive Gαo protein. J. Neurosci. *33*, 4369–4377.

Lan, K.L., Sarvazyan, N.A., Taussig, R., Mackenzie, R.G., DiBello, P.R., Dohlman, H.G., and Neubig, R.R. (1998). A point mutation in Galphao and Galphai1 blocks interaction with regulator of G protein signaling proteins. J. Biol. Chem. *273*, 12794–12797.

Masu, M., Iwakabe, H., Tagawa, Y., Miyoshi, T., Yamashita, M., Fukuda, Y., Sasaki, H., Hiroi, K., Nakamura, Y., Shigemoto, R., et al. (1995). Specific deficit of the ON response in visual transmission by targeted disruption of the mGIuR6 gene. Cell *80*, 757–765.

Mojumder, D.K., Qian, Y., and Wensel, T.G. (2009). Two R7 Regulator of G-Protein Signaling Proteins Shape Retinal Bipolar Cell Signaling. J. Neurosci. *29*, 7753–7765.

Morgans, C.W., Brown, R.L., and Duvoisin, R.M. (2010). TRPM1: the endpoint of the mGluR6 signal transduction cascade in retinal ON-bipolar cells. Bioessays *32*, 609–614.

Rao, A., Dallman, R., Henderson, S., and Chen, C.-K. (2007). Gβ5 Is Required for Normal Light Responses and Morphology of Retinal ON-Bipolar Cells. J. Neurosci. *27*, 14199–14204.

Ray, T.A., Heath, K.M., Hasan, N., Noel, J.M., Samuels, I.S., Martemyanov, K.A., Peachey, N.S., McCall, M.A., and Gregg, R.G. (2014). GPR179 Is Required for High Sensitivity of the mGluR6 Signaling Cascade in Depolarizing Bipolar Cells. J. Neurosci. *34*, 6334–6343.

Schindelin, J., Arganda-Carreras, I., Frise, E., Kaynig, V., Longair, M., Pietzsch, T., Preibisch, S., Rueden, C., Saalfeld, S., Schmid, B., et al. (2012). Fiji: an open-source platform for biological-image analysis. Nat. Methods *9*, 676–682.

Shen, Y., Rampino, M.A.F., Carroll, R.C., and Nawy, S. (2012). G-protein-mediated inhibition of the Trp channel TRPM1 requires the Gβγ dimer. Proc. Natl. Acad. Sci. U.S.A. *109*, 8752–8757.

Shim, H., Wang, C.-T., Chen, Y.-L., Chau, V.Q., Fu, K.G., Yang, J., McQuiston, A.R., Fisher, R.A., and Chen, C.-K. (2012). Defective Retinal Depolarizing Bipolar Cells in Regulators of G Protein Signaling (RGS) 7 and 11 Double Null Mice. J. Biol. Chem. *287*, 14873–14879.

Song, J.H., Song, H., Wensel, T.G., Sokolov, M., and Martemyanov, K.A. (2007). Localization and differential interaction of R7 RGS proteins with their membrane anchors R7BP and R9AP in neurons of vertebrate retina. Molecular and Cellular Neuroscience *35*, 311–319.

Tagawa, Y., Sawai, H., Ueda, Y., Tauchi, M., and Nakanishi, S. (1999). Immunohistological Studies of Metabotropic Glutamate Receptor Subtype 6-Deficient Mice Show No Abnormality of Retinal Cell Organization and Ganglion Cell Maturation. J. Neurosci. *19*, 2568–2579.

Talbot, J.N., Jutkiewicz, E.M., Graves, S.M., Clemans, C.F., Nicol, M.R., Mortensen, R.M., Huang, X., Neubig, R.R., and Traynor, J.R. (2010). RGS inhibition at G(alpha)i2 selectively potentiates 5-HT1A-mediated antidepressant effects. Proc. Natl. Acad. Sci. U.S.A. *107*, 11086–11091.

Young, A., Jiang, M., Wang, Y., Ahmedli, N.B., Ramirez, J., Reese, B.E., Birnbaumer, L., and Farber, D.B. (2011). Specific interaction of Gαi3 with the Oa1 G-protein coupled

receptor controls the size and density of melanosomes in retinal pigment epithelium. PLoS ONE *6*, e24376.

Zhang, J., Jeffrey, B.G., Morgans, C.W., Burke, N.S., Haley, T.L., Duvoisin, R.M., and Brown, R.L. (2010). RGS7 and -11 Complexes Accelerate the ON-Bipolar Cell Light Response. IOVS *51*, 1121–1129.

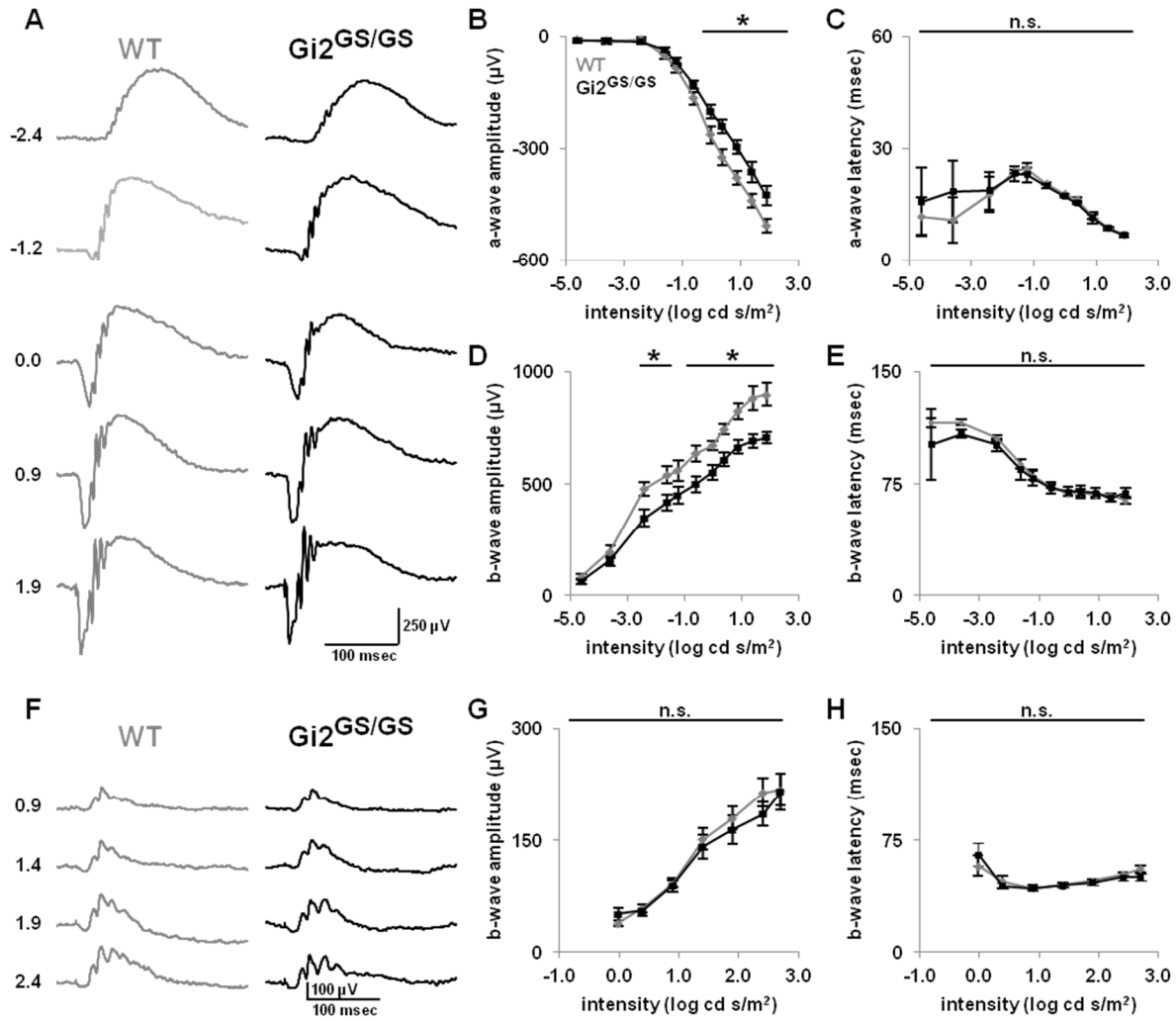

Figure 1. Gi2$^{GS/GS}$ mice have diminished ERG a-wave and b-wave amplitude.

A. Representative ERG responses from dark-adapted WT and Gi2$^{GS/GS}$ mice (~3 months) were obtained over the indicated range of flash intensities (log cd s/m^2). **B-C.** Disruption of RGS regulation of Gi2 diminishes a-wave amplitude (B) but does not affect a-wave latency (C). **D-E.** Gi2$^{GS/GS}$ mice exhibit diminished dark-adapted b-wave peak amplitude (D) with no change in latency (E). **F.** Representative ERG responses of light-adapted WT and Gi2$^{GS/GS}$ mice over the photopic range of flash intensities (log cd s/m^2). **G-H.** Similar ERG b-wave peak amplitude (G) and latency (H) in light-adapted WT and Gi2$^{GS/GS}$ mice were observed. Error bars represent ±SEM. Asterisks denote p value, $p<0.05$.

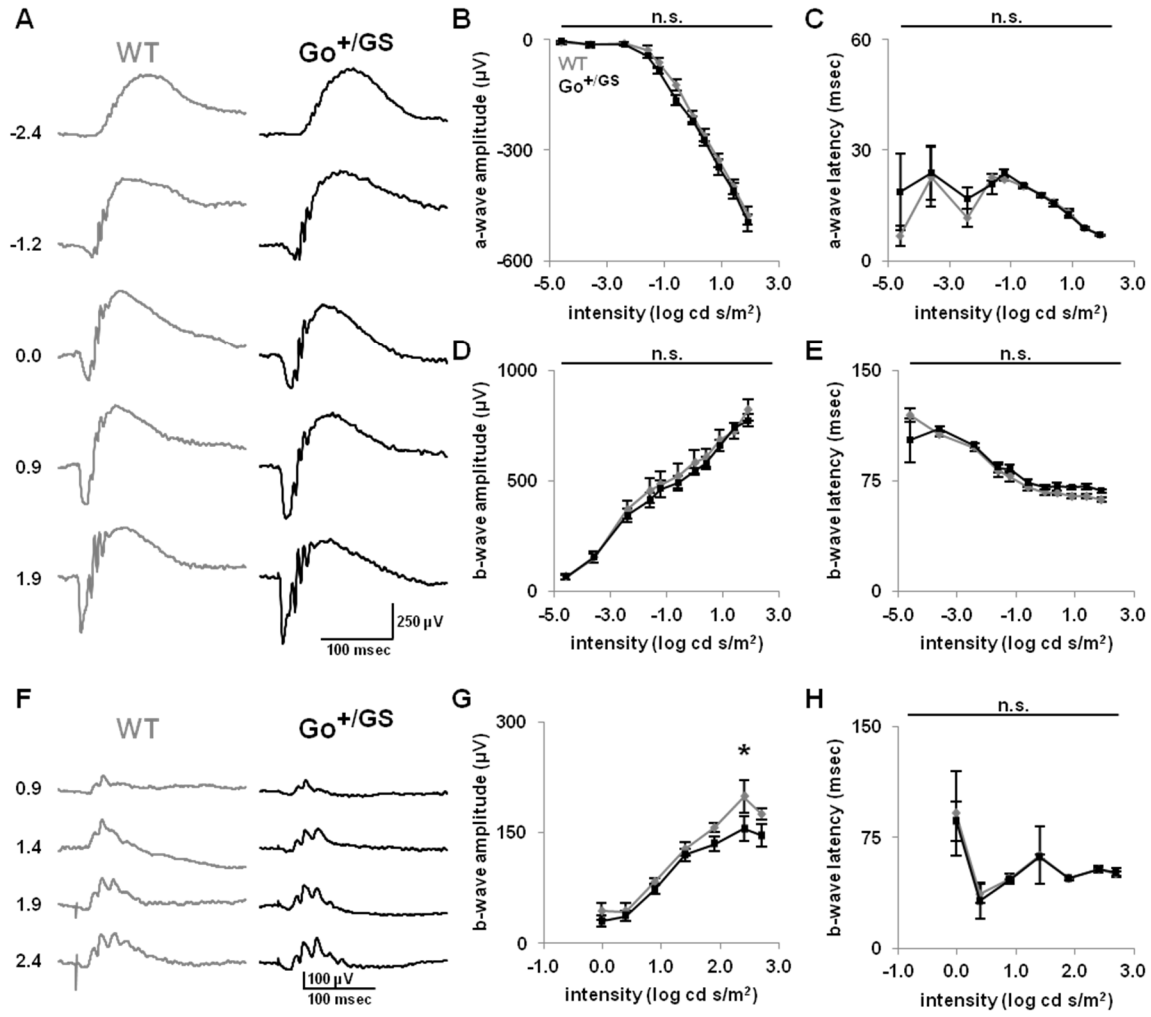

Figure 2. Go$^{+/GS}$ have normal dark-adapted photoreceptor and ON bipolar cell activity.

A. Representative ERG responses from dark-adapted WT and Go$^{+/GS}$ mice (~3 months) were obtained over the indicated range of flash intensities (log cd s/m^2). **B-C.** Quantification of ERG a-wave peak amplitude (B) and latency (C) in adult dark-adapted WT (gray) and Go$^{+/GS}$ (black) mice. **D-E.** Go$^{+/GS}$ mice exhibit normal dark-adapted b-wave peak amplitude (D) or latency (E). **F.** Representative ERG responses of light-adapted WT and Go$^{+/GS}$ mice over the photopic range of flash intensities (log cd s/m^2). **G-H.** Decreased ERG b-wave peak amplitude (G) but normal latency (H) in light-adapted Go$^{+/GS}$ mice were observed. Error bars represent ±SEM. Asterisks denote p value, $p<0.05$.

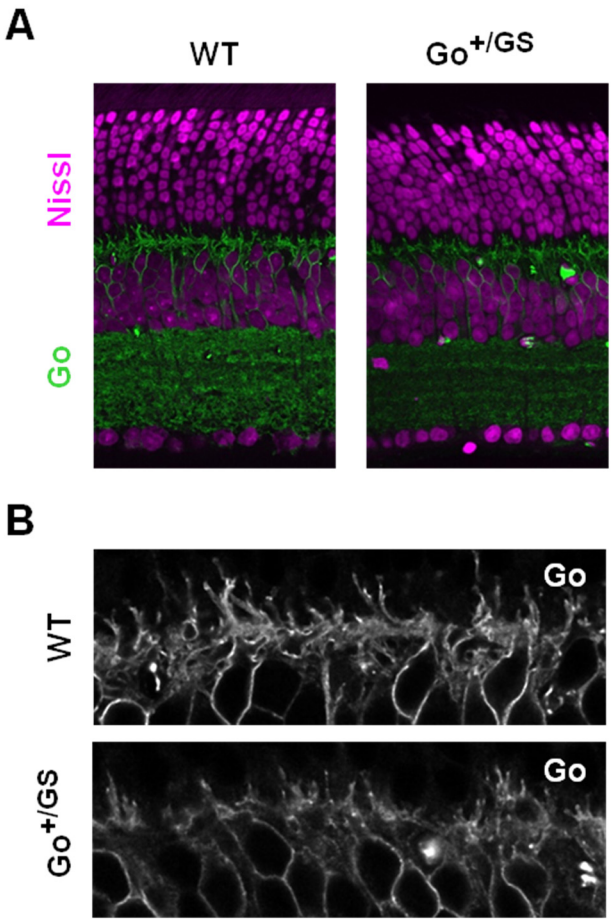

Figure 3. Normal Go expression and rod bipolar cell dendritic morphology in $Go^{+/GS}$ retina. **A.** Normal distribution of Go in WT and heterozygous RGS-insensitive $Go^{+/GS}$ knock-in mutants in retina vertical slices. **B.** Rod bipolar cell morphology, marked by Go immunostaining, is not impaired by expression of $Go^{+/GS}$.

Chapter 5:

Preliminary characterization of RGS6$^{-/-}$ visual function

Acknowledgements:

I must thank Ken Blumer for being willing to let me investigate another mouse line so late in my graduate study. The RGS6$^{-/-}$ mice were provided by Rory Fisher (U. of Iowa). Anne Hennig helped train me on the BigShot ERG system used in this study. Again, I would like to thank members of the Blumer lab for helpful advice and discussion. This work was supported by grants from the National Institutes of Health (GM44592 and HL075632 (K.J.B) and EY02687 (Department of Ophthalmology and Visual Sciences, Washington University) and from Research to Prevent Blindness, Inc. (DOVS). During this work I was supported by predoctoral training grants from the NIH (GM 007067 and T32-EY013360).

Abstract

R7-RGS family members are critical regulators of GPCR signaling in outer retinal function. It is unknown if R7-RGS proteins regulate Gi/o signaling in the inner retina. In this preliminary study, we address this question by analyzing the effects of genetically ablating RGS6, an uncharacterized R7-RGS family member that is highly expressed in the inner retina. We found that RGS6 is predominately expressed in starburst amacrine cells. We demonstrate that RGS6 and R7BP are not interdependent for expression and localization in SACs. Using electroretinography, we demonstrate that photoreceptor and ON bipolar cell light responses are normal in RGS6$^{-/-}$ mice. We also found that ablation of RGS6 impaired scotopic spatial vision as measured by optomotor response. Taken together these findings provide preliminary evidence that RGS6 is a novel regulator of the visual system downstream of the outer retina.

Introduction

In the retina and CNS, the R7-RGS (regulators of G protein signaling) family (RGS6, 7, 9, 11) accelerate G protein deactivation by functioning as GTPase-activating proteins (GAPs) specifically for Gi/o subunits (Hooks et al., 2003). RGS7, RGS9, and RGS11 have been demonstrated to be important regulators of outer retinal function. RGS9 regulates phototransduction by deactivating transducin (Cowan et al., 1998; He et al., 1998). RGS7 and RGS11 cooperatively regulate the mGluR6/Go cascade in ON bipolar cells to facilitate light-evoked depolarization (Cao et al., 2012; Chen et al., 2010; Mojumder et al., 2009; Rao et al., 2007; Shim et al., 2012; Zhang et al., 2010). However, additional Gi/o coupled receptors modulate synaptic transmission in the inner retina (Clark et al., 2009; Gleason, 2012; Guimarães-Souza and Calaza, 2012; Huang et al.; Jensen, 2006; Jensen and Daw, 1986; Kothmann et al., 2009). The GAPs that regulate these Gi/o signaling cascades are not known.

RGS6, like other members of the R7-RGS family, functions as a GAP specific for Gi/o subunits. Recent evidence has demonstrated that it plays unique roles in murine CNS. For example, RGS6 regulates GABA(B) signaling in cerebellum to promote motor coordination and regulates serotonin and 5-HT1AR signaling in the hippocampus to promote depression and anxiety (Maity et al., 2012; Stewart et al., 2014).

In the retina, RGS6 is expressed primarily in the inner plexiform layer. This location suggests that it may modulate Gi/o signaling and inner retinal function (Song et al., 2007). Furthermore, RGS6 likely does not regulate outer retinal function as it is unable to compensate for loss of RGS7, 9, or 11 in outer retina (He et al., 1998; Makino et al., 1999; Shim et al., 2012).

Based on these findings, we hypothesize that ablation of RGS6 will augment Gi/o signaling evoked by endogenous GPCR agonists specifically in the inner retina, and this process could potentially impair retinal function.

Here we performed a preliminary characterization of RGS6 function in the visual system. We investigated its cellular expression and coupling to the allosteric regulator R7 RGS-binding protein (R7BP). Functional characterization of RGS6$^{-/-}$ mice revealed no deficit in outer retinal function, but it suggests RGS6 may be necessary for normal spatial vision.

Results

RGS6 is expressed highly in starburst amacrine cells but is not necessary for lamination.

RGS6 is the last R7-RGS family member to be characterized in mammalian retina. To investigate RGS6 function in the retina, we first identified RGS6 expression by probing vertical retinal slices of adult mice with anti-RGS6 antibodies. Specific RGS6 staining was primarily detected in S2/S4 of the IPL with additional expression in somata of the inner nuclear and ganglion cell layers (Figure 1A, 1B). This staining was absent from $RGS6^{-/-}$ vertical slices (Figure 1A). Due to background staining in the IPL, we were unable to distinguish RGS6 expression in other sublaminae of the IPL. Several results indicated that starburst amacrine cells (SACs) express RGS6. First, co-staining of RGS6 and choline acetyltransferase (ChAT, a marker of SACs) was evident in S2 and S4 which indicates the presence of RGS6 in SAC processes (Figure 1B). Second, RGS6 also was expressed strongly on the somatic plasma membrane of ChAT-positive SACs in the INL and displaced SACs in the GCL (Figure 1B, indicated by arrowheads). Previous research has shown RGS6 can colocalize with VACHT, a marker for SAC plexi (Song et al., 2007), but our data is the first to demonstrate RGS6 expression in SACs from colamination in the IPL. Despite expression in SACs, ablation of RGS6 had no effect on lamination of SACs or general retinal morphology (Figure 1C).

RGS6 and R7BP are not interdependent for expression or localization in SACs.

Previous studies have demonstrated that RGS6 and R7BP co-immunoprecipitated in retina (Song et al., 2007). Therefore, R7BP may function through the regulation of RGS6. As we had previously characterized subtle inner retina phenotypes in $R7BP^{-/-}$ mice, we wanted to determine if it was reasonable to expect that the phenotype of $RGS6^{-/-}$ mice would be distinct

from phenotypes described in R7BP$^{-/-}$ mice (Cain et al., 2013). R7BP is predicted to be a critical regulator of R7-RGS plasma membrane localization (Drenan et al., 2005). Therefore, we determined RGS6 localization in R7BP$^{-/-}$ vertical retina slices. RGS6 correctly colocalized with ChAT and SAC plexi in S2/S4 sublaminae of the IPL (Figure 2A) which suggests that R7BP is not necessary for RGS6 trafficking in SACs. While R7BP may not affect RGS6 trafficking to these plexi, it may affect localization to specific membrane compartments in SAC plexi or act as an allosteric regulator. R7BP stability is dependent on its interaction with R7-RGS DEP domains (Grabowska et al., 2008; Martemyanov et al., 2005). To ascertain the extent to which R7BP is coupled to RGS6, we measured R7BP expression both in RGS6$^{-/-}$ retinal lysates (Figure 2B) and by immunostaining for R7BP in retinal vertical slices (Figure 2C). R7BP expression was minimally decreased in RGS6$^{-/-}$ retinas which suggests that a majority of R7BP is not dependent on RGS6$^{-/-}$ for stability. Similarly, R7BP expression in starburst amacrine cells appeared diminished but relatively normal. However, RGS7 levels have been reported to increase with loss of expression of other R7-RGS family members (Chen et al., 2010). To determine if R7BP was being stabilized by compensatory expression of RGS7, we also measured RGS7 expression in RGS6$^{-/-}$ retinal lysates using western blotting. As shown in Figure 2C, we observed no change in RGS7 retinal expression. Together these data indicate that a majority of RGS6 and R7BP reside in distinct functional pools and that RGS6$^{-/-}$ mice may be phenotypically different from R7BP$^{-/-}$ mice.

RGS6$^{-/-}$ have normal light-evoked photoreceptor and ON bipolar cell activity.

RGS6 is absent from photoreceptors and is unable to compensate for loss of RGS7 and RGS11 in ON bipolar cells. This finding suggests that RGS6 does not regulate R7-RGS targets

in the outer retina (Cao et al., 2012; Shim et al., 2012; Song et al., 2007). To determine whether RGS6 ablation alters photoreceptor or ON bipolar cell light responses, we performed electroretinography of dark-adapted (Figure 3A) and light-adapted mice (Figure 3F). In dark-adapted WT and RGS6$^{-/-}$ mice (n=7), we observed no difference in a-wave amplitude or latency corresponding to light-evoked hyperpolarization of rods (low light intensities) or rods and cones (higher intensities) (Figure 3B/C). The ERG b-wave, which primarily is caused by ON bipolar cell depolarization, was not different in amplitude or latency in dark-adapted RGS6$^{-/-}$ mice (Figure 3D/E). Similarly, photopic (cone-specific) responses revealed by constant background illumination and high intensity flashes revealed no change in b-wave amplitude (Figure 3G). RGS6$^{-/-}$ photopic b-wave latency was significantly decreased at 2.4 log cd s/m^2 ($p=0.004$); however, all other intensities or latencies were indistinguishable from wild-type (Figure 3H). These data indicate that RGS6 ablation has no significant effect on light-evoked responses in outer retina.

RGS6$^{-/-}$ mice have normal oscillatory potentials.

Additionally, we extracted ERG oscillatory potentials (OPs) from ERG curves. Oscillatory potentials arise from activity in the inner retina and are seen as higher frequency oscillations on the b wave. In dark-adapted RGS6$^{-/-}$ ERGs, OP1-4 amplitudes and latencies were indistinguishable from WT values. At higher intensities of light-adapted ERGs, OP3 and OP4 were diminished in RGS6$^{-/-}$ mice but did not reach levels of statistical significance ($p=0.08$ and $p=0.07$). In both dark- and light-adapted mice, the latency of OP1-4 was not affected by RGS ablation. Analysis of OPs suggest there are no dramatic changes to inner retinal function in RGS6$^{-/-}$ retina.

Abnormal spatial vision in RGS6$^{-/-}$ mice.

As a preliminary analysis of vision in RGS6$^{-/-}$, we evaluated the optomotor responses of RGS6$^{-/-}$ mice as means of determining visual acuity and contrast sensitivity under scotopic (-4.5 log cd/m^2) and photopic (1.8 log cd/m^2) conditions. we show that outer retinal function is normal in RGS6$^{-/-}$ mice; any spatial vision defects would suggest that RGS6 functions in a downstream of the outer retina, potentially the inner retina. Interestingly, scotopic contrast sensitivity was significantly decreased in RGS6$^{-/-}$ mice ($p=0.04$). However, scotopic visual acuity was not significantly affected. Similarly, photopic contrast sensitivity and visual acuity were not significantly different in this preliminary data set.

Discussion

We provide preliminary evidence that RGS6 is necessary for proper spatial vision. While we demonstrate that RGS6 is expressed in the retina, we cannot yet conclude how RGS6 is functioning to maintain normal spatial vision. Principally, it is unclear if RGS6 specifically regulates circuits governing the optomotor response or has broader impact on the visual system. While outer retina dysfunction can impair optomotor responses, RGS6 likely functions downstream of the outer retina because photoreceptor and ON bipolar cell light responses are normal in the absence of RGS6.

The idea that RGS6 functions in SACs to regulate optomotor responses is intriguing. SACs and the direction-selective RGCs that they regulate are critical in encoding directional movement that elicits the optomotor response (Sugita et al., 2013; Yoshida et al., 2001). Indeed, immunotoxin-mediated ablation of SACs eliminates optokinetic eye movement, an analogous reflex that is driven by similar subcortical pathways as the optomotor head tracking (Yoshida et al., 2001). Assessing if there is any loss of directional preference in DS-RGCs would help determine if RGS6 is acting in retina to regulate optomotor responses.

It is also possible that RGS6 is regulating optomotor responses downstream of the retina in the accessory optic system in the brain. We previously demonstrated that R7-RGS complexes are expressed in other visual centers of the brain like the dLGN. Therefore, a survey of RGS6 expression in the relevant accessory optic system will be needed. Alternatively, the deficits in spatial vision in RGS6$^{-/-}$ may represent a broader retinal dysfunction. Assessing if RGS6

ablation affects RGC activity to full field stimuli would aid in determining the extent that RGS6 is necessary for inner retinal function.

Material and Methods

Animals

All animal procedures used protocols approved by the Washington University Animal Studies Committee (Protocols #20110184 and #20140036). $RGS6^{+/-}$ mice were generated by Texas A&M Institute for Genomic Medicine (TIGM). $RGS6^{-/-}$ mice were interbred to produce $RGS6^{-/-}$ mice of either sex and compared to C57BL/6 wild-type mice (Charles River Laboratories).

Tissue preparation and immunostaining

Mice were euthanized by CO_2 asphyxiation followed by cervical dislocation. Enucleated eyes were fixed with paraformaldehyde (4%) in PBS (pH 7.4). Retinas were isolated in PBS and embedded in 4% low-melting point agarose. Vertical retina slices were cut (60 μm) with a vibratome. Slices were blocked with 10% normal horse serum (NHS) in PBS and incubated with primary antibodies overnight in 5% NHS and 0.05% Triton X-100 (Sigma-Aldrich). The following antibodies were used: affinity purified rabbit anti-R7BP (Grabowska et al., 2008), rabbit anti-RGS6 (1:500), provided by Rory Fisher, goat anti-ChAT (#AB143 Millipore; 1:100), Alexa Fluor 568-conjugated anti-rabbit and Alexa Fluor 488-conjugated anti-goat (Invitrogen; 1:1000) antibodies. Slices were mounted using VectaShield (Vector Labs) and imaged with Olympus FluoView FV500 (Bakewell NeuroImaging Laboratory, WUSM). Retinal immunofluorographs were median filtered (1 pixel surround) using NIH Fiji (Schindelin et al., 2012).

Western Blot

Mice were euthanized by CO_2 asphyxiation followed by cervical dislocation. Enucleated eyes were isolated in PBS. Isolated retinas were homogenized in 1% Triton x-100 in PBS (pH 8.0) using teflon microcentrifuge tube pestle. Homogenates were further lysed by rotating at 4°C for 30 min. Lysates were cleared by centrifugation at 16,000xg (20 min). Soluble fractions were quantified using Bradford reagent (BioRad). For western blots, samples were electrophoresed through 10% SDS-polyacrylamide gels and transferred to PVDF membranes (Millipore). Membranes were blocked with 5% milk in TBST (1 hr) and incubated overnight at 4°C with primary antibody in TBST or 5% milk in TBST. The following antibodies were used: affinity purified rabbit anti-R7BP (1:1000), rabbit- RGS6 (1:1000), provided by Rory Fisher, and rabbit anti-RGS7 (1:1000), provided by Ted Wensel. Blots were washed three times in TBST (10 min) prior to incubation with HRP-conjugated anti-rabbit antibody in TBST. Secondary antibody was washed three times with TBST (10 min) and blots were imaged using ECL reagent (General Electric) and ChemiDoc XRS+ system (BioRad)

Electroretinography

Flash ERG measurements were performed with a UTAS Visual Electrodiagnostic System with BigShot Ganzfeld running EM for Windows (LKC Technologies). Mice (~3 months old) were dark-adapted overnight. Under dim red illumination, mice were anesthetized with a cocktail of 80 mg/kg ketamine and 15 mg/kg xylazine. The body temperature of the mice was maintained at 37 ^{o}C with a heating pad controlled by a rectal temperature probe. After positioning mice in the Ganzfeld dome, the recording Bruian-Allen contact lens electrodes were positioned on the corneal surface of each eye in a drop of 0.5% atropine sulfate (Bausch & Lomb) and 1.25% hydroxypropol methylcellulose (GONAK; Akorn Inc.). Reference and ground

electrodes were placed at the vertex of the skull and back, respectively. For dark-adapted analysis, we recorded the responses to white light flashes of increasing intensity (-4.6 to 1.9 log cd s/m^2) in total darkness. Mice were then light-adapted to a constant white background illumination of 2.3 log cd s/m^2 for 10 min. Light-adapted responses to a series of light flashes (-0.01 to 2.9 log cd s/m^2) were obtained in the presence of constant background illumination. Responses to multiple trials were averaged at each light intensity level. The a-wave amplitude and latency were measured and quantified for comparison. B-wave amplitude and latency were measured using a custom MatLab script. Briefly, ERG curves were filtered using a lowpass zero-phase Butterworth digital filter (15 Hz) to remove high frequency oscillations. B wave peak was defined as the maximum post-flash amplitude from lowpass filtered curves. Oscillatory potentials (OPs) were isolated by bandpass Butterworth filter (45-300 Hz). The amplitude of OPs was calculated from the OP peak to preceding trough. Latency was defined as the time of the OP peak. OPs were identified by MatLab script with the highest amplitude OP being defined as OP2 and all other OPs being identified relatively.

Spatial vision measured by optomotor reflexes

For testing spatial vision, we measured optomotor responses in WT and R7BP$^{-/-}$ mice (~3 months old) using the OptoMotry virtual optomotor system (Cerebral Mechanics) (Prusky et al., 2004). This system utilizes a reflex in which mice move their heads to track a moving vertical sine wave grating. Mice were placed on a pedestal surrounded by computer monitors that displayed the grating and monitored with a video camera under normal or IR illumination. Stimuli were presented for a period of 5 sec before returning to 50% gray illumination. The protocol implemented a two-alternative, forced choice method in which the observer was blind to

the direction of rotation of the grating and was forced to identify the direction based on the mouse's observed head movement (Umino et al., 2006). A staircase paradigm was used for assessing contrast and spatial frequency thresholds, defined as a correct observer response of 70%. For determining contrast sensitivity, testing was performed under optimal tuning conditions in which spatial frequency were set at 0.128 cyc/deg and temporal frequencies were set at 0.75 or 1.5 Hz for scotopic and photopic conditions, respectively (Umino et al., 2008). Contrast sensitivity was defined as the inverse of the contrast at threshold (Prusky et al., 2004). For testing visual acuity, contrast (100%) and speed (Scotopic: 5.4 deg/s, Photopic: 12.0 deg/s) were kept constant while spatial frequency was gradually increased. Visual acuity was defined as the spatial frequency at threshold. For scotopic (-4.5 log cd/m^2) testing, mice were dark-adapted overnight, and neutral density film filters were placed between mice and the computer monitors. For photopic (1.8 log cd/m^2) testing, mice were light adapted, and the acuity and contrast sensitivity examinations were repeated without filters.

Statistics

Statistical analysis of electroretinograms was performed using repeated measures ANOVA followed by Holm-Sidak post-test. Significance was determined before post-test. Student's t-test was used to determine significance of optomotor response data. Statistical significance was defined as $p<0.05$.

References

Cain, M.D., Vo, B.Q., Kolesnikov, A.V., Kefalov, V.J., Culican, S.M., Kerschensteiner, D., and Blumer, K.J. (2013). An allosteric regulator of R7-RGS proteins influences light-evoked activity and glutamatergic waves in the inner retina. PLoS ONE *8*, e82276.

Cao, Y., Pahlberg, J., Sarria, I., Kamasawa, N., Sampath, A.P., and Martemyanov, K.A. (2012). Regulators of G protein signaling RGS7 and RGS11 determine the onset of the light response in ON bipolar neurons. PNAS *109*, 7905–7910.

Chen, F.S., Shim, H., Morhardt, D., Dallman, R., Krahn, E., McWhinney, L., Rao, A., Gold, S.J., and Chen, C.-K. (2010). Functional Redundancy of R7 RGS Proteins in ON-Bipolar Cell Dendrites. IOVS *51*, 686–693.

Clark, B.D., Kurth-Nelson, Z.L., and Newman, E.A. (2009). Adenosine-Evoked Hyperpolarization of Retinal Ganglion Cells Is Mediated by G-Protein-Coupled Inwardly Rectifying K+ and Small Conductance Ca2+-Activated K+ Channel Activation. J. Neurosci. *29*, 11237–11245.

Cowan, C.W., Fariss, R.N., Sokal, I., Palczewski, K., and Wensel, T.G. (1998). High expression levels in cones of RGS9, the predominant GTPase accelerating protein of rods. Proceedings of the National Academy of Sciences of the United States of America *95*, 5351.

Drenan, R.M., Doupnik, C.A., Boyle, M.P., Muglia, L.J., Huettner, J.E., Linder, M.E., and Blumer, K.J. (2005). Palmitoylation regulates plasma membrane–nuclear shuttling of R7BP, a novel membrane anchor for the RGS7 family. J Cell Biol *169*, 623–633.

Gleason, E. (2012). The influences of metabotropic receptor activation on cellular signaling and synaptic function in amacrine cells. Visual Neuroscience *29*, 31–39.

Grabowska, D., Jayaraman, M., Kaltenbronn, K.M., Sandiford, S.L., Wang, Q., Jenkins, S., Slepak, V.Z., Smith, Y., and Blumer, K.J. (2008). Postnatal induction and localization of R7BP, a membrane-anchoring protein for regulator of G protein signaling 7 family-Gβ5 complexes in brain. Neuroscience *151*, 969–982.

Guimarães-Souza, E. m., and Calaza, K. c. (2012). Selective activation of group III metabotropic glutamate receptor subtypes produces different patterns of γ-aminobutyric acid immunoreactivity and glutamate release in the retina. Journal of Neuroscience Research *90*, 2349–2361.

He, W., Cowan, C.W., and Wensel, T.G. (1998). RGS9, a GTPase Accelerator for Phototransduction. Neuron *20*, 95–102.

Hooks, S.B., Waldo, G.L., Corbitt, J., Bodor, E.T., Krumins, A.M., and Harden, T.K. (2003). RGS6, RGS7, RGS9, and RGS11 stimulate GTPase activity of Gi family G-proteins with differential selectivity and maximal activity. J. Biol. Chem. *278*, 10087–10093.

Huang, H., Wang, Z., Weng, S.-J., Sun, X.-H., and Yang, X.-L. Neuromodulatory role of melatonin in retinal information processing. Progress in Retinal and Eye Research.

Jensen, R.J. (2006). Activation of group II metabotropic glutamate receptors reduces directional selectivity in retinal ganglion cells. Brain Research *1122*, 86–92.

Jensen, R.J., and Daw, N.W. (1986). Effects of dopamine and its agonists and antagonists on the receptive field properties of ganglion cells in the rabbit retina. Neuroscience *17*, 837–855.

Kothmann, W.W., Massey, S.C., and O'Brien, J. (2009). Dopamine-Stimulated Dephosphorylation of Connexin 36 Mediates AII Amacrine Cell Uncoupling. J. Neurosci. *29*, 14903–14911.

Maity, B., Stewart, A., Yang, J., Loo, L., Sheff, D., Shepherd, A.J., Mohapatra, D.P., and Fisher, R.A. (2012). Regulator of G protein signaling 6 (RGS6) protein ensures coordination of motor movement by modulating GABAB receptor signaling. J. Biol. Chem. *287*, 4972–4981.

Makino, E.R., Handy, J.W., Li, T., and Arshavsky, V.Y. (1999). The GTPase activating factor for transducin in rod photoreceptors is the complex between RGS9 and type 5 G protein beta subunit. Proc. Natl. Acad. Sci. U.S.A. *96*, 1947–1952.

Martemyanov, K.A., Yoo, P.J., Skiba, N.P., and Arshavsky, V.Y. (2005). R7BP, a Novel Neuronal Protein Interacting with RGS Proteins of the R7 Family. J. Biol. Chem. *280*, 5133–5136.

Mojumder, D.K., Qian, Y., and Wensel, T.G. (2009). Two R7 Regulator of G-Protein Signaling Proteins Shape Retinal Bipolar Cell Signaling. J. Neurosci. *29*, 7753–7765.

Prusky, G.T., Alam, N.M., Beekman, S., and Douglas, R.M. (2004). Rapid Quantification of Adult and Developing Mouse Spatial Vision Using a Virtual Optomotor System. IOVS *45*, 4611–4616.

Rao, A., Dallman, R., Henderson, S., and Chen, C.-K. (2007). Gβ5 Is Required for Normal Light Responses and Morphology of Retinal ON-Bipolar Cells. J. Neurosci. *27*, 14199–14204.

Schindelin, J., Arganda-Carreras, I., Frise, E., Kaynig, V., Longair, M., Pietzsch, T., Preibisch, S., Rueden, C., Saalfeld, S., Schmid, B., et al. (2012). Fiji: an open-source platform for biological-image analysis. Nat. Methods *9*, 676–682.

Shim, H., Wang, C.-T., Chen, Y.-L., Chau, V.Q., Fu, K.G., Yang, J., McQuiston, A.R., Fisher, R.A., and Chen, C.-K. (2012). Defective Retinal Depolarizing Bipolar Cells in Regulators of G Protein Signaling (RGS) 7 and 11 Double Null Mice. J. Biol. Chem. *287*, 14873–14879.

Song, J.H., Song, H., Wensel, T.G., Sokolov, M., and Martemyanov, K.A. (2007). Localization and differential interaction of R7 RGS proteins with their membrane anchors R7BP and R9AP in neurons of vertebrate retina. Molecular and Cellular Neuroscience *35*, 311–319.

Stewart, A., Maity, B., Wunsch, A.M., Meng, F., Wu, Q., Wemmie, J.A., and Fisher, R.A. (2014). Regulator of G-protein signaling 6 (RGS6) promotes anxiety and depression by attenuating serotonin-mediated activation of the 5-HT(1A) receptor-adenylyl cyclase axis. FASEB J. *28*, 1735–1744.

Sugita, Y., Miura, K., Araki, F., Furukawa, T., and Kawano, K. (2013). Contributions of retinal direction-selective ganglion cells to optokinetic responses in mice. Eur. J. Neurosci. *38*, 2823–2831.

Umino, Y., Frio, B., Abbasi, M., and Barlow, R. (2006). A two-alternative, forced choice method for assessing mouse vision. Adv. Exp. Med. Biol. *572*, 169–172.

Umino, Y., Solessio, E., and Barlow, R.B. (2008). Speed, Spatial, and Temporal Tuning of Rod and Cone Vision in Mouse. J. Neurosci. *28*, 189–198.

Yoshida, K., Watanabe, D., Ishikane, H., Tachibana, M., Pastan, I., and Nakanishi, S. (2001). A key role of starburst amacrine cells in originating retinal directional selectivity and optokinetic eye movement. Neuron *30*, 771–780.

Zhang, J., Jeffrey, B.G., Morgans, C.W., Burke, N.S., Haley, T.L., Duvoisin, R.M., and Brown, R.L. (2010). RGS7 and -11 Complexes Accelerate the ON-Bipolar Cell Light Response. IOVS *51*, 1121–1129.

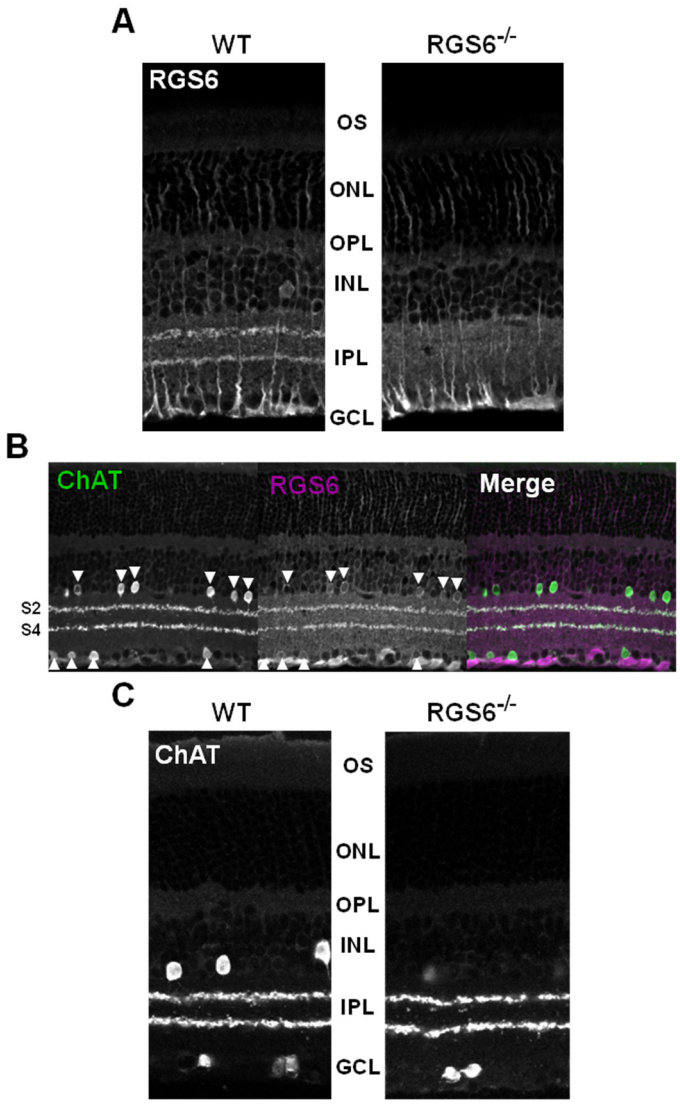

Figure 1. RGS6 is expressed in starburst amacrine cells but is not necessary for proper SAC lamination.

A. Immunostaining of RGS6 in the IPL in wild-type retina (A) as compared to RGS6$^{-/-}$ retina. **B.** Expression of RGS6 in starburst amacrine cells (SACs). Co-staining of the SAC marker (ChAT; green) and RGS6 (magenta) in the S2/S4 sublaminae of the IPL and somata of the INL and GCL. Arrowheads mark ChAT-positive somata. **C.** RGS6 ablation does not disrupt gross retinal morphology or lamination of starburst amacrine cells.

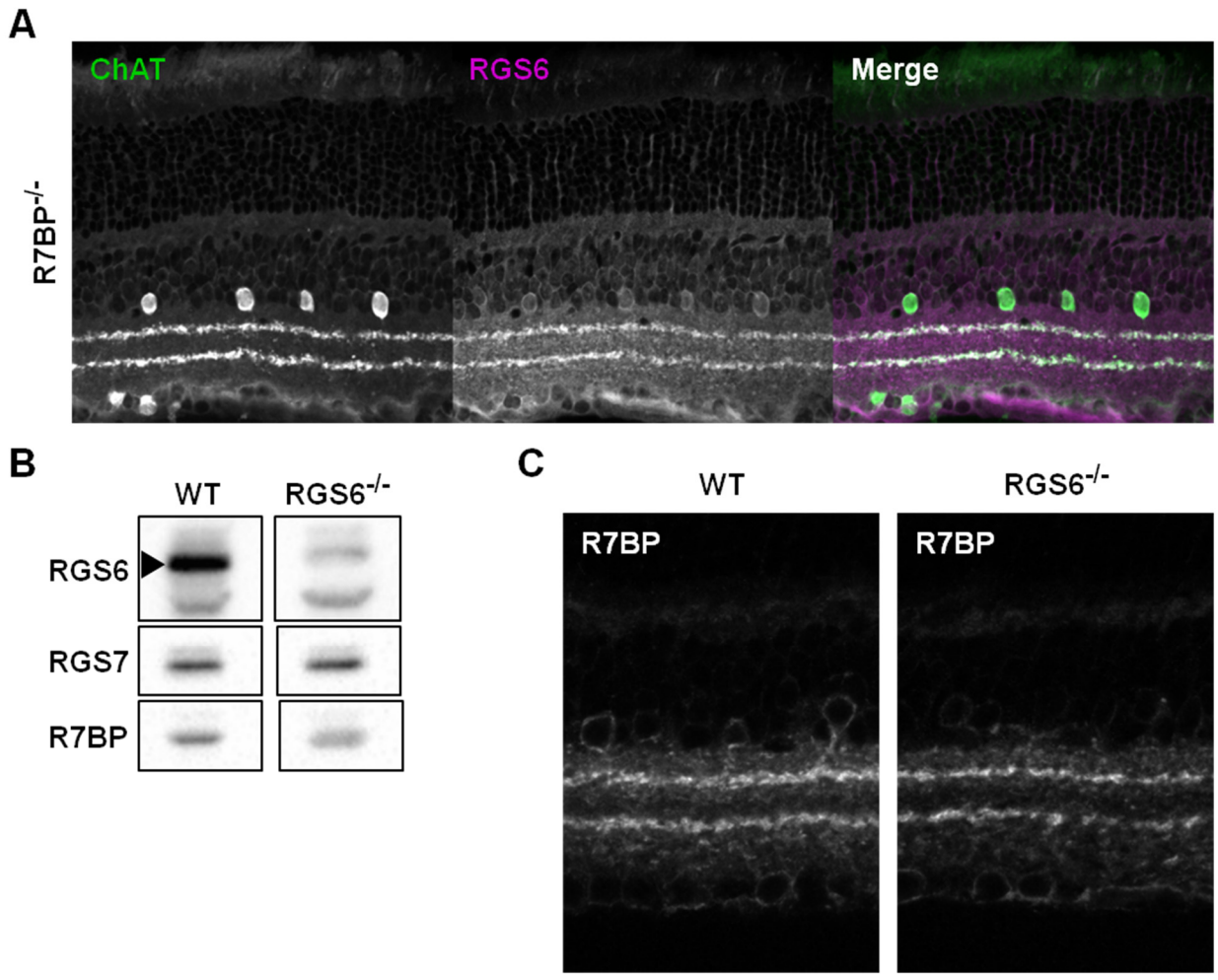

Figure 2. RGS6/R7BP expression and localization are not interdependent.

A. R7BP is not necessary for RGS6 localization in SAC plexi. Co-staining of the SAC marker (ChAT; green) and RGS6 (magenta) in the S2/S4 sublaminae of the IPL of adult R7BP$^{-/-}$ retinas.

B. Ablation of RGS6 does not drastically alter RGS7 and R7BP retinal expression. RGS6, RGS7, and R7BP in wild-type and RGS$^{-/-}$ total retinal lysates were detected by western blotting.

C. Immunostaining of R7BP in adult wild-type and RGS6$^{-/-}$ vertical retinal slices reveal RGS6 is not necessary for R7BP expression in IPL

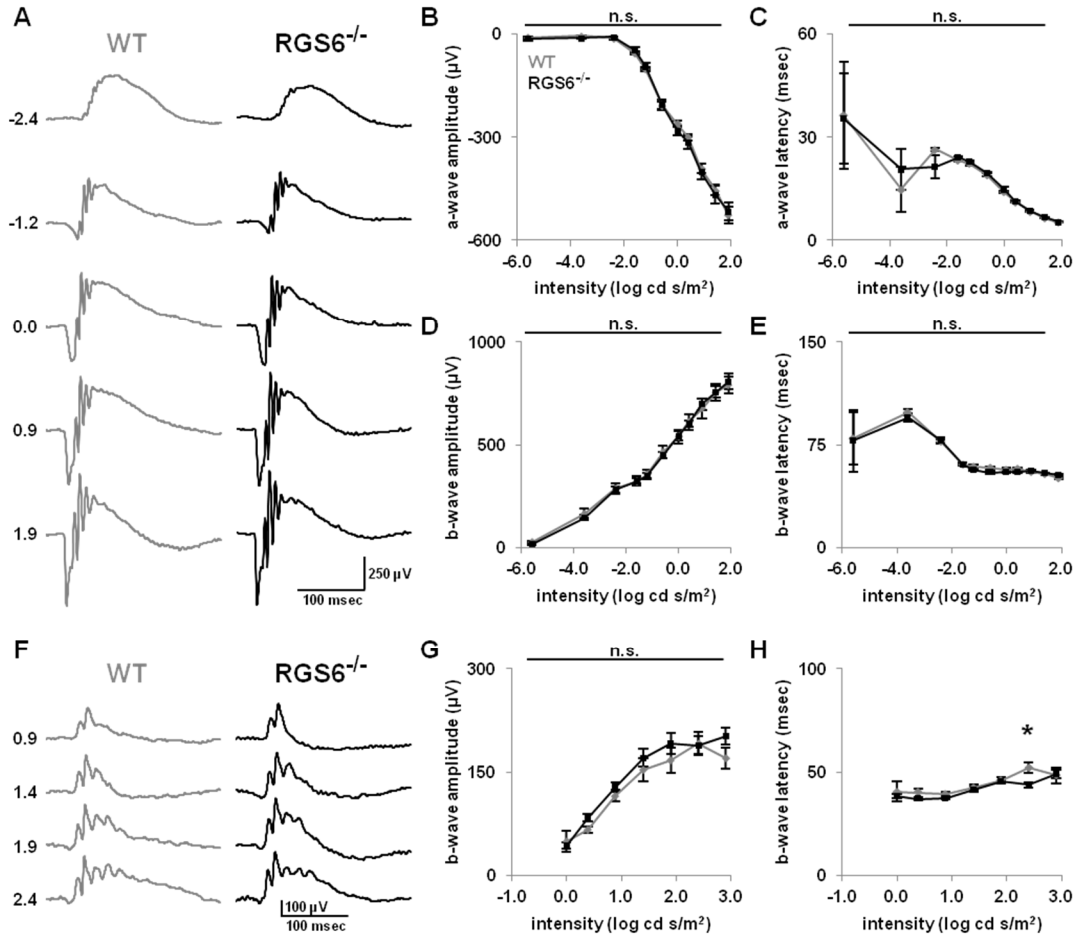

Figure 3. RGS6$^{-/-}$ mice have normal light-evoked photoreceptor and ON bipolar cell activity.

A. Representative ERG responses from dark-adapted WT and RGS6$^{-/-}$ mice (~3 months) were obtained over the indicated range of flash intensities (log cd s/m^2). **B-C.** Quantification of ERG a-wave peak amplitude (B) and latency (C) in adult dark-adapted WT (gray) and RGS6$^{-/-}$ (black) mice. **D-E.** Ablation of RGS6 does not alter dark-adapted b-wave peak amplitude (D) or latency (E). **F.** Representative ERG responses of light-adapted WT and RGS6$^{-/-}$ mice over the photopic range of flash intensities (log cd s/m^2). **G-H.** Similar ERG b-wave peak amplitude (G) and latency (H) in light-adapted WT and RGS6$^{-/-}$ mice were observed. Error bars represent ±SEM. Asterisks denote p value, $p<0.05$.

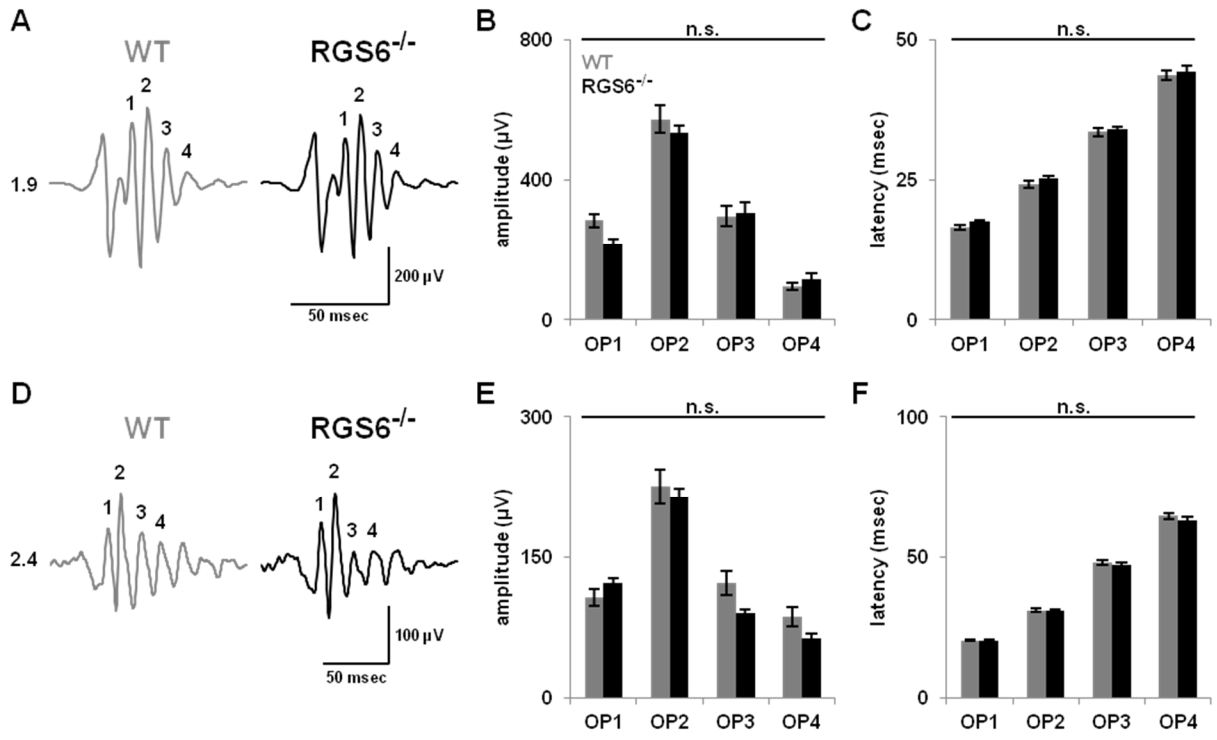

Figure 4. RGS6$^{-/-}$ mice have essentially normal ERG oscillatory potentials.

A. Representative oscillatory potentials (OPs) from dark-adapted WT and RGS6$^{-/-}$ mice at maximum intensity (1.9 log cd s/m^2). OP1-4 are designated. **B-C.** Ablation of RGS6 does not significantly alter dark-adapted OP1-4 amplitude (B) or latency (C). **D.** Representative oscillatory potentials (OPs) from light-adapted WT and RGS6$^{-/-}$ mice at 2.4 log cd s/m^2. OP1-4 are designated. **E-F.** Ablation of RGS6 does not significantly alter light-adapted OP1-4 amplitude (E) or latency (F). Error bars represent ±SEM.

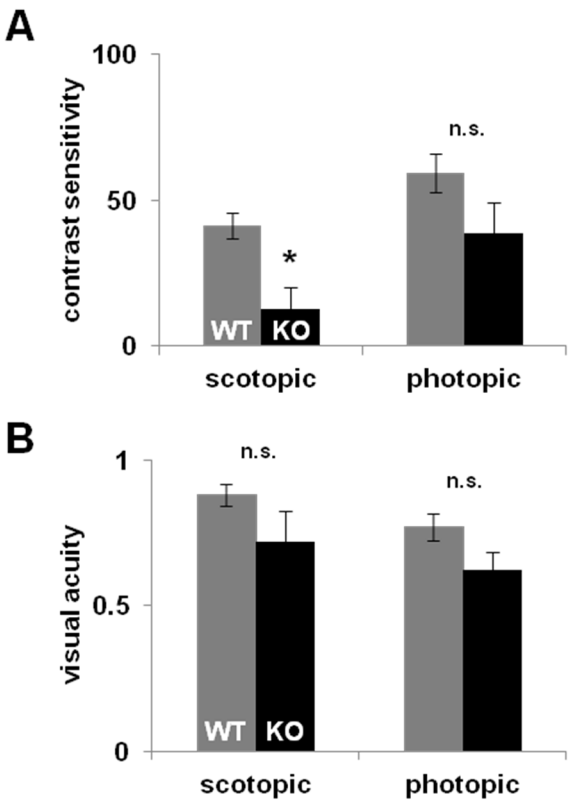

Figure 5. Abnormal spatial vision in RGS6$^{-/-}$ mice.

A. Significantly reduced contrast sensitivity of RGS6$^{-/-}$ mice under scotopic but not photopic conditions, as measured by optomotor response. **B.** Ablation of R7BP does not significantly disrupt scotopic and photopic visual acuity. Error bars represent ±SEM. Asterisks denote p value, $p<0.05$.

Chapter 6:

Discussion and Future Directions

Findings of the Dissertation

At the initiation of this project in 2009, the function of R7-RGS complexes in the CNS had begun to be investigated. Although R7-RGS biochemical function was well understood, less was known about R7-RGS function *in vivo*. Studies had demonstrated the necessity of R7-RGS function in the outer retina. RGS9-1 and its membrane targeting protein R9AP had been identified as important regulators of transducin and phototransduction in photoreceptors (He et al., 1998; Nishiguchi et al., 2004). Similarly, R7-RGS/Gβ5 complexes were identified as necessary components of mGluR6 cascades regulating ON bipolar cell light responses (Cao et al., 2012; Rao et al., 2007; Shim et al., 2012). However, the expression of R7-RGS complex proteins in the inner retina led us to hypothesize: 1) R7-RGS proteins regulate inner retinal function, and 2) perturbation of R7-RGS function will reveal visual circuits sensitive to RGS and G protein regulation. The results presented in this dissertation provide evidence supporting these hypotheses, and it extends our knowledge of R7-RGS protein function and G protein signaling in the retina.

To test these hypotheses, we analyzed the retinal function and vision of multiple mouse strains that disrupted RGS regulation of Gi/o signaling. First characterized was R7BP, a positive allosteric regulator of R7-RGS complexes. R7BP was found to be expressed in both starburst amacrine cells and retinal ganglion cells (RGCs) in the inner retina. We demonstrated that R7BP is not necessary for normal light-evoked photoreceptor and ON bipolar cell activity, as assessed by ERG. In parallel to our studies, Martemyanov and colleagues reported similar findings of the dispensability of R7BP in rod light responses using an independently generated $R7BP^{-/-}$ mouse line (Cao et al., 2008). Using multielectrode array recording of RGCs, we demonstrated R7BP

increased the firing rate and accelerated the latency of ON RGCs to mesopic intensity light. Looking at R7BP function in the developing retina, we found that R7BP regulated the burst duration of glutamatergic waves but had no effect on cholinergic waves. Despite these perturbations in light-evoked and spontaneous RGC activity, we found that ablation of R7BP had no effect on spatial vision or segregation of retinogeniculate projections. We also identified that R7BP formed complexes with RGS6, RGS7, and Gβ5 in the dorsal lateral geniculate nucleus (dLGN), the major relay center for retinal projection to the visual cortex. However, R7BP was not necessary for membrane targeting of R7-RGS complexes in lateral geniculate nucleus.

In a separate study, we analyzed the effect of disruption of RGS regulation of two specific Gi/o subunits, Gi2 and Go, using two RGS-insensitive (G184S) mutant knock-in lines. We demonstrated RGS regulation of Gi2 was necessary for maximal rod light responses. Unexpectedly, expression of a RGS-insensitive Go mutant was insufficient to perturb dark-adapted photoreceptor and ON bipolar cell light responses. This finding was not consistent with previous studies that demonstrated necessity of RGS7/RGS11/Gβ5 complexes for ON bipolar cell light responses (Cao et al., 2012; Rao et al., 2007; Shim et al., 2012).

In our final study, we report preliminary characterization of RGS6$^{-/-}$ vision. We demonstrated that RGS6 was expressed in starburst amacrine cells (SACs) but was not necessary for their proper lamination in the inner plexiform layer (IPL). We further demonstrated that RGS6 localization to SAC plexi in the IPL was independent of R7BP and that R7BP expression was not dependent on RGS6 expression. In assessing RGS6$^{-/-}$ retinal function, we showed that RGS6 was not necessary for light-evoked photoreceptor and ON bipolar cell activity. However,

we demonstrated that RGS6 was necessary for normal spatial vision as measured by optomotor responses.

Discussion of Results and Future Directions

Measurement of optomotor responses of RGS6$^{-/-}$ suggest that RGS6 is necessary for normal spatial vision. Further study is required to determine if RGS6 functions in the retina or in the subcortical visual system. For retinal studies, investigation of RGS6 ablation on direction selective (DS) RGCs directional preference should be a high priority. Stimulation of Gi/o coupled Group II mGluR receptors in starburst amacrine cells (SAC) reduces neurotransmitter release and impairs directionally selective responses in DS RGCs (Jensen, 2006). Does ablation of RGS6 augment Gi/o signaling in SACs? As SACs and DS RGCs are essential for the optomotor response (Sugita et al., 2013; Yoshida et al., 2001), this remains a strong candidate pathway to explain the optomotor phenotype observed in RGS6$^{-/-}$ mice.

We identified that R7-RGS/R7BP complexes are expressed in dLGN. This is the first indication that R7-RGS complexes are expressed in extraretinal components of the visual system. There are several open questions in regards to how R7-RGS complexes may be functioning in dLGN. The fact that thalamocortical relay neurons activity is affected by Gi/o coupled receptors, such as GABA(B) and Group II mGluRs, makes exploration of R7-RGS regulation in relay neurons a pertinent goal (Bickford et al., 2010b; Crunelli et al., 1988; Govindaiah and Cox, 2006; Lam and Sherman, 2013; Perreault et al., 2003; Ziburkus et al., 2003). RGS6$^{-/-}$ or RGS7$^{-/-}$ mouse lines can be used immediately in dLGN slice preps, as optic track stimulation is unaffected by any retinal phenotypes associated with the R7-RGS knockouts.

Our study and prior analysis of Gi2$^{-/-}$ mice indicate that Gi2 is critical to outer retinal function. Our data indicates that augmented Gi2 activity promotes rod dysfunction. However,

the identities of outer retina neurons affected by loss of Gi2 remain unknown. Further exploration of Gi2 function in outer retina is therefore warranted. As transducin and Go are necessary for phototransduction and ON bipolar cell light responses, it is likely that Gi2 functions peripherally to these primary cascades (Dhingra et al., 2000b, 2002). Similarly, developmental and morphological changes would be of both concern and interest because $Gi2^{GS/GS}$ mice exhibit a complex developmental phenotype and partially penetrant embryonic lethality (Huang et al., 2006).

Our data suggest that R7BP interacts with other R7-RGS family members in addition to RGS6 in SACs. As further investigation of R7-RGS function in SACs is of interest, the other R7-RGS proteins expressed in SACs should identified. RGS7 is the best candidate for this additional R7-RGS. Like RGS6, RGS7 is expressed in inner retina (Liapis et al., 2012; Song et al., 2007). Although, its expression in SACs has not been as clear. Ablation of RGS7 substantially decreases R7BP expression suggesting that they do interact; however, it is unclear if this reflects loss of R7BP in the inner or outer retina (Cao et al., 2012).

A majority of this study centered on identifying the function of R7BP *in vivo*. We demonstrated that R7BP regulates light-evoked and spontaneous activity in the inner retina. However, from a more mechanistic perspective, our data challenge the hypothesis that R7BP is a critical regulator of R7-RGS membrane association *in vivo*. R7BP does not affect RGS6 localization in SACs nor is it necessary for R7-RGS/Gβ5 membrane association in the lateral geniculate nucleus. Other studies have demonstrated that R7BP is dispensable for a majority of R7-RGS membrane association in retina (Cao et al., 2008). Instead, it seems that R7-RGS

associate with other integral membrane proteins in the retina. In rods, RGS9 interacts with R9AP (Keresztes et al., 2004). In ON bipolar cells, RGS7 and RGS11 require GPR179 to facilitate targeting to dendritic tips (Orlandi et al., 2012). Taken together R7BP does not appear to be necessary for trafficking or membrane association of R7-RGS proteins in retina or dLGN. It is possible that the visual system is tuned to require R7-RGS to associate preferentially with these integral membrane proteins for rapid response. However, with the exception of R9AP, there are many DEP-binding integral membrane proteins that are expressed throughout the CNS including: GPR158, GPR179, and muscarinic M3 and dopamine D3 receptors (Orlandi et al., 2012; Sandiford and Slepak, 2009; Zheng et al., 2011).

If transmembrane proteins facilitate the majority of R7-RGS membrane association, then what is the advantage conferred by the palmitate moieties of R7BP? The most interesting characteristic to consider is the reversibility of the palmitate modification. This reversibility allows R7BP to be responsive to cellular signaling. Indeed, we have reported previously that Gi/o signaling inhibits R7BP depalmitoylation, suggesting that R7BP could shuttle to regions of high Gi/o signaling (Jia et al., 2011). While the palmitoyltransferase DHHC2 has been identified to facilitate de novo palmitoylation and palmitoylation turnover, the serine hydrolase that mediates R7BP depalmitoylation is unknown (Jia et al., 2014). Identification of the hydrolase that regulates R7BP will be valuable in determining the extent to which R7BP is regulated by cellular conditions and signaling.

In additional to membrane targeting, R7BP may be better regarded as an allosteric regulator of R7-RGS proteins. It is capable of modulating the interaction of R7-RGS with

various DEP-binding proteins *in vitro* (Sandiford and Slepak, 2009; Zheng et al., 2011). However, to which extent this represents an *in vivo* function is unclear. The most relevant evidence of this allosteric function is that R7BP causes conformational change in R7-RGS exposing interfaces that facilitate its interaction with GIRK channels (Zhou et al., 2012a). This interaction is dependent on residues on Gβ5 that are conserved with interfaces in Gβγ signaling but are less exposed in the absence of R7BP (Ford et al., 1998; Masuho et al., 2011; Narayanan et al., 2007; Zhou et al., 2012b). It is intriguing to consider if R7BP facilitates interaction of R7-RGS with other classic Gβγ effectors. Therefore, comparison of R7-RGS/Gβ5/R7BP heterotrimer structure to existing R7-RGS/ Gβ5 dimer (Cheever et al., 2008) will further inform future studies of R7BP function as an allosteric modulator.

References

Bickford, M.E., Slusarczyk, A., Dilger, E.K., Krahe, T.E., Kucuk, C., and Guido, W. (2010). Synaptic development of the mouse dorsal lateral geniculate nucleus. J. Comp. Neurol. *518*, 622–635.

Cao, Y., Song, H., Okawa, H., Sampath, A.P., Sokolov, M., and Martemyanov, K.A. (2008). Targeting of RGS7/Gβ5 to the Dendritic Tips of ON-Bipolar Cells Is Independent of Its Association with Membrane Anchor R7BP. J. Neurosci. *28*, 10443–10449.

Cao, Y., Pahlberg, J., Sarria, I., Kamasawa, N., Sampath, A.P., and Martemyanov, K.A. (2012). Regulators of G protein signaling RGS7 and RGS11 determine the onset of the light response in ON bipolar neurons. PNAS *109*, 7905–7910.

Cheever, M.L., Snyder, J.T., Gershburg, S., Siderovski, D.P., Harden, T.K., and Sondek, J. (2008). Crystal structure of the multifunctional Gbeta5-RGS9 complex. Nat. Struct. Mol. Biol. *15*, 155–162.

Crunelli, V., Haby, M., Jassik-Gerschenfeld, D., Leresche, N., and Pirchio, M. (1988). Cl- - and K+-dependent inhibitory postsynaptic potentials evoked by interneurones of the rat lateral geniculate nucleus. J. Physiol. (Lond.) *399*, 153–176.

Dhingra, A., Lyubarsky, A., Jiang, M., Pugh, E.N., Birnbaumer, L., Sterling, P., and Vardi, N. (2000). The Light Response of ON Bipolar Neurons Requires Gαo. J. Neurosci. *20*, 9053–9058.

Dhingra, A., Jiang, M., Wang, T.-L., Lyubarsky, A., Savchenko, A., Bar-Yehuda, T., Sterling, P., Birnbaumer, L., and Vardi, N. (2002). Light Response of Retinal ON Bipolar Cells Requires a Specific Splice Variant of Gαo. J. Neurosci. *22*, 4878–4884.

Ford, C.E., Skiba, N.P., Bae, H., Daaka, Y., Reuveny, E., Shekter, L.R., Rosal, R., Weng, G., Yang, C.-S., Iyengar, R., et al. (1998). Molecular Basis for Interactions of G Protein βγ Subunits with Effectors. Science *280*, 1271–1274.

Govindaiah, G., and Cox, C.L. (2006). Metabotropic Glutamate Receptors Differentially Regulate GABAergic Inhibition in Thalamus. J. Neurosci. *26*, 13443–13453.

He, W., Cowan, C.W., and Wensel, T.G. (1998). RGS9, a GTPase Accelerator for Phototransduction. Neuron *20*, 95–102.

Huang, X., Fu, Y., Charbeneau, R.A., Saunders, T.L., Taylor, D.K., Hankenson, K.D., Russell, M.W., D'Alecy, L.G., and Neubig, R.R. (2006). Pleiotropic phenotype of a genomic knock-in of an RGS-insensitive G184S Gnai2 allele. Mol. Cell. Biol. *26*, 6870–6879.

Jensen, R.J. (2006). Activation of group II metabotropic glutamate receptors reduces directional selectivity in retinal ganglion cells. Brain Research *1122*, 86–92.

Jia, L., Linder, M.E., and Blumer, K.J. (2011). Gi/o Signaling and the Palmitoyltransferase DHHC2 Regulate Palmitate Cycling and Shuttling of RGS7 Family-binding Protein. J. Biol. Chem. *286*, 13695–13703.

Jia, L., Chisari, M., Maktabi, M.H., Sobieski, C., Zhou, H., Konopko, A.M., Martin, B.R., Mennerick, S.J., and Blumer, K.J. (2014). A mechanism regulating G protein-coupled receptor signaling that requires cycles of protein palmitoylation and depalmitoylation. J. Biol. Chem. *289*, 6249–6257.

Keresztes, G., Martemyanov, K.A., Krispel, C.M., Mutai, H., Yoo, P.J., Maison, S.F., Burns, M.E., Arshavsky, V.Y., and Heller, S. (2004). Absence of the RGS9.Gbeta5 GTPase-activating complex in photoreceptors of the R9AP knockout mouse. J. Biol. Chem. *279*, 1581–1584.

Lam, Y.-W., and Sherman, S.M. (2013). Activation of both Group I and Group II metabotropic glutamatergic receptors suppress retinogeniculate transmission. Neuroscience *242*, 78–84.

Liapis, E., Sandiford, S., Wang, Q., Gaidosh, G., Motti, D., Levay, K., and Slepak, V.Z. (2012). Subcellular localization of regulator of G protein signaling RGS7 complex in neurons and transfected cells. Journal of Neurochemistry *122*, 568–581.

Masuho, I., Wakasugi-Masuho, H., Posokhova, E.N., Patton, J.R., and Martemyanov, K.A. (2011). Type 5 G Protein Subunit (G 5) Controls the Interaction of Regulator of G Protein Signaling 9 (RGS9) with Membrane Anchors. Journal of Biological Chemistry *286*, 21806–21813.

Narayanan, V., Sandiford, S.L., Wang, Q., Keren-Raifman, T., Levay, K., and Slepak, V.Z. (2007). Intramolecular Interaction between the DEP Domain of RGS7 and the Gβ5 Subunit†. Biochemistry *46*, 6859–6870.

Nishiguchi, K.M., Sandberg, M.A., Kooijman, A.C., Martemyanov, K.A., Pott, J.W.R., Hagstrom, S.A., Arshavsky, V.Y., Berson, E.L., and Dryja, T.P. (2004). Defects in RGS9 or its anchor protein R9AP in patients with slow photoreceptor deactivation. Nature *427*, 75–78.

Orlandi, C., Posokhova, E., Masuho, I., Ray, T.A., Hasan, N., Gregg, R.G., and Martemyanov, K.A. (2012). GPR158/179 regulate G protein signaling by controlling localization and activity of the RGS7 complexes. J. Cell Biol. *197*, 711–719.

Perreault, M.-C., Qin, Y., Heggelund, P., and Zhu, J.J. (2003). Postnatal development of GABAergic signalling in the rat lateral geniculate nucleus: presynaptic dendritic mechanisms. J Physiol *546*, 137–148.

Rao, A., Dallman, R., Henderson, S., and Chen, C.-K. (2007). Gβ5 Is Required for Normal Light Responses and Morphology of Retinal ON-Bipolar Cells. J. Neurosci. *27*, 14199–14204.

Sandiford, S.L., and Slepak, V.Z. (2009). The Gβ5−RGS7 Complex Selectively Inhibits Muscarinic M3 Receptor Signaling via the Interaction between the Third Intracellular Loop of the Receptor and the DEP Domain of RGS7†. Biochemistry *48*, 2282–2289.

Shim, H., Wang, C.-T., Chen, Y.-L., Chau, V.Q., Fu, K.G., Yang, J., McQuiston, A.R., Fisher, R.A., and Chen, C.-K. (2012). Defective Retinal Depolarizing Bipolar Cells in Regulators of G Protein Signaling (RGS) 7 and 11 Double Null Mice. J. Biol. Chem. *287*, 14873–14879.

Song, J.H., Song, H., Wensel, T.G., Sokolov, M., and Martemyanov, K.A. (2007). Localization and differential interaction of R7 RGS proteins with their membrane anchors R7BP and R9AP in neurons of vertebrate retina. Molecular and Cellular Neuroscience *35*, 311–319.

Sugita, Y., Miura, K., Araki, F., Furukawa, T., and Kawano, K. (2013). Contributions of retinal direction-selective ganglion cells to optokinetic responses in mice. Eur. J. Neurosci. *38*, 2823–2831.

Yoshida, K., Watanabe, D., Ishikane, H., Tachibana, M., Pastan, I., and Nakanishi, S. (2001). A key role of starburst amacrine cells in originating retinal directional selectivity and optokinetic eye movement. Neuron *30*, 771–780.

Zheng, M., Cheong, S.-Y., Min, C., Jin, M., Cho, D.-I., and Kim, K.-M. (2011). β-arrestin2 plays permissive roles in the inhibitory activities of RGS9-2 on G protein-coupled receptors by maintaining RGS9-2 in the open conformation. Mol. Cell. Biol. *31*, 4887–4901.

Zhou, H., Chisari, M., Raehal, K.M., Kaltenbronn, K.M., Bohn, L.M., Mennerick, S.J., and Blumer, K.J. (2012a). GIRK channel modulation by assembly with allosterically regulated RGS proteins. PNAS.

Zhou, H., Chisari, M., Raehal, K.M., Kaltenbronn, K.M., Bohn, L.M., Mennerick, S.J., and Blumer, K.J. (2012b). GIRK channel modulation by assembly with allosterically regulated RGS proteins. Proc. Natl. Acad. Sci. U.S.A. *109*, 19977–19982.

Ziburkus, J., Lo, F.-S., and Guido, W. (2003). Nature of inhibitory postsynaptic activity in developing relay cells of the lateral geniculate nucleus. J. Neurophysiol. *90*, 1063–1070.